

UNIVERSIDAD DE CASTILLA-LA MANCHA

---

**Spatiotemporal characteristics of solar resource  
and photovoltaic productivity over the  
Euro-Mediterranean area: a climate perspective**

---

Memoria para optar al grado de Doctor

Departamento de Ciencias Ambientales

Instituto de Ciencias Ambientales (ICAM)

Toledo, 2019

Doctoranda:

Claudia Gutiérrez Escribano

Director:

Miguel Ángel Gaertner

Co-director:

Oscar Perpiñán





# **Características espacio-temporales del recurso solar y la productividad fotovoltaica en el área Euro-Mediterránea: perspectiva climática**

Claudia Gutiérrez Escribano



A los ingobernables,  
a los incondicionales:

a Yuri, a Igor.



A Diego.  
Que hoy esté escribiendo  
estas líneas es gracias a ti  
y a una clase de física cuántica.





---

## Agradecimientos

En el momento que escribo estas líneas, poco o nada queda de aquella que comenzó esta andadura hace ya algo más de cuatro años. Atrás han quedado la ilusión y la inocencia, barridas por el pragmatismo y la realidad de un trabajo diario solitario y absorbente, llevado a término en la presente forma gracias a una tenacidad y dedicación casi inagotable.

A pesar de la ausencia de un sentimiento profundo al llevar a término este trabajo, como probablemente esperaba que fuera en otro tiempo, la conciencia de cada uno de los pasos que me han llevado hasta aquí es plena, y el agradecimiento para todos y cada uno de los que han ayudado, en una u otra manera a que esto sea posible, es de justo reconocimiento.

Gracias a Miguel Ángel por darme la oportunidad de empezar esta tesis doctoral sin conocerme, sin ninguna referencia sobre mí y en una convocatoria contrarreloj solicitada en pleno verano.

Cuento con los dedos de una mano los profesores que en mi paso por la universidad consiguieron despertar motivación y entusiasmo a pesar de tener de su lado el atractivo de la física. El sistema ahoga a los profesores que quieren ser investigadores y a los investigadores que quieren ser profesores, perjudicando al alumnado que casi inerte recibe clases aburridas de profesores aburridos sobre cosas aburridas. Tuve que pasar por un posgrado de orientación profesional para encontrar la ilusión que para entonces había desaparecido y darme cuenta de que mi camino no pasaba por dedicar mis días a calcular el *return of investment* en una hoja de cálculo. Gracias Oscar porque tu trabajo y ayuda incondicional te definieron, entonces y ahora, como un gran profesor. Gracias además por tu enseñanza de las herramientas y metodología de trabajo con las que poder abrirme paso en el futuro.

La realidad de la investigación ha llevado a que sean unas cuantas las personas que han pasado por el laboratorio 0.14 dejándolo un poco huérfano con su marcha. Gracias Marta por tu carácter, tu disponibilidad infinita, tu amistad y tu comprensión, que hizo que aquellos primeros meses sean ahora un bonito recuerdo y ha ayudado a que los más difíciles sean una

---

lección de la que aprender. Gracias a todo el grupo Momac, los de antes y los de ahora, por hacer los días más amenos. Gracias Juanje porque siempre fuiste un paso por delante, y cada uno de tus consejos fueron valiosos para sobrevivir. Gracias Kike, el antagonismo entre tu optimismo y mi carácter encontraron el equilibrio. Todo esto hubiera sido mucho más difícil sin tu apoyo. Gracias María por tu amistad y por estar cada día para escucharme y apoyarme.

\*\*\*

I especially want to thank you all the scientific help and disinterested support to everybody who I shared time with in Tolouse. This work would hardly have been possible without their help.

Thank you, Samuel. You welcomed me as part of your group and make me feel at home since the beginning. Thanks for your help, your advice, your endless curiosity and every of your lessons. It has been a privilege having shared with you that time and I will always be thankful.

Thank you Pierre, because of your kindness and availability, and your valuable help. Thank you Marc, for your time and your ability of doing always the right questions.

No quiero olvidarme de agradecer a todos los que hicieron más amable mi paso por aquella ciudad también fuera del trabajo. Gracias a aquellos que buscaron un hueco en su vida para conocerme un poco durante esos meses. De manera especial, gracias Danila por tu amistad.

\*\*\*

Es necesario dirigir a mis padres y mi hermana estas líneas porque siempre creyeron en mí un poco más de lo que debían. Gracias por enseñarme la riqueza de los libros y fomentar la curiosidad que me ha llevado a ser quien soy. En gran medida, terminar este trabajo es también fruto de todo aquello.

Por último, si he llegado hasta aquí ha sido posible gracias a Diego. Por acompañarme, por compartir este aprendizaje conmigo y llegar al final del camino a mi lado. Nadie sabe mejor que tú lo que esto significa.

\*\*\*



---

## Preface

*"Habiendo accedido tarde a los estudios, sentía ahora urgencia por estudiar. A veces, inmerso en sus libros, le venía a la cabeza la conciencia de todo lo que no había leído y la serenidad con la que trabajaba se hacía trizas cuando caía en la cuenta del poco tiempo que tenía en la vida para aprender tantas cosas, para aprender todo lo que tenía que saber"*

—Stoner

Applied science has made societies evolve thanks to the existing link between the basic science and the inventions, which implement the structural and basic knowledge into the daily reality of the individuals. The bridge between the fundamental studies and its evolution or transformation into something useful for the societies development, has been a matter of interpretation or “translation” to find the accurate language to exchange this knowledge.

Transversality between the fundamental disciplines of physics, chemistry or biology, and the different applied sciences, most of them under the umbrella of engineering, end unavoidably into a transformation of the abstraction into something tangible with the premise or ideal of improving wellbeing of present and future societies.

However, it is very likely that this conception of the scientific application and what is called “developement” has led at the same time to the most challenging problems that humanity has to face regarding its existance, climate change, pollution, environmental degradation, loss of biodiversity etc. The anthropocentrism has become a problem and all the science and technology that made better human lifes should be re-thought.

The inter-disciplinary and multi-disciplinary approaches are the only way to solve the complex problems that we will have to face. In his book, “El pensador intruso”, where boundaries between knowledge disciplines are explored, Jorge Wagensber wrote about the evolution

---

of science and the underlying progress as follows:

*Existen sobre todo dos vicios que tienden a inyectar ideología precocinada en la ciencia. Una de ellas se basa en las distintas formas de antropocentrismo y consiste en situar instintivamente al sujeto del conocimiento en el centro del cosmos. La historia del conocimiento es testigo: cada vez que barremos el Yo del centro del escenario el conocimiento avanza, y avanza sólo por ello.*

Despite of the character of most applied science about solving “just” humanity problems, a holistic approach to these challenges would undoubtedly lead to better, more sustainable and responsible solutions, clearly showing the limitations and consequences of our propositions. In a complex world, with complex societies and problems, answers must come from deep scientific reflection.

# Resumen

## Introducción y motivación

La transición energética en marcha y el crecimiento de la participación de las tecnologías renovables en el sistema energético, especialmente en el mix de generación eléctrico, han aumentado el interés por conocer las características espacio-temporales de los distintos recursos renovables. Esta demanda de conocimiento por parte de los sectores involucrados, ha crecido no sólo en las escalas temporales más cortas, necesarias en la operación y gestión de las plantas, sino también en las escalas temporales denominadas climáticas, que afectan a distintas etapas de su desarrollo como la planificación y la financiación. Es en el estudio y caracterización de estas escalas climáticas en lo que se sustenta la presente tesis doctoral.

Especialmente relevante es el creciente interés sobre la disponibilidad de los recursos bajo condiciones de cambio climático, los posibles cambios en su cantidad o variabilidad pueden afectar a la planificación futura y a la operación de plantas que sean proyectadas en el momento en el que nos encontramos. De igual manera, los resultados obtenidos pueden proporcionar información relevante para la elaboración de políticas orientadas al aumento de la participación renovable en el sector energético.

## Objetivos

El presente trabajo aborda el problema de variabilidad en escalas climáticas desde tres perspectivas distintas, dando a su vez respuesta a preguntas concretas en cada uno de los capítulos destinados a los resultados. Estos tres puntos pueden resumirse de la siguiente manera:

1. Estudio de la variabilidad interanual de la producción fotovoltaica y de su complejidad en la Península Ibérica a través de metodologías de clustering.

- 
2. Cuantificación del impacto de los aerosoles en la variabilidad espacio-temporal de la productividad fotovoltaica en el área Euro-Mediterránea.
  3. Evolución de las proyecciones de potencial fotovoltaico bajo condiciones de cambio climático en Europa.

## Resultados

El primer estudio [Gut+17], propone un método para analizar la variabilidad y complementariedad del recurso solar y de la productividad fotovoltaica en la Península Ibérica. El empleo de técnicas de clustering sobre la zona de estudio ha permitido encontrar una partición óptima de regiones (o clusters) a partir de la variabilidad, lo que facilita el análisis espacial, especialmente el de complementariedad. Un modelo paramétrico de producción fotovoltaica es utilizado para obtener la producción potencial en cada punto del dominio estudiado.

La zona de estudio presenta una variabilidad interanual baja, lo que la hace especialmente relevante para el desarrollo e integración masiva de tecnologías solares, existiendo aún así diferencias entre las distintas zonas. Además, se ha encontrado cierto grado de complementariedad entre ellas, lo que podría ayudar a la compensación espacial cuando la disponibilidad del recurso sea baja. Este estudio puede servir de base para futuros trabajos que estudien la complementariedad con otros recursos como el eólico, lo que facilitaría la gestión de la producción en un sistema con alta penetración de ambas tecnologías.

\* \* \*

En segundo lugar, dentro de los factores que originan la variabilidad tanto del recurso solar por un lado, como de la producción fotovoltaica por otro, el papel de los aerosoles es analizado mediante una cadena de modelado utilizando simulaciones climáticas y el modelo fotovoltaico paramétrico. A pesar de que la nubosidad es el factor que más impacta normalmente en la producción fotovoltaica, reduciendo la radiación directa que llega al generador, el impacto de los aerosoles puede ser muy alto en algunas zonas. Mediante el diseño de un test de sensibilidad, determinamos la variabilidad espacio-temporal que es consecuencia de los aerosoles en el área Euro-Mediterránea.

Los resultados [Gut+18] muestran una influencia importante de los aerosoles en el patrón espacial, el ciclo estacional y las tendencias de largo plazo de la producción. La sensibilidad de la producción anual es alta en la zona de Europa central y el tipo de seguidor del sistema fotovoltaico considerado es relevante en el cálculo.

En este aspecto, se concluye que los aerosoles no pueden despreciarse en la producción en escalas temporales largas. Además, el crecimiento potencial debido a una reducción de aerosoles antropogénicos se muestra mediante la simulación del periodo de 'brightening' ocurrido a partir de los años 80 en Europa. Los resultados ilustran la posible evolución de

---

otras zonas con alta contaminación y el potencial aumento en el recurso y la producción fotovoltaica.

Los resultados de este punto muestran además la utilidad los modelos regionales para estudios de sensibilidad y atribución concretos que pueden ayudar a entender mejor la variabilidad espacio-temporal de los recursos renovables.

\* \* \*

El tercer problema estudiado en este documento se centra en las proyecciones futuras en condiciones de cambio climático. La zona Euro-Mediterránea es evaluada para determinar los potenciales cambios en la radiación solar como recurso de la energía fotovoltaica y el impacto en la producción como consecuencia de ello. La influencia de los aerosoles, como factor determinante en las proyecciones propuestas con diferentes modelos climáticos regionales, es analizada con el objeto de determinar su papel en la productividad futura.

Para abordar este tercer punto, se parte del hecho de que las anomalías de radiación proyectadas en Europa por los modelos globales, GCMs, son de signo opuesto a la mayoría de las proyecciones de los modelos regionales, RCMs. En este aspecto, se ha analizado el papel de los aerosoles en las simulaciones de los modelos regionales como un factor determinante en el cambio proyectado de radiación solar.

Los resultados muestran que las proyecciones de los modelos regionales que incluyen la evolución temporal de aerosoles en los escenarios, coinciden en el signo con la anomalía proyectada por los modelos globales, es decir, proyectan un aumento del potencial fotovoltaico en Europa. La magnitud del cambio proyectado depende del modelo, con valores de más de un 10% para la productividad en verano para al menos uno de los modelos en la zona de Europa Central, lo que supone una información importante para los países involucrados.

Estos resultados suponen información relevante para la transición energética en marcha en muchos de los países de la zona, así como para el desarrollo de los servicios climáticos cada vez más presentes.





---

## Abstract

The ongoing energy transition and the growth of the share of renewables technologies in the energy system, especially in the electricity mix generation, have risen concern about the spatio-temporal characteristics of the resources. This knowledge demand from the involved stakeholders, has increased not only for the short-term time scales, but also in the climatic scales that affect to different stages of the renewables deployment and development. The interest about the availability of renewable resources under climate change conditions is especially relevant. The possible changes in the resource amount or its variability might affect the planning and future operation activities in power plants that are being projected at this time.

The present work is based on the study of solar resource and photovoltaic production over the Euro-Mediterranean area with a climatic perspective. The variability issue, that makes most of the renewable technologies not available by demand, is addressed from three different perspectives. At the same time, these three approaches give answers to concrete scientific questions in each of the results chapters.

In the first place, the interannual variability and complementarity of solar resource and photovoltaic productivity in the Iberian Peninsula is analysed using a multi-step scheme that includes a regionalization through clustering algorithms. The method allows to systematize intercomparison among zones inside the region studied.

Secondly, the role of aerosols in the spatio-temporal variability of the photovoltaic production is analysed for the Euro-Mediterranean area, which is highly influenced by aerosols from different sources.

Finally, future projections of photovoltaic energy are analysed under climate change conditions over Europe.

---

The three studies show that climate time-scales are also relevant in terms of solar resource and photovoltaic productivity and deserve attention for a better integration of photovoltaic energy in the energy system.



---

# Contents

<b>Contents</b>	<b>xv</b>
<b>Nomenclature</b>	<b>xix</b>
<b>I Introduction</b>	<b>1</b>
<b>1 Context and introduction</b>	<b>3</b>
1.1 A changing world . . . . .	3
1.2 Renewable Energy . . . . .	4
1.3 Photovoltaic Energy . . . . .	6
1.4 Links between climate and renewable energy . . . . .	6
1.5 Climate change and the Mediterranean area . . . . .	9
1.6 Organization of the document . . . . .	10
<b>2 State of knowledge</b>	<b>13</b>
2.1 Variable renewable energies: VRE . . . . .	13
2.2 Variability sources in PV . . . . .	15
2.3 Short-term variability . . . . .	18
2.4 From short to long term issues . . . . .	22
2.5 Future projections and trends . . . . .	28
2.6 Objectives and scientific questions . . . . .	31

<b>II Data &amp; Methods</b>	<b>33</b>
<b>3 Data</b>	<b>35</b>
3.1 Solar Radiation data . . . . .	36
3.2 Aerosols datasets . . . . .	42
3.3 Photovoltaic production data . . . . .	43
3.4 Other data . . . . .	44
<b>4 Methods</b>	<b>45</b>
4.1 Clustering algorithm applied to climate data . . . . .	46
4.2 Simulating a photovoltaic system . . . . .	50
4.3 Using Regional Climate Models . . . . .	55
4.4 Future projections and scenarios . . . . .	58
<b>III Results</b>	<b>61</b>
<b>5 Multi-step scheme over the Iberian Peninsula</b>	<b>63</b>
5.1 Introduction . . . . .	66
5.2 Data sources . . . . .	67
5.3 Methods . . . . .	67
5.4 Results . . . . .	73
5.5 Conclusion . . . . .	81
<b>6 Impact of aerosols on photovoltaic production</b>	<b>91</b>
6.1 Introduction . . . . .	94
6.2 Data and Methods . . . . .	95
6.3 Results . . . . .	100
6.4 Discussion . . . . .	111
6.5 Conclusions . . . . .	112
<b>7 Future projections of solar and photovoltaic potential in Europe</b>	<b>115</b>
7.1 Introduction . . . . .	118
7.2 Climate data . . . . .	119
7.3 Methods . . . . .	121
7.4 Results . . . . .	123
7.5 Discussion . . . . .	129
7.6 Conclusion . . . . .	129

<b>IV Discussion &amp; Conclusion</b>	<b>135</b>
<b>8 Discussion and Conclusion</b>	<b>137</b>
<b>9 Perspectives</b>	<b>141</b>
<b>Bibliography</b>	<b>149</b>
<b>List of Figures</b>	<b>181</b>
<b>List of Tables</b>	<b>184</b>





---

## Nomenclature

*AC* Alternate current

*ANN* Artificial Neural Networks

*AOD* Aerosol Optical Depth

*B(0)* Direct (beam) irradiance on the horizontal plane

*B<sub>0</sub>(0)* Direct (beam) extra-terrestrial irradiation

*B<sub>d</sub>(0)* Daily direct (beam) irradiation on the horizontal plane

*BSRN* Baseline Surface Radiation Network

*c* number of clusters where the 2 fit-lines split

*c<sub>j</sub>* Centroid of the cluster j

*CH* Calinski-Harabasz validity index

*CM – SAF* The Satellite Application Facility on Climate Monitoring

*CV* Coefficient of variability

*D(0)* Diffuse irradiance on the horizontal plane

*D<sub>d</sub>(0)* Daily diffuse irradiation on the horizontal plane

*F<sub>D,d</sub>* Diffuse fraction

*G(0)* Global irradiance on the horizontal plane

$G(\alpha, \beta)$  Global irradiation at the plane of the array. Alpha and beta correspond to the inclination and orientation angles of the panel

$G_{eff}(\alpha, \beta)$  Global effective irradiation at the tilted panel

$GCMs$  Global Climate Models

$G_d(0)$  Daily global irradiation on the horizontal plane

$GHG$  Greenhouse Gases

$I_m$  Intensity from the photovoltaic module

$I_{mpp}$  Intensity for the maximum power point from I-V curve

$IP$  Iberian Peninsula

$IPCC$  The Intergovernmental Panel on Climate Change

$I_{sc}$  Short circuit current

$J$  Objective function of the Kmeans clustering method: summation over euclidean distances

$k$  number of clusters

$k_i^o$  Coefficients of the efficiency curve of a inverter

$K_{Td}$  Clearness index

$NAO$  North Atlantic Oscillation

$NWP$  Numerical Weather Prediction

$P_{out}$  Power output from the photovoltaic module

$P_{inv}$  Nominal power of the inverter

$p_o$  Normalized output power of a inverter

$POA$  Plane of the Array

$PV$  Photovoltaic.

$R(0)$  Albedo component

$RCMs$  Regional Climate Models

$RMS_{left}$  Root mean squared error of the left-side linear regression

$RMSE_{right}$  Root mean squared error of the right-side linear regression

$RMSE_T$  Total root mean square error

$RTM$  Radiative Transfer Model

$SSR$  Surface solar radiation

$T_a$  Ambient temperature

$T_c$  Cell temperature

$TMY$  Typical Meteorological Year

$TOA$  Top Of the Atmosphere

$TSO$  Transmission system operator

$V_m$  Voltage of a photovoltaic module

$V_{mpp}$  Voltage for the maximum power point from I-V curve

$VRE$  Variable Renewable Energies

$V_{oc}$  Open circuit voltage

$x_i$  Each point in the cluster, where the point is a vector with elements comprising the daily irradiation time series values at a pixel obtained from satellite images



## **Part I**

# **Introduction**



## CHAPTER

# 1

---

## Context and introduction

*"Begin at the beginning," the King said gravely, "and go on till you come to the end: then stop."*

— Lewis Carroll, *Alice in Wonderland*

### 1.1 A changing world

It is said that nothing is permanent except for change. We are in a constantly evolving world where, unavoidably, some of these changes will occur without us being able to adapt to them. Meanwhile, other changes will go unnoticed because of their slowness or because they are not part of our main concerns. It seems paradoxical to think that some of those human induced changes, consciously or unconsciously, willingly or by mistake, will make human beings resist and get adapted as a species against the consequences of something that they themselves created.

The evolution and development of nations has been linked since the first Industrial Revolution to an increment of the energy demand. The use of fossil fuels since the vapor engine has changed the well-being of societies. Related to this increase, the greenhouse gases (GHG) emissions and their concentration in the atmosphere has risen dramatically in contrast to pre-Industrial times. Global warming, with its origin in human activities, is one of the biggest challenges of adaptation for human beings.

The *anisotropic* character of the associated impacts of climate change puts our solidarity with the most vulnerable and less responsible communities on the test.

Some people believe we are in what has been described as the Third Industrial Revolution [Rif12], a process of exponential scientific-technological development, characterized as a convergence of the evolution of renewable energy technologies and the massive use of new communication technologies. The ongoing energy transition should be the answer to committed citizens that find those technologies as an alternative and an answer to the environmental challenges and associated consequences.

The actual context is characterized by an advanced globalization where borders have been blurred through the development of telecommunications and more feasible international migration movements. In 2015, there were 100 millions more people living in a different country from its birth country than in 1990 [Mig18]. Most of those movements are related to work opportunities or family issues. However, the increase in population and the rising demand for natural resources to support a system based on the continuous growth, lead to geopolitic conflicts and the depletion of natural resources [RD12; Com91], meaning an increase in migration movements of different character. Populations migrate away from conflict areas or most affected areas by natural disasters [Mig18]. In that sense, these movements affect most vulnerable people and require special attention.

In order to address the human needs in a juncture of population growth, increase of energy demand and environmental crisis, a paradigm shift is needed. This change would mean recognizing the importance of nature itself and recognizing our interdependence with every ecosystem. In 1962, Thomas Kuhn wrote in his book "The Structure of Scientific Revolutions" that a paradigm shift does not occur until the adherents of the old paradigm are replaced with the new generation. We should then wait to see the end of this paradigm shift hoping that it is not too late.

### 1.2 Renewable Energy

In the context of energy consumption in societies we call **primary energy sources** those from whom, after a process of extraction or transformation and transport, we are able to obtain final energy to be used. Regarding that, we consider fossil fuels as a primary energy source, as well as hydro-power, solar energy or biomass.

These primary energy sources can be classified depending on their origin, being **renewable** those ones that are inexhaustible. The sun, despite of its unquestionable finitude is considered inexhaustible as well, because of the difference in the temporal scale of human existence and the life of such star, which is several magnitude orders above.

### 1.2.1 History and evolution

The use of renewable energy has come along with development of humanity since ancient times. From the use of biomass to get thermal energy to the transformation of wind energy into mechanical energy to be used in the traditional windmills or for shipping. It was around the middle of the 19th century, with the invention of the vapor engine that fossil fuels started to be used massively and linked to that occurred what was called the *First Industrial Revolution*. This period meant a big technological development that directly impacted positively on the well being of society, at least to those from the richest or western countries.

This economic development brought about an increase on the fossil fuels demand that grew up exponentially during the 20th century. Societies were more and more dependent on energy and evolved turning a blind eye to the reality that the base of their development were finite resources unequally distributed around the globe.

The first step to diversify sources of primary energy did not take place until the 70's, with the first petroleum crisis in 1973 (and the second crisis in 1979) [Sør91]. The embargo of the petroleum producer countries had some important economic consequences on the importer ones, resulting in the fact that some of them started to consider new sources of energy in order to ensure stability and supply.

In the last decades, in addition to the socio-economic and geopolitic factors that have led to the need of limiting petroleum dependence from importer countries, the stimulus for the big increase of these alternative technologies, has come about due to their decreasing costs, which have its origin in the promotion of support policies. These policies have been upheld by different organisms and governments that have created a virtuous cycle around these technologies. The decrease in costs thanks to the support and long-term view policies favors, at the same time, more national target commitments in the use of renewable energy to reduce greenhouse gases, GHG, emissions and to fight against Climate Change. In 2017 more than 170 countries had established goals of renewable generation [Age17]

In the actual context, the global energy demand is growing based on the needs of developing countries. It has been estimated that for 2040 it will be up by more than a quarter and it will have an associated shift from Europe to Asia, which will account for 40% of the energy demand (led by China) by that time [Age18].

Energy systems account for approximately 3/5 of all anthropogenic greenhouse gases emissions [Age18] which force us to find the way for a sustainable development that is able to cover human needs. This, unavoidably needs a decarbonization scenario in the following years.

In 2018 renewable energies account for the 18.2% of the **final energy consumption** according to the *REN21* report [REN18], with a share of 27% in heat generation and 25% for electricity generation. Transport remains the sector with less share of renewable energies with only a 3%. These numbers, reflect that contribution of RE to the mix is continuously growing, with increasing relevance in the electricity sector.

Future scenarios continue to project an increase in the energy demand with an overall decrease of the fossil fuel's share. At the same time, it is expected that the power sector will increase its share in the final energy consumption distribution. According to that, renewable energies and especially solar and wind are key for delivering low carbon electricity [Tro18].

In 2017, the renewable capacity added was about 178 GW, accounting for the first time for more than 2/3 of global net electricity capacity growth and it was the PV the one that expanded the most with 97 GW [IEA].

### 1.3 Photovoltaic Energy

Among all the renewable energy technologies that had started to increase their installed capacity all over the world, the photovoltaic (PV) energy has been the one with higher ratios of installation in recent years and bigger rates of decreasing prices (80% since 2008 [Age17]). Based on the completed projects in 2010, the leveled cost of energy, LCOE of PV projects fell 73% between 2010-2017 [REN18].

It has been mentioned that in 2017, RE had its largest annual increase of generation capacity [REN18], 178 GW, from which 55% correspond to PV energy. It means that more capacity from solar PV than for any other technology was installed. Nowadays, the total amount of solar PV capacity reaches 402 GW.

It is also forecasted that the PV capacity can grow by 600 GW more, which is more than the projected increase for any other technology combined. Within this framework, China would lead the PV installations, as it happened in 2017 when from the 97 GW of added PV capacity more than a half were installed there [REN18].

### 1.4 Links between climate and renewable energy

The energy sector and in particular, the electricity power sector is highly dependent on the state of the atmosphere. For renewable energy technologies, the amount of resource available at each time determines the final energy that can be generated. In addition, the meteorological conditions impact on the electricity demand most notably in extreme events like heatwaves or cold spells.

The energy market and different stakeholders, as well as the need of keeping balance between supply and demand, requires an accurate and high resolution meteorological information in order to predict the amount of energy that can be generated with each technology.

In addition, meteorological conditions also affect indirectly in other aspects. For instance, the maintenance and operating activities in an offshore wind farm are a complex process due to the accessibility of the wind turbines. To know beforehand the weather forecast is necessary in order to plan the activities and avoid the risk exposure of the employees.

Although the short-term activities are in the core of the operational side of a renewable energy project, there are also some stages that require the study of longer temporal scales. Firstly, in order to establish the suitability of a renewable power plant, it is necessary to develop a resource assessment phase or potential assessment phase. This allows the owners to estimate the maximum power output of a project depending on the meteorological conditions and assess the amount of energy that they will be able to produce, what becomes important in order to finance the project.

The term bankability makes reference to the suitability of a project for being profitable and reliable to be financed. In order to determine that, long term information about the resource is considered in renewable projects. Bankability [Vig+12] of a project depends on two main factors: in the first place the availability of the resource and in the second place the benefits obtained from the project. Benefits depend on the operation time and the amount of energy supplied during the lifetime of the project. Due to that, an accurate assessment, not only of the available resource, but also of its variability and trends, is necessary.

The relevance of the seasonal and sub-seasonal scale for the operation and maintenance of power plants has to be noticed. The improvement in the climate forecast on these scales will impact directly on their activities and will help the TSOs (Transmission System Operators) and market operator in the management activities. For instance, knowing in advance if next Autumn is going to be especially rainy, will help to assess the amount of electricity that can be produced with hydro-power plants, making the system more reliable and efficient.

#### **1.4.1 Climate change and the energy sector**

In a global warming context, the link between energy and climate has usually been related to the impact that a big share of renewable in the generation mix can cause regarding the possible reduction of GHG in this way. However, the fact that climate change can cause at the same time variations in the availability or distribution of the

resources, as well as in the electricity demand patterns, should be taken into account and thoroughly researched.

One of the associated problems to the possible medium to long-term changes in renewable resources, like wind patterns, is the possibility of profitability loss of some projects that are now in the final stage of their lifetime. Repowering of these projects with upgraded technology, like the replacement of old wind turbines by new ones with larger nameplate capacity or more efficient, is one of the options for the power plants installed almost two decades ago [RCI11]. Changes in the resource can alter the conditions of the project because of the turbines used and because of the availability of the resource.

In addition, the rising temperature due to climate change can directly affect the energy generation and infrastructure in different ways. For the conventional power plants, that increase in air temperature means a decrease in their conversion efficiency as well as some problems related to their refrigerating activities [BC15].

The projected increase in extreme events also have potential hazards and risks for the industry that have to be considered. One example is the increase in the temperature of the river flow due to the above normal air temperature in a heatwave episode, which are projected to be more frequent and severe [Tro18]. That increase can affect the nuclear power plants operations, because the impacted plants are not able to use the river for their refrigeration purposes [Tro18; FS10]. Also, the more frequent drought events impacts hydropower generation directly.

The energy infrastructure can be also affected by the rising temperature. The exposure of air transmission lines to higher temperatures impacts their capacity. In addition, under extreme events they can be damaged in rainfall episodes or extreme winds [Tro18].

### 1.4.2 Climate services

Due to the intrinsic characteristics of renewable energy resources, related to their high space-time variability and the potential impacts on the energy sector mentioned above, there is an increasing demand for information about climate forecasts, projections and hazards. Although the energy sector is one of the most interested actors in the development of an operational system of climate information, there are also other sectors that would benefit from that, like agriculture or tourism.

This increasing demand for predictions and climate projections from different sectors, has led to the development of the climate services, in order to systematize, to organise and to target the information for different stakeholders [Tro18].

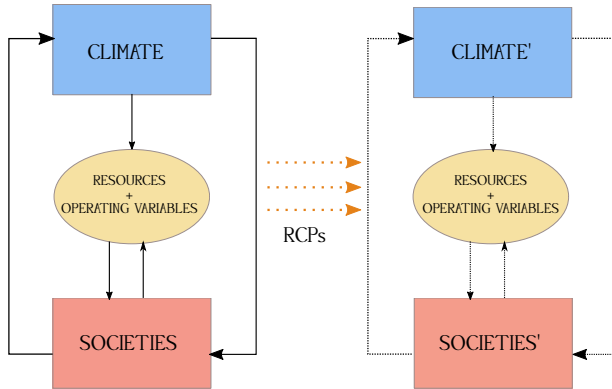


Figure 1.1: Scheme: conceptual representation of the relationships between climate, energy sector and societies. Left side of the scheme represents actual conditions and right side is the future relationships after the evolution following a RCP scenario.

From the renewable energies side, climate information is especially relevant for strategic decisions, evaluation risks, planning and trading operations. As can be seen in figure 1.1, interaction processes between society and the variables involved in the energy generation are two-way relations. On one hand, the energy supply would depend on the availability of the resources and constraints due to climate change; and on the other hand, demand is directly influenced by those factors. Due to that, development of climate services should be based on the improvement of the models and the offered products considering the two sides.

## 1.5 Climate change and the Mediterranean area

The climate system has varied constantly and significantly throughout the Earth's history. Climate variability can be explained due to external factors and the response of the climate system or, on the other hand, due to the internal instabilities and non-linear relationship between different components of the system, occurring the last ones with independence of the external forcings.

External forcings can be astronomic factors, like changes in the intensity of solar radiation or in the orbital parameters, or they can be terrestrial factors like changes in the composition of the atmosphere due to human activity, changes in the Earth's surface due to land use, etc.

Since the Industrial Revolution the Earth has experimented an increase in the global temperature that cannot be explained due to natural external forcings like changes on solar activity or volcanic emissions [Bin+13], neither can it be explained as part of

the internal variability of the system. The IPCC in its last report, assures that human activity and more precisely, GHG emissions generated since 1850 are responsible for the climate change that causes the increase in global temperature and this might have caused that the last 30 years between 1983-2012 have been the warmest in the last 1400 years in the northern hemisphere (IPCC). In spite of the large interannual variability, the global character of the temperature increase in the last decades is clear [Sto+13].

Despite the fact that climate change is a global concept, its consequences and impacts are perceived in a local and regional scale. These hazards and impacts affect communities and population unequally depending on its vulnerability, adaptation capabilities and resilience. Due to that, the socio-economic response to mitigate climate change impacts has to be applied in that scale despite the need for a consensus on the urgency and some common compromises.

One of the first works on quantification of climate change impacts in a regional scale was the one published by Giorgi in 2006 [Gio06]. They used an index for the first time, RCCI (Regional Climate Change Index), to measure and compare geographically the climate sensitivity of different areas to climate change. The conclusion of the research showed the Mediterranean area as one of the most affected areas in terms of climate response to climate change, and since then it has been referred to as a climate change hot-spot.

The climate models project scenarios in which the main consequences of global warming in the Mediterranean area are a generalized decrease of precipitations (with the exception of some areas like the Alps) [Gio+16], due to an increase in the anticyclonic circulation, that is associated with a northward shift of the Atlantic storm track [Yin05]. An increase in interannual variability of temperature and precipitation is also projected, mostly in the warm season [GL08; Pla+12]. In terms of extreme events, less frequent but more intense precipitation events are projected [Dro+18] and with respect to temperature, some authors have evaluated the probability of an increase in heatwaves over the Mediterranean area [Mee04; FS10]. All these climate perspectives should be considered in order to plan and prepare the adaptive capacity of the region.

## 1.6 Organization of the document

This thesis is organized as follows:

The **first part** of the text contains two chapters: the first one is the previous **Introduction**, that aims to introduce the context in which the thesis has been elaborated. In

the second chapter, **State of knowledge**, there is an introduction on the main contributions related to this topic over the literature. It includes a general overview about intermittency of PV and how the short-term problems have been managed. After that, the long-term problems and the main contributions about this topic over the area are reviewed.

The **second part** is composed by two chapters including the **Data** description and the **Methodology** used along the studies. It is important to remark that each results chapter has its own 'Data and Methodology' section used for the specific chapter. The contents of this *part II* are related to general description of ground stations, satellite, climate data and models as well as general methodologies.

The **results** are presented in the **third part** of this document. There is a different chapter for each of the main aspects investigated here and described in the above section. The organization of this chapter has been adapted from the journal papers where these results have been published.

Finally, the **fourth part** contains a chapter with an integrative **discussion** of the results previously presented and the main **conclusions**. This section also summarizes the main questions emerged from the work, which will lead future research.



---

## State of knowledge

*"Commençons par les systèmes les plus simples et les plus faciles à cerner pour monter graduellement à la compréhension des plus complexes."*

— René Descartes, *Le Discours de la Méthode*

### 2.1 Variable renewable energies: VRE

The variable nature of renewable energy resources, in space and time, is a key aspect for their high penetration into the conventionally designed electricity systems. Due to the requirement that supply and demand have to match at every time-step, the forecast and management of the generated electricity is needed for accomplishing this match, which becomes more difficult in the case of variable renewable energy (VRE) plants.

In the traditional electricity systems, a portfolio of centralized power plants (coal, nuclear, gas...) dispatches electricity as the customer loads demand it. The conventional power plants are able to store the primary energy that they use and produce electricity only when it is needed. With the increase of renewable power plants, mostly wind and solar, the supply of electricity demand approach has changed. The VRE power plants only produce electricity when enough resource is available and in the case of

photovoltaic power plants, only during the daylight time. This concept is referred to as **intermittency**, to recall the fact that solar and wind resources are not available at any time and that they are variable by nature. Nevertheless, there are renewable power plants that are able to provide energy by demand, like biomass power plants or hydropower (with some restrictions in drought events). They are dispatchable and can operate as conventional thermal power plants.

Due to the rising penetration of the non-dispatchable power plants (wind and solar) the management and the operation of the system has to be adapted. However, the alternatives for energy storage for VRE plants are increasing in different ways: batteries for wind and photovoltaic power plants, hydrogen or pumping hydro-power [Lun+15; BF18; SMH04], which favors the integration of the alternative energy sources.

Research in storage for VRE is rising but different approaches are also being adopted to integrate high share of this alternative technologies. The term **flexibility** is one of the most used referred to the new strategies followed from demand and supply sides in order to adapt to the new system [Kro17]. From the demand side, flexibility refers to means related to load shape and demand patterns, like peak shaving, load shifting, valley filling etc [Lun+15].

On the other hand, flexibility of the supply side depends on the power plants, whose output can be controlled to obtain power balance. It is important in terms of flexibility to consider the response time of different power plants as well as the different nature of each one. As the availability of solar and wind resources is not related to the geographical distribution of the demand, a highly interconnected grid is one of the main needs for a high penetration of VRE. Once this is considered, geographically spread portfolios of VRE plants are able to smooth variability of power output [Kro17; Mar+12; HP10; HP12]

There are also studies that try to identify complementary features of different energy resources, either in time or in space, in order to address the intermittency issue through the smoothing of the total power output. The complementarity studies are made using different technologies like hydro-power and wind power [DDCC09; Sil+16] or hydro-power and solar photovoltaic [Fra+16; BKK12; Kou+16]. In [HR11] complementarity of wind and solar is investigated for a region in Canada and also in Italy [Mon+14]. In addition, over the Iberian Peninsula [SA+12; Jer+13a] and Great Britain [BT16] it has also been investigated from a more climatological approach. A recent study also shows the complementarity of wind and solar over Europe for future projections [Jer+19].

As much as we were able to forecast the variability of solar/wind resources in the short term and to characterize the resource in the long-term for projections, better flexibil-

ity measures and strategies could be applied to integrate high rates of VRE without compromising reliability and efficiency.

## 2.2 Variability sources in PV

It is important to notice that every power system has associated an inherent variability and uncertainty, as a non-exclusive characteristic of a renewable energy system. In the case of PV systems, the variability of PV outputs depends on two items: in the first place, it depends on the variability linked to the solar irradiation reaching the generator (resource variability), and secondly, it also depends on the behavior of the electrical components.

Solar radiation varies in multiple time-scales, from seconds to multi-decadal variations, as well as spatially, affecting PV production. For the operating activities in PV plants, an accurate forecasting of solar irradiation, which means being able to reproduce its short-term variability, leads to better forecasting of the PV output, demanded by TSOs and used for trading. On longer time-scales, understanding variability features improves the projection of the PV output for a period of time: seasonal, year-to-year produced energy, multi-year trends or climate change projections. That helps in the plannification, the strategy, the financing activities, and can influence the policy-makers' decisions.

Different factors are responsible for the variability of either solar resource or the electrical components of the PV generator and affect them across different time and spatial scales.

### 2.2.1 Astronomical factors

The amount of solar energy that reaches the photovoltaic generator depends on the first place on the sun position with respect to the orientation of the PV panels, which is a deterministic factor that only depends on the time of the year, the time of the day and the relative position of the generator surface. It means that the first factor causing PV intermittency is the fact that no energy can be produced during nighttime. However, although this daily scale intermittency is the one that affects the PV power production most, there is no uncertainty associated to this fact, which is a very important concept in order to manage VRE.

### 2.2.2 Atmospheric factors

#### Clouds

There are other factors that reduce the amount of solar energy reaching the surface and their influence depends on the composition of the atmosphere at each time. When solar radiation goes through the atmosphere it can be reflected, absorbed or scattered. The presence of clouds is the most affecting factor in the transmission of solar radiation to the surface. The condensed particles that form clouds scatter and reflect solar radiation and part of it can also be absorbed. Different types of clouds affect solar radiation differently[Pag12]. High thin clouds are less dense than low clouds, becoming more transparent to solar radiation [KC80].

For partially cloudy skies, solar irradiance (direct component) can drop in seconds [Pag12] due to clouds. In overcast periods, short-term variations depend on the type of clouds.

Low frequency changes in cloud cover for large areas are related to changes in large scale circulation patterns, which are linked to changes in solar resource for those places [CW10; San+09].

#### Aerosols

Aerosols is the term used to refer to the solid particles suspended on gas. In this work we are referring to the atmospheric aerosols, which are the solid particles suspended on the atmosphere but the hydrometeors like ice crystals [Bou15]. In the absence of clouds, aerosols are the main source of variability for solar resource.

Aerosols impact solar radiation in two ways: directly, scattering, absorbing or reflecting solar radiation or indirectly, acting as condensation nuclei favoring the formation of clouds [Bou15]. They can be classified depending on its source origin. Natural sources emit aerosols from oceans, wild fires and vegetation, whereas anthropogenic sources emit aerosols from industrial activities, burning fuels and human-caused fires.

Aerosols vary greatly in time and across space [KTB02]. Despite of the aerosols' relatively short residence time in the atmosphere (of the order of hours to weeks), they have a strong influence on climate through their impact on the radiative budget and clouds [Nab+14; Nab+15]. Aerosols from natural sources, like airborne dust, which last some days, have a very strong seasonality, affecting regional and continental scales periodically. Also, due to the relationship between aerosols and human activities, long time cooling trends have been detected in China in the last decades related to the

increase in aerosols optical thickness [Gio02] and other studies had shown the relationships between the “dimming” and “brightening” periods and the anthropogenic aerosols emissions [Wil05; Wil12; Wil09].

### 2.2.3 PV system factors

#### Spatial aggregation

There are two factors related to the spatial dimension that influence the photovoltaic power variability:

- Power plant size: a PV power plant acts like a low-pass filter for short fluctuations, which means that higher frequencies of power fluctuations (less than a minute) from the PV generator are smoothed as a function of the PV plant size [PL11; PML13].
- Distance between power plants: on the other hand, it has been also concluded that for a fleet of dispersed PV plants, short-term power output fluctuations are attenuated. Some authors observed that short-term fluctuations are essentially uncorrelated for distances between PV plants over 6 km.[OMK97; Wie+01; HP12]

#### Other factors

As it has been noted at the beginning of the section, there are other factors that affect the performance of a PV system, causing variations in the power output. These factors are related to the electrical components of the system and they can be divided into internal and external factors.

The most important external factor affecting the PV system is **temperature**. It affects cells performance and if temperature is highly different from the optimum cell temperature the efficiency will drop. Also some external factors like **dust deposition** and **soiling** can affect the electrical performance, limiting the energy reaching the cells [Fan86; MSK12; DSS13].

Internal factors affecting the PV output that can cause variability are related to the transmission lines, wires and interconnections, or the inverter, whose functioning is not always constant and can present variations.

## 2.3 Short-term variability

From the different factors that influence variability of PV power production, it can be followed that variability studies can be made from the solar **resource** point of view or from the **power** variability side [Wid+15].

### 2.3.1 Resource Variability

The research of short-term variability from the resource perspective, started with the research on the characterization of solar irradiation at the surface. Those studies had the objective of the statistical modeling of solar irradiation behavior at the Earth's surface in short-term time scales [LJ60]. Others, were motivated by the solar energy development and the need for characterizing the resource for a better performance of the PV plants [CPR79]. In that sense, variability studies have been generally focused on local aspects.

For different operation activities, forecasting the amount of energy fed into the grid from a PV system or plant, is essential in order to manage the associated photovoltaic power production intermittency. In order to accomplish that, it is needed, in the first place, to forecast the amount of incident solar energy on the photovoltaic generator and secondly, to model the system's behavior in order to forecast the AC produced.

#### Solar irradiation forecasting

There are different types of forecasting methods for solar irradiation. There are two different approaches: **physical methods** and **statistical methods**. Physical methods are based on the radiative transfer equation and physical variables whereas the statistical or empirical methods are based on historical data.

The application of each kind of forecasting models is closely related to the **forecast horizon** that wants to be addressed, as well as the horizontal resolution. In the operation activities, 3 time forecasting horizons were described by Kostylev and Palovsky [KPO11]: intra-hour, intra-day, day-ahead. For other activities like trading, the day-ahead forecast is very important as well as for planning operations. The statistical approach is applied in shorter scales whereas the physical approach has been proved to have a better performance for longer time scales [Per+10; Dia+13; Wid+15].

- Physical Methods

The physical modeling of solar radiation is based on physical equations of the interaction between atmospheric components and solar radiation (aerosols, water vapor, clouds...). When solar radiation goes through the atmosphere, it

can interact with its components being absorbed by molecules, back-scattered to space or scattered in any other direction. Thus, only part of the solar radiation at the top of the atmosphere (TOA) will reach the Earth's surface.

This process is the physical process of energy transfer described by the radiative transfer equation (RTE) and its solution needs a radiative transfer model (RTM). The radiative transfer is a very complex process that needs to be simplified to be solved numerically and some parametrizations are needed. However, from these models it is possible to reproduce the solar radiation behavior across the atmosphere and at the surface. RTMs are in the core of numerical weather prediction models, NWP, and climate models and sometimes they are used to obtain solar radiation from satellite images, although in this case empirical or semi-empirical approaches are also commonly applied.

Numerical weather prediction models are very useful for intraday time horizons larger than 4h [Per+10]. It is very frequent to apply a post-processing process to the output of NWP that enhances the forecast. Some statistical tools like bias correction can be applied to reduce some systematic errors or local effects [Dia+13].

- Statistical methods

Solar radiation on the surface can be estimated also using statistical methods. In this case it is necessary to have enough accurate historical data to create and validate the model and these models will unlikely be able to reproduce solar behavior universally. However, they can be very useful for local applications and at very high time-resolution.

On these methods traditionally used to forecast time-series, relies the idea of predicting some variables through the statistical analysis of historical data and its relationship with other variables called predictors. Many models have been developed in this sense from the most simple approach, the persistence model or autorregressive models, to more sophisticated ones [Rei09; BMN09; IPC13]. Also, with the development of the ANN (artificial neural networks), these models have been additionally applied to the solar forecasting field [QR+15], with their predictions based on a learning algorithms [MK08].

- Hybrid methods

It is very common to apply a combination of more than one model to enhance the prediction accuracy. Many studies have shown the overcome of a combination of two different approaches with respect to a simpler approach [KI16;

Yan+14]. For instance, some studies show the application of ANN methods after the obtention of NWP output [CPB15] or after obtaining a satellite-based model output [MPC13; QR+15]

Different models are applied depending on the forecast horizon. A summary of different methods for solar irradiation can be found in the figure 2.1, which also includes the wind and wave forecasting. For shorter periods, statistical methods are preferred to derive solar irradiation from satellite measurements. As the time horizon increases, the NWP models are used to forecast irradiance.

### Aerosols in solar irradiation forecasting

Although clouds are the main driver of variability of solar resource, under cloudless conditions, aerosols reduce the amount of solar energy reaching the Earth's surface. Some models compute solar irradiance in clear sky conditions, which means that they calculate attenuation of solar irradiation only due to the constituents of the atmosphere. Many clear-sky models have been proposed on the literature [Gue12]. The difference between clear-sky models is based on the parameters used to predict solar irradiance. The most simplest ones only consider the zenith angle and extraterrestrial irradiation. The higher the complexity of the model, the more parameters are included to characterize the state of the atmosphere: different aerosols content, water vapor etc. Performance of these models depends on the parametrizations of each model and the knowledge of the atmospheric composition.

These models are commonly used to derive solar irradiation from satellite observations (see chapter data). As satellites are able to give observations of the cloudiness at

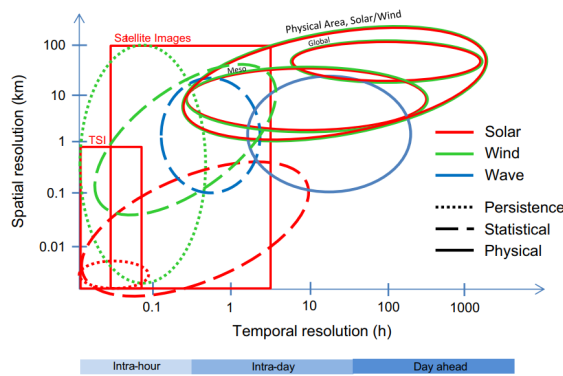


Figure 2.1: Models to forecast irradiance, wind and waves, depending on the time horizon from [Wid+15]).

---

a given time and site, the use of a clear sky model in combination with these observations makes it easy to establish a relationship between the cloud index and the clear sky index. The role of aerosols input in these satellite-based methods to derive solar irradiation has been investigated in [Pol+14].

On the other side, under high loads of AOD, NWP usually presents a systematic bias in solar radiation forecast [Rie+17]. This fact is due to the design of the models that normally use climatological values for the representation of aerosols with spatially and temporally homogeneous concentrations. This fact led to an overestimation of solar irradiation in the dust outbreak of 4 April 2014 in Germany, which caused significant economic losses [Rie+17].

### 2.3.2 PV variability

#### PV power forecasting methods

Once the solar radiation is either modeled or measured, the AC output from a PV system can be modeled following two main principles [APN15]:

- Parametric models
- Nonparametric models

In the first place, **parametric models** are a set of equations that model each step of the electricity generation: decomposition of solar irradiation in different components, its transposition to the tilted panel of the generator, the behavior of the PV generator and the inverter to finally get the electricity output. The advantage of this type of models is that they can be applied independently to each location. This approach has been used by many authors [Bof06; Lor+10; Lor+11] with differences in the sub-models applied in each case.

The **nonparametric models**, on the other hand, consider the whole PV system as a black box and only takes into account the input data (variables as solar irradiation and temperature) and historical output data, developing a statistical model from the measured values. The constraints related to this approach is that this method can only be applied when the historical time-series are long enough to be representative of the PV plant [BMN09].

#### Smoothing effect

Variability of PV production from an individual power plant or from a cluster of them, can be approached from the perspective of what is called “smoothing effect”. This

refers to the before mentioned factor that affects variability, the spatial aggregation of the considered units. Whereas the power output of a PV system varies highly in time, the power time series of a group of inverters spatially dispersed is less noisy than the individual series. The same could happen to the aggregation of PV power plants allocated in different places. Therefore, intermittency can be addressed from the study of these two factors:

- Generator size
- Distance between power plants

### Aerosols

The impact of aerosols on photovoltaic energy production has been also studied from the power side. In the short-term, some extreme events like dust outbreaks have been analyzed, due to the impact on a daily basis that they have on PV production. Some authors have seen reductions of PV production in semi-arid regions up to 48% , like the Sahel zone [Neh+17]. For the western Mediterranean, the impact of two extreme events of high loads of dust on the one side and smoke on the other were studied and they showed a reduction of 34% for smoke and 6% for dust on daily averages [GA+19]. For larger areas, the impact of an extreme event in April 2014 over Germany, shows that aerosols could reduce PV production in a country causing large economic losses if these events are not previously forecasted [Rie+17].

## 2.4 From short to long term issues

Despite the variable behavior of surface radiation in the short-term, there was a belief that solar radiation was stable in longer time scales. However, relatively recent observational evidences has shown that variability of solar resource is also present in longer time-scales with substantial changes. For solar energy applications, these long-term changes can affect different stages of the projects, from feasibility to finance, and they can also have an influence in strategic decisions from some stakeholders like operators and policymakers.

It deserves to be mentioned, that at the same time that frequency of time variability decreases, the horizontal extension in which different patterns can be observed, expands [Eng+17]. That is because lower frequency changes in solar resource (and other renewable resources linked to atmospheric conditions) are most of the times related to large-scale atmospheric patterns that affect a larger geographical area. On the contrary, short-term frequency changes, are related to weather regimes as well, but are

affected locally by specific conditions like the transition of clouds. That means that for longer time scales, not only individual PV projects are the target of the analysis, but also an overall study of bigger areas can arise from it. For instance: developing strategies for deploying renewable energies in a country, the analysis of the portfolio's variability of a company, future strategies related to trends and low frequency variations, etc.

### 2.4.1 Solar Resource Variability

From the resource side, much of the research in long-term variability of solar irradiation has not been focused on its application for solar energy. Long-term variations in solar irradiation have been studied because of its main role in the Earth's energy budget [Wil12], which is key to understand the climate system and its variability. First observational studies about surface solar radiation, SSR, started in the early 90s [Ohm+98; Dut+06] when the first results of monitoring solar radiation arised from different stations around the world.

Since then, the stations network and observational research have increased, although the density still remains scarce in many places around the world. The use of satellite data since the 80's in order to address the uncovered areas has helped, despite the fact that surface solar radiation cannot be directly measured from satellites.

Over time, more solar radiation research has been oriented to application for renewable energy, focusing on variability in seasonal to interannual scales related to large-scale circulation modes and teleconnections across different areas [DT12; Jer+13b; JT13]. In addition, some recent studies have focused on the impact of resource variability into practical stages of solar projects and its relation to the risk analysis [Bry+18].

#### **Large-scale circulation modes**

From **seasonal** to **interannual** time scales, local or regional climate is the main driver of solar irradiation variability. Regional climate variability is partly due to patterns of variability (modes) of the atmospheric circulation. These *modes* are the dominant spatial patterns and their temporal variation also accounting for teleconnections. Teleconnections are the mechanisms that are able to describe climate links between geographically separated regions.

Climatic variability of surface solar radiation over the **Euro-Mediterranean** area has been associated to large-scale circulation patterns in several studies [JT13; CW10; San+09; PV+04]. This large-scale modes, are drivers of cloudiness patterns, which consequently influence variability of solar irradiation.

The **North Atlantic Oscillation**, NAO, is the variation in the pressure differences between the Azores' High and Iceland's Low. This difference has an associated index, whose sign, positive or negative, determines if the difference is lower or higher than the mean difference in time. The former, causes the midlatitude storm track to affect southern Europe, which means more clouds in the south, whereas the latter, increases the difference between the High and Low systems, shifting the storm track to northern Europe. These changes in cloudiness associated to the NAO phase are therefore, associated to changes in surface solar radiation.

A dipole pattern has been described for the correlation between the NAO index and sunshine duration measurements [PV+04] over Europe. The maximum of the dipole is found over the Iberian Peninsula for the positive phase and the minimum over Norway. Anomalies of sunshine duration over IP have been reported to be around 10-20% for the positive phase and -20 to -30% for the negative phase. The interannual variability of wind and solar irradiation over the Mediterranean area is highly influenced by the NAO [PV+11].

Another study analyzed solar, wind and hydropower resources for the Iberian Peninsula and its relationship with different large-scale modes: NAO index, Scandinavian (SCAND) and East Atlantic (EA). Only the NAO had a significant impact on the **inter-annual variability** of the resources. In the case of solar radiation, a strong correlation is found between the index and the monthly time series [JT13] showing significant results from October to March.

In order to characterize interannual variability of some regions with a comparable metric, the coefficient of variability has been used in different studies across different regions. One of the first efforts to characterize not only interannual variability but also spatial variability was made by Wilcox [GW11], where the CV was identified for individual sites among the State of Washington finding variations from low to high (15%) interannual CV.

In the Euro-Mediterranean area, different works have evaluated interannual variability of solar resource through the CV. However, due to the lack of dense network with long-term observations of solar irradiation over the same area, some authors have analyzed the interannual variability through the sunshine duration measurements [Gil+15]. In that study, the **coefficient of variability** is used to quantify interannual variability over the IP, showing in general a quite stable solar resource, with differences among the stations.

### Low frequency changes

The studies of low frequency changes of surface solar radiation started with the analysis of the observed long term series from stations as mentioned before. These studies were the first on detecting a decrease in SSR between the 50s and the 80s. Following studies have referred to these multi-year variability as periods of “dimming” and “brightening” [Wil12]. These trends and low-frequency changes in SSR have been evaluated extensively through the literature from observations, with a modeling approach and through satellite observations [WHD13; Wil05; Wil09; San+09; Mat+14; Pfe+18a].

A decline in surface radiation, the **dimming** period, was observed from the 1950s to the 1980s in regions from USA, Europe, China, Japan and India. Since then, some studies have shown a reverse in that trend, a **brightening** period, for some areas until the 2000s. Although the dimming period was observed in many regions around the world, the later increase was not that coherent, and some areas still presented negative trends, like India [Wil12].

The magnitude of the multi-decadal trends differs not only on the sign but also in the magnitude, depending on the period and the area [Wil09; Wil12]. From the year 2000, USA and Europe have showed an increasing trend in surface radiation of 5 and 2  $W/m^2$  (per decade) respectively, but China and India still shows a significant decreasing trend of  $-4W/m^2$  and  $-10W/m^2$  per decade respectively.

These low-frequency changes cannot be explained by changes in sun's luminosity as it was showed by [WM03]. As a consequence, they only can come from changes in the atmosphere's transparency. Long-term changes in cloud cover are responsible for most of the interannual variability of solar radiation, but they are not able to completely explain decadal changes [NW07; San+09].

The global dimming phenomena has been studied as a result of the increase in anthropogenic aerosols emissions, finding consistent changes in surface radiation related to sulfur and black carbon emissions between 1980-2000 [SWC06; NW07]. In Europe, the dimming period is being associated with the collapse of the former Soviet Union and the implementation of pollution control measurements [Wil05; Wil09].

Over Europe, low-frequency changes in solar irradiation are less correlated with changes in cloud cover than some of the seasonal series in the area [San+09; CW10]. For instance, as it was previously commented, winter series are highly correlated with the NAO index. Ciacchio and Wild [CW10] found that on decadal seasonal changes, there are other influencing parameters, suggesting changes in anthropogenic aerosols emissions, like it was pointed out in other studies [San+09; SLCW13; SL+17]. Also,

they suggested that the indirect effect of aerosols is also responsible for changes in the correlation between surface radiation and NAO.

The analysis of multi-year variations was also made through clear-sky series showing significant trends over areas of central and eastern Europe for some decades that are clearly related to dimming and brightening periods.

Over the Iberian Peninsula, some long-term series of sunshine duration and its relationship with cloud cover were analyzed by [San+09]. For most of the seasons, sunshine records and total cloud cover are strongly negative correlated, although some areas in the southern part and in summer have weaker correlations. The results are part of the large scale dipole pattern between the North and the South of the Euro-Atlantic sector [PV+04]. Besides, other more regional atmospheric patterns influence variability of sunshine duration series. It is worth mentioning that for residual clear sky sunshine duration series, a correlation with particular atmospheric circulation pattern is found, which might be related to the impact of anthropogenic aerosols emission on the dynamics of the atmospheric circulation at synoptic scales [San+09]. More recent studies have included a new methodology for quantifying the effects of aerosols and clouds in the intense brightening observed in the Iberian Peninsula since the early 2000s. They conclude that aerosols are responsible for one fourth of the brightening and clouds are responsible for the rest [Mat+14].

The use of satellite datasets of solar radiation, and clouds in some cases [Pfe+18a], has helped in order to see spatial patterns and analyze multi-decadal variability in large areas with no available irradiation data. For Europe, they have been used to analyze long-term series and trends of surface solar radiation. For the period between 1983-2010 an overall mean increase of  $2 \text{ W/m}^2$  per decade has been reported over Europe after the analysis of satellite-derived data. This result is due to changes in cloud cover, due to the lack of aerosols variation in satellite products. Further analysis has shown that for the same period, some residual trends obtained from the difference between the satellite and on ground measurements, showed a higher increase in central and eastern Europe suggesting the brightening period related to anthropogenic aerosols reduction.

Further research using more recent satellite dataset products for the period 1983-2015 and 1983-2010 shows a general increase in surface solar radiation over Europe (between 1.9 and  $2.4 \text{ W/m}^2$  per decade), also attributed to a decrease in cloud cover. The difference with respect to observations and the trends in residual series are attributed to changes in direct aerosols effect and snow cover [Pfe+18b; SL+17].

### 2.4.2 Resource assessment

Characterization of solar irradiance for a region or a specific location over an historical period is called *resource assessment*. It is the first step for the initial phase of a solar project, the feasibility phase, and for the later design phase. In the first stage, developers of the future power plant look for site selection, where an estimation of average solar irradiation at the site is the first selection criterion used. After that, a more specific approach for the selected place is needed to consider local climate conditions.

The resource assessment stage is usually developed applying a solar irradiation database that accounts for long-term historical data in order to estimate the amount of energy that can be obtained with the project. However, as seen before, it is not an easy task to obtain solar irradiation measurements, which makes necessary the use of other types of data. Different products are nowadays available, most of them derived from satellite observations [Sen+17b].

One of the common practices that has been historically applied for solar resource assessment is the use of a TMY dataset: a typical meteorological year dataset for a certain location. These datasets are derived from longer time data and summarize the average behavior of meteorological variables in a 12 month dataset. Although this practice has been extensively applied for modeling power generation and evaluating the economic value of photovoltaic power plants, there are by now many studies that have proved that these datasets are not the best to capture the whole variability of the resource and, moreover, some extreme events, that can lead to a higher economical impact, are underestimated [Bry+18; Vig+12; Sen+17b]. These could be especially critical for solar projects in desert areas, where higher loads of desert dust can drop energy production significantly [Gue14].

Related to low-frequency variability of solar resource, an interesting contribution was made in order to consider the decadal variations of solar resource in the resource assessment phase [Mül+14]. The uncertainty related to these long-term variations is not usually considered, but it has been shown that these trends are not negligible in the horizontal plane, and they are higher for tilted panels. Their contribution recommended to use the last 10 years of accurate data for estimate trends in solar radiation as an indicator of the future evolution of solar irradiation. Due to the decadal changes in surface solar radiation and brightening and dimming periods, a selection of the last 10 years of data is more precise to determine real trends in this variable [Mül+14].

#### Resource risk

As in every energy project, there are associated risks that compromise the revenues of the project. Some of them, like technical or commercial risks, are also in other power

projects. However, the uncertainty in the resource that is the “fuel” of the power plant is inherent to some renewable energy projects. That is called “resource risk” and most of the financing activities of the project are related to it. The goal of every project is to estimate that risk and to minimize it.

In the first place, in order to know if a photovoltaic project is going to be profitable, the amount of energy that can be produced by the potential project is assessed. In order to do that, it is necessary to characterize the solar resource in the area and to model the performance of the PV plant. This first step is the previously explained solar resource assessment, and should consider different time-scale variability of the resource: interannual, multi-year, long-term trends.

Variability of the resource has some commercial implications to be considered. From the variations in electricity prices, which would depend on the contract between the project owners and the energy grid operator, to the necessity of matching some delivery requirements, or forecasting requirements, if the energy produced has to be forecasted in advance for the TSOs, etc. [MGV13].

Some risk management techniques are developed in order to address the issue of resource variability. The **probability of exceedance** gives the probability of exceeding a certain amount of energy in different time-scales of the project. This measure helps the financial steps giving some threshold based on the historical data.

Secondly, the source of variability in the projected energy has to be considered. In this case there are three clear sources to be considered: the inherent variability of the resource, the uncertainty in the dataset selected and the modeling assumptions for the PV system.

## 2.5 Future projections and trends

In a context of climate change, the climate system will evolve and renewable energy resources might be affected. In a scenario of high penetration of renewables, the relationship between changes or constraints in power supply due to changes in resources and, on the other hand, changes in the demand side as a consequence of climate change is a first order issue to be addressed in coming years [Dam+17; Blo+16].

From the supply side, climate change might impact traditional power plants like large nuclear and coal-fire plants [BC15; Tro18] due to an increase in air temperatures and river flow temperature, which affects the cooling system of the plants. However, systems based on these traditional power supply will evolve to a higher renewables penetration scenario. In that sense, a research across western US shows that a higher

share of renewables makes the power system less vulnerable to climate change risks like events of extreme temperature and severe droughts [BC15].

Different power supply scenarios can be less vulnerable to climate change depending on the technologies. Due to the projected changes in precipitation patterns [Dor05; GPG06] and the expected increase in extreme events like droughts [Hoe+12], hydropower is likely to be highly impacted under global warming conditions at least over certain regions. Over Europe, the impact of climate change in power generation has been investigated through its impact on different technologies. It has been found that those impacts can double from a 1°C warming scenario to a 3°C. Generally, southern areas in Europe will be more affected due to limited impact on solar and PV but higher impacts on hydropower and thermoelectric generation [Tob+18] as previously commented.

Some studies have evaluated projections of wind power potential over the same area, analyzing the availability of the resource for future scenarios. They show a slight decrease of wind power potential over Mediterranean areas and Western Europe; and an increase in the Northern areas [Tob+15; Tob+16] projected for 2020 and 2050. In general, there are no projected changes in the interannual variability.

From a solar perspective, modifications in the large scale atmospheric circulation related to global warming have to be considered, due to its direct link with cloudiness patterns and the storm-track [PV+04; CW10; CV12]. In the Northern Hemisphere summer, an intensification of the monsoonal regime and associated cloudiness over northern Africa and southern Asia is expected [Gae+14]. The intensification of the Hadley meridional circulation will produce downward vertical motions, and associated subsidence and clear sky conditions at subtropical latitudes. On the other hand, for the southern hemisphere winters, a modification of the mid-latitude atmospheric circulation and associated storm-track is expected, which will result in a high-low pressure dipole in the Euro-Atlantic sector, which orientates the westerly flow toward the Scandinavian peninsula, with a consequent excess of cloudiness over the North Atlantic storm-track [Gae+14].

As a result of these changes in the atmospheric circulation, an increase in cloudiness over northern Africa, and more clear sky conditions over western Europe and the Mediterranean [Gae+14] might be expected. The conditions in the Euro-Atlantic sector can also result in a reduction of solar radiation in northern and eastern Europe.

Projected changes in solar irradiation potential under climate change scenarios have been investigated in several works addressing different areas [Bar10; Cro+11; Gae+14; Wil+15; Jer+15b]. Some of them are focused on solar radiation rather than in photovoltaic potential because they have a climate perspective. Different tools have been

used in each of the studies mentioned before. On one hand, global climate models, with coarser resolution have been used to analyze changes in solar irradiation globally, using ensembles of different projects CMIP5, CMIP3 or a specific model to run sensitivity cases. Other studies, have been focused on regional scales, using regional climate simulation models, from PRUDENCE, ENSEMBLES and more recently Euro-CORDEX project.

Global projections using GCMs have been evaluated in [Cro+11] and later in [Wil12] showing an overall solar radiation decrease in large areas around the globe with exceptions in some regions like Europe, southeastern China and to a lesser extent southeastern of North-America. In the later study, that uses CMIP5 climate simulations, projected changes between 2006 and 2049 under the RCP8.5 scenario overall are on the order of 1% per decade for horizontal planes, but they might be larger for tilted or tracked planes, as well as on shorter (decadal) timescales.

Other works show regional results making use of regional climate models, RCMs. Main results in solar resource for Europe show a discrepancy between Global Models, GCMs, and Regional Climate Models, RCMs. Whereas most of the global model simulations show an increase of solar resource and photovoltaic potential over Europe, some research with RCMs have shown a small decrease of photovoltaic potential in the same area, mostly for northern and central part of Europe, associated with an increase in the total cloud cover [Jer+15b]. Although some studies have investigated the discrepancy between Global and Regional Climate models projections over Europe [Bar+17], there are still some uncertainties that deserves attention.

In some local studies, the effect of changes in solar irradiation and temperature has been evaluated with RCM simulations. For Greece, some bias corrected simulations have been evaluated and different signals across the country have been found. Generally, an increase between 1 and 3% is projected in the south and a decrease of roughly the same magnitude in the north [Pan+14].

Another local analysis has been recently made over the Iberian Peninsula, investigating changes in the interannual variability under climate change scenarios. The analysis is conducted using different RCMs and it is found that solar resource over the IP will increase and also a decrease in the interannual variability is also projected [Gil+18].

### Aerosols

One of the sources of uncertainty in future climate projections is the evolution of anthropogenic aerosols emissions and its interaction with climate. The direct and indirect effects of aerosols in climate and the hydrological cycle needs further research.

Interactions and feedbacks between aerosols and climate system are difficult to unravel due to the high variety of shapes and forms in aerosols but also because of its high spatiotemporal variation [KTB02]. In this regard, it is also important to notice that the representation of aerosols in regional climate simulations is not always taken into account and a research effort is needed.

Therefore, due to the aerosols potential impact not only on climate but directly on solar irradiation, it is a matter to be considered for renewable resource projections.

A sensitivity analysis has been performed to show the impact of different aerosols emission scenarios on solar potential and wind potential [Gae+14]. Global simulations with the ECHAM5 GCM projected changes in temperature and surface solar radiation globally considering different scenarios of GHG emissions and aerosols emissions.

Results of this work show significant positive changes in surface solar radiation, SSR, in the tropics, at mid and high latitudes, and negative changes in the subtropical areas in all the 2030 simulations. The extension and intensity of the simulated changes increase as the aerosol emissions decrease, indicating that the climate change signal related to GHG increase is augmented by the reduction of anthropogenic aerosols emissions [Klo+08; Klo+10]

## 2.6 Objectives and scientific questions

The main objective of this work can be described after having introduced the framework: the underlying idea is to analyze the long-term characteristics of solar resource and photovoltaic production in a specific area, the Euro-Mediterranean region. On one hand, most of the Mediterranean region has high potential of solar resource, which makes the area suitable for its deployment. On the other hand, from the electrical point of view, Europe is well interconnected and can be considered as a whole system, which is important for the development of solar energy. In addition, due to the especially high sensitivity to climate change of the Mediterranean area and the projected increase in renewable energy generation, characterization in long time scales becomes an important matter.

We approach the main problem in three different chapters. Each one analyses a key aspect of the long-term features of solar resource and photovoltaic production and it is made using different approaches.

1. The first objective addressed in chapter 5 is the characterization of the interannual variability of solar resource and photovoltaic productivity over the Iberian Peninsula using clustering techniques.

The selected area contains multiple climates in a relatively small region and its electrical system interconnection is constrained by the rest of the European electrical system. A multi-step scheme approach is used, including a regionalization step and an inter-comparison step, which systematize the variability study. The process can be applied to different spatial or temporal scales.

2. Secondly, the objective is to quantify the impact of aerosols as a specific cause of SSR variability (in space and time) and how it affects PV production. In this chapter, the spatial scale is broadened to the Euro-Mediterranean region. Other transversal questions can be also studied through this chapter, like the use of RCM for renewable energy resource assessment.
3. Finally, the objective is to analyze future projections of solar resource and photovoltaic potential over the Euro-Mediterranean. The evaluation is made focusing on the role of evolving aerosols in the future runs in different regional climate models. This chapter allows to investigate not only the possible scenarios for solar resource, but also, diverging results from GCMs and RCMs for future projections of solar resource and the limitations of an ensemble approach if some sources of uncertainty are not limited.

## **Part II**

# **Data & Methods**



CHAPTER

**3**

---

## Data

In the present chapter, the data used in the document are described. Different types of data are used in each of the studies due to the fact that different problems are addressed. A more specific description is included in later chapters.

There are many applications from meteorology to agriculture or even health sciences, that would benefit from an accurate station network that provides high quality radiation measurements at the surface. However, it is well-known that the lack of well spread solar radiation measurements has been a constraint, not only for the development of solar forecasting or resource assessment techniques, but also for the study of the whole atmospheric/climatic processes in which solar radiation takes place. The progress and improvement in the satellite-based products has helped to overcome some of these issues providing gridded data at a high spatial and temporal resolution.

Part of this work has been developed through what could be called a modeling chain approach, which is explained in the following chapters. This modeling chain is formed by a model that provides solar radiation data and a model that computes PV production from this input. Due to that, the data input of the PV model is also included in this section, which is solar radiation from observations and climate models.

As this work is focused on long time scales and wide areas, time and horizontal resolution of gridded data used are not considered a constraint to our analysis in most cases. Due to that, as explained below, finest temporal resolution used in this work

is daily and the horizontal resolution of the gridded datasets goes from  $0.05^\circ$  for a satellite-based product to  $0.44^\circ$  for data from regional climate models.

### 3.1 Solar Radiation data

#### 3.1.1 Solar radiation measurements

The measurement of solar radiation is based on radiometers that measure the solar energy reaching the Earth's surface. These radiometers are able to measure electromagnetic solar radiation at different wavelengths. For energy purposes, the interest of solar radiation measurements is on the shortwave range of the spectrum.

Solar radiation can be decomposed in three components: direct beam normal irradiation  $B(0)$ , the diffuse component,  $D(0)$ , and the albedo component,  $R$ . The three components form the global solar irradiation  $G(0)$  and different instrumentation can be used to measure each of the components.

Historically, the first instruments that measured solar radiation were based on mechanisms to calculate the duration of bright sunshine, following the needs of agriculture to understand evaporation [Sen+17a]. For that time, the Campbell-Stokes sunshine recorder was the most widely used [Sen+17a], although it was not a radiometer. It worked focusing the direct beam of solar irradiation to create burn marks in a record paper when it exceeded a certain value. Through the comparison of the burned length to the day length it was possible to characterize solar radiation at each place [Iqb83].

By the early 20th century, the pyranometer was developed to measure global solar irradiation. Pyranometers are also able to measure the diffuse component through a shading device that excludes direct radiation from the sun. For direct solar irradiation, the instruments are called pyrheliometers and they measure direct solar beam at normal incidence.

Actual radiometers are of three different types: thermopile, blackbody cavity, and solid state [GM08]. The detector of the instrumentation has a known spectral response to incident radiation and it is protected with an optical window that can be used to limit the spectral range of the radiation measured, which is important for energy purposes [GM08].

Different research programs are in charge of assuring the quality of some important solar radiation measurements databases. These significant research initiatives are the Baseline surface radiation network, BSRN [KL+13], the International Daylight Measurement Program [DK99], the Global Energy Balance Archive, GEBA [GWO98] or the

World Radiation Data Center, WRDC (<http://wrdc.mgo.rssi.ru/>). All of them are only applicable for research purposes and no-commercial activities. To these databases, different country-level databases that manage dense station networks can be added, but the availability of global solar irradiation measurements and, to a further extent, different components is not always assured.

## **BSRN**

One of the main sources of high quality data, as it has been previously commented, is the *Baseline Surface Radiation Network*, BSRN [KL+13].

The BSRN project was born with the aim of detecting changes in the Earth's radiation field that could be a consequence of climatic changes. The monitoring network provides high-quality and high-frequency data of short and long-wave radiation fluxes from different stations around the globe, which correspond to different climatic zones. In figure 3.1 all the available stations from BSRN are displayed.

The World Climate Research Program (WCRP) Radiative Fluxes Working Group initiated the Baseline Surface Radiation Network (BSRN) to support the research projects of the WCRP and other scientific programs related to solar radiation. By the time this document is written, 52 BSRN stations are in operation. There are some stations with "candidate" status and some that will be closed in 2019. Among these stations there are different levels of data provided, from the basic measurements that include the components of solar radiation, air temperature and pressure to other variables and synoptic observations.

### **3.1.2 Satellite data**

Satellite datasets have become one of the main used sources of solar irradiation data for energy resource assessment and forecasting. Solar irradiation derived from satellites is itself a product of modelization and their main advantage is their high spatial and temporal resolution as well as their increasing accuracy.

There are different methods to retrieve solar radiation from satellite images that goes from physical models to empirical ones. In the first case, the models try to explain the radiance observed by the satellite instrumentation with a radiation transfer model (RTM). In order to do that, it is necessary to know the composition of the atmosphere. On the other hand, empirical models are based on simple regression models between the visible-channel's recorded intensity and ground measurements.

It is possible to extract cloudiness information from the satellite radiance information due to the fact that intensity of the measurements change depending on the composition of the atmosphere and the cloud cover. Considering that, a simple equation can



Figure 3.1: Solar radiation stations from BSRN. Figure from the BSRN website.

describe the relationship between the radiance measured and the amount of clouds, this was called **cloud index** [Can+86]

To retrieve solar radiation from satellites, most empirical methods consider a linear relationship between the cloud index and atmospheric transmittance [Can+86; Dia+87; IP99; ZRP05; PZR08].

There are also some approaches that are in between these two sides: the semi-empirical models, which have become the most common approach [PZR08]. They use a simple radiative-transfer scheme and some statistical regressions between data from satellite sensors and observed data [Sch89; PFL95; Kle13].

There are two types of satellites orbiting the Earth: the polar orbiting, closer to the Earth's surface, with high spatial resolution but limitations in the temporal coverage, and the geostationary satellites (36000km from the Earth's surface) with high spatial and temporal resolution. This last kind of satellites are the commonly used to derive solar radiation at the surface.

The uncertainty in the satellite radiation estimation comes from different sources. First, Sun elevation affects the determination of cloud position due to the increase of reflections, increasing the uncertainty for low Sun elevation. Other sources are related to geographical factors. The high albedo of some surfaces like deserts or ice areas makes the determination of clouds difficult, increasing uncertainty [CSG11].

There are many solar irradiation datasets derived from satellite products available nowadays: Meteonorm, SolarGIS, CM-SAF, Helio-Clim etc. Their differences are based on different parameters that go from the data source, one or several satellites, the spatial coverage and resolution, the time resolution or its accessibility related to its private/commercial purposes. An in detail review of 16 of the most common satellite derived datasets is made in [VPB14].

In our work the CM-SAF (The Satellite Application Facility on Climate Monitoring) solar irradiation products are used due to its spatial and time coverage and availability as well as its free access for research purposes.

### **Climate Monitoring Satellite Application Facility: CM-SAF**

The aim of CM-SAF consortium from EUMETSAT is to develop satellite-data-based-products for climate monitoring since 2000 when the importance of using satellite data for this purpose was recognized [Sch+09].

The CM SAF products are derived from several instruments on-board operational satellites in geostationary and polar orbits. There are two main types of products that can be obtained from the CM-SAF: operational products and climate data records (CDR). The main purpose of the CDR is to provide a high-quality database to monitor climate variability and changes [Mül+15], as well as to detect trends. Operational products, on the other hand, are not accurate enough for this purpose because some errors like inter-satellite biases or sensors degradation are not corrected.

The SARAH dataset from CM-SAF has been used in chapters 6 and 7 of this document for the analysis of solar radiation at the surface. The data is based on the records from Meteosat images, first and second generation, using the on-board MVIRI and SEVIRI instruments respectively [Pos+12]. As the purpose of the CDR is to provide long time series covering more than 20 years, a retrieval algorithm that can be applied to SEVIRI instruments as well as to the older MVIRI is necessary. This algorithm has been called MAGIC SOL and has two parts: first, the modified **Heliosat** method is used to obtain the cloud effective albedo (CAL), also called *cloud index*; and second, the **MAGIC** approach is used to obtain all sky surface radiation based on CAL [Pos+12].

The **clear sky index**,  $k$ , can be defined as the ratio between all-sky irradiation and the clear sky irradiation. For most of the conditions it can be generalized a relationship between the clear sky index and the effective cloud albedo, CAL:

$$k = 1 - CAL \quad (3.1)$$

Clear sky radiation is obtained through the MAGIC algorithm [Mue+09] that consists of simulations of a radiative transfer model (RTM) and an interpolation method using discrete values of the RTM runs, which reduce the computational time [Mue+09]. Inputs of atmospheric state are needed: aerosols, water vapor etc. After that, with the knowledge of the clear sky index and the the clear sky surface radiation, the all-sky radiation on the surface can be derived. A scheme representing the process to obtain direct and global solar irradiation is presented in Figure 3.2

Information about **aerosols** to be used in the MAGIC algorithm is obtained from the ECMWF-MACC reanalyses. The MACC [CAM19] data are a combination of a model for aerosol composition and dynamic [Mor+09] and a data assimilation system [Ben+09]. Monthly mean aerosol information is included in the algorithm to obtain clear sky irradiation. The MACC data has to be regridded to a higher resolution ( $0.5^\circ \times 0.5^\circ$ ) to the use within CM-SAF.

### 3.1.3 Solar radiation from climate models

Solar irradiation at the Earth's surface can be measured using the above mentioned instrumentation or can be obtained through modelization, with physical or statistical methods, as it was explained in chapter 2.

Climate models are a representation of the whole climatic system. In order to solve the Earth's radiation budget equation, they use a radiative transfer scheme. By solving the radiative transfer equation, they are able to give solar radiation at the surface. Due to the complexity of the climate system, and the coarse spatial resolution of climate models, some processes have to be simplified and others need to be parametrized. Climate models parameterize convection processes, aerosol processes, cloud micro-physics etc. Thus, different RTMs can be implemented depending on the climate model.

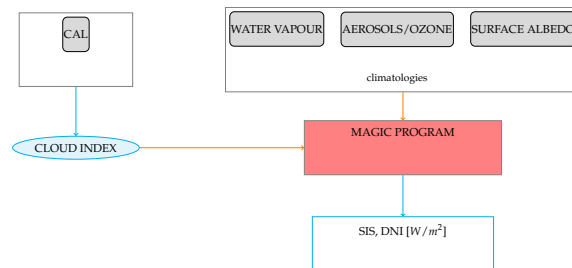


Figure 3.2: Algorithm scheme: Retrieval of shortwave solar radiation from satellite images.

In chapters 6 and 7 different climate models are used as main source of solar radiation data. The output of each model will be the result of the radiative scheme inside their codes and it can be used as the input variable for a photovoltaic production model to analyze photovoltaic potential under different climate conditions.

### CORDEX initiative

Under the acronym of CORDEX (Coordinated Regional Downscaling Experiment) a wide range of regional climate models has been applied in a coordinated way to provide downscaled climate simulations<sup>1</sup> for different areas around the globe<sup>2</sup>. Whereas GCMs give an overview of the evolution of global conditions, their coarse resolution is not enough to understand some small scale processes of climate and to project climate change impacts at a local scale. The higher resolution of the regional climate models is needed not only for purely physical knowledge, but for supporting adaptation and mitigation plans.

Two different domains from CORDEX are used in this study both focus on the Mediterranean area: Euro-CORDEX and Med-CORDEX (in figure 3.3). The horizontal resolution of the simulations included in Euro/Med-CORDEX goes from 0.44° to 0.11° (from 50km to 12km).

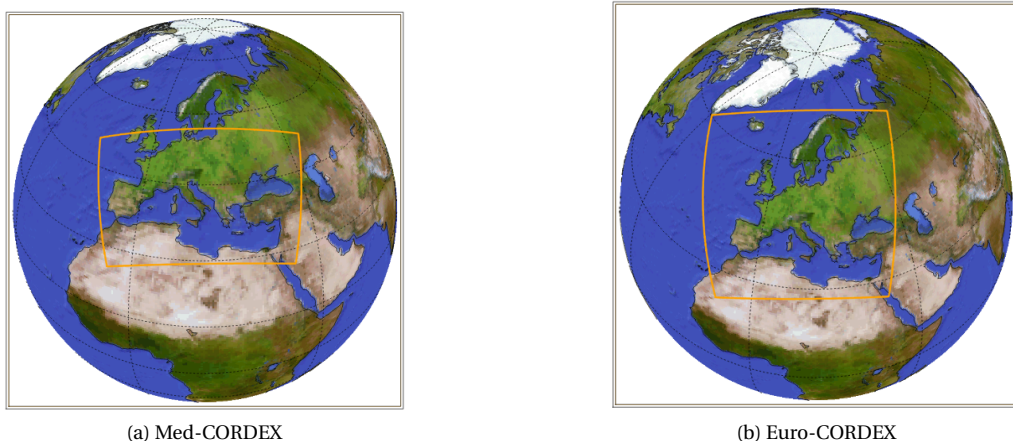


Figure 3.3: Domains from Med-CORDEX and Euro-CORDEX. Images from WRCP-CORDEX website.

<sup>1</sup>The chapter 4 explains the origin of regional climate modeling and the simulations used in the thesis

<sup>2</sup>Cordex website:<http://www.cordex.org/>. This international framework is under the umbrella of the world climate research program, WRCP

The main difference between the two initiatives, in addition to the studied domain represented in figure 3.3, is that simulations from Med-CORDEX [Rut+16] are runs from coupled ocean-atmosphere climate models, whereas the Euro-CORDEX [Jac+14] ensemble includes atmosphere models only.

## 3.2 Aerosols datasets

Atmospheric aerosols content can be summarized by the AOD, aerosol optical depth, parameter; which is the integration among an atmospheric column of the incident light that is scattered or absorbed by aerosols. Since the 1980s, different sensors from satellites have been used to derived AOD and at the same time, some models have been developed and provide AOD climatologies as well as the contribution of different species to the total AOD [Nab+13].

From the measurements side, the **AERONET** network [Hol+98] was initiated by NASA in the 90s and it has grown to become a widely spread network of radiometers across different continents based on international cooperation. This ground-based aerosols monitoring network allows to characterize from local to global profiles directly related with Earth's radiation budget studies. It has become also an important database for evaluation of satellite derived and model AOD products.

There are different aerosols datasets for the **Mediterranean area**, which is very influenced by natural and anthropogenic aerosols [Lel02]. These datasets are derived from satellite observations like MODIS, MISR, or SEVIRI; or from model simulations like LMDz-OR-INCAR or MACC reanalysis. An intercomparison of aerosols datasets in the area can be found in [Nab+13] where an improved 4-D climatology of aerosols is developed.

### 3.2.1 Aerosols in RCMs

The representation of aerosols in RCMs varies from one model to another. Despite of the high influence of aerosols in the Mediterranean climate variability [Nab+14] and its role in the brightening period over Europe (1980-2012) that has been also investigated [Nab+14; Nab+15; Wil09], the representation of aerosols in RCMs is still scarce. The AOD is often used for calculating aerosols radiating forcing in RCMs simulations. Some of the RCMs simulations include a fixed climatology of AOD, like Tegen or the old one of Tanré [Teg+97; TGS84], whereas others do not include any aerosols. The most complex include an interactive aerosols scheme, that is necessary for daily scales and also for future projections.[Nab+13]

In future climate projections over the Euro-Mediterranean area with RCMs (under the Med-CORDEX or Euro-CORDEX frame), few models include aerosols time evolution. Most of them include a fixed climatology for present climate conditions that is also applied invariantly for future projections. The models that include time evolving aerosols in their runs apply different inventories like [Szo+13] or [Lam+10].

### 3.3 Photovoltaic production data

In order to evaluate the performance of a PV model it is necessary to use the data from real PV plants. However, these data are not easy to obtain, due to the fact that they belongs to private companies and it could compromise some of their strategies. This makes it necessary to get agreements and confidential contracts between these companies and researchers that are not always easy to obtain if an immediate benefit does not arise from those relationships.

Some alternatives are the databases of aggregated data that are available for the European countries through the ENTSO-e data portal website [HMB18]. However, these data will be only useful for certain modeling exercises but have limitations due to the fact that there is a lack of information related to the power plant locations in each country.

In this work two power plants data have been used in order to compare simulations with the real data. The limitations of these two plants is that they are both located in the Iberian Peninsula, and the length of the time series is limited. However, due to the difficulties to obtain these kind of data, it is useful to compare the modeling chain approach used in chapter 6 with the real data.

### 3.4 Other data

In addition to the direct relationship between solar irradiation and photovoltaic energy conversion, there are other atmospheric variables that influence the performance of solar cells, like temperature or wind speed. The model used in this work considers only temperature as a second order factor that reduces cell efficiency, as it is explained in chapter 4.

Temperature data are easier to obtain than solar radiation data. Numerous weather stations provides temperature data at 2m over the surface at a local scale. For studies over a large area gridded products are useful and easier to combine with the satellite products than station data.

In this work, temperature from climate models is used in chapters 6 and 7 to compute photovoltaic productivity. In chapter 5, temperature from the E-OBS dataset is combined with solar radiation from a satellite dataset.

#### 3.4.1 E-OBS dataset

E-OBS is a gridded dataset derived from interpolation from the ECA&D data based on stations that provides daily temperature data over Europe and the Mediterranean area<sup>3</sup>. This product has been validated in several research papers [Beg+08; Hof+09] finding some inaccuracies related to an over-smoothing in areas where there are few stations, which affects extreme analyses mostly.

The horizontal resolution of the gridded products is 0.25° or 0.44° whereas the time resolution is daily, with time series going from January 1950 until June 2018.

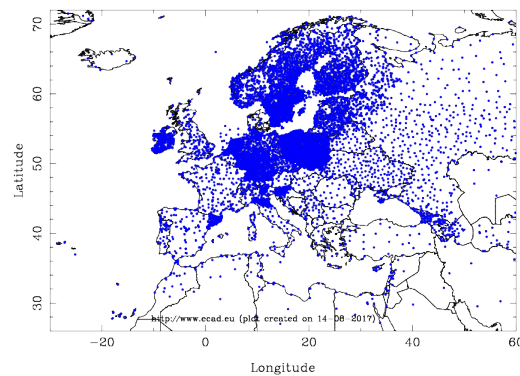


Figure 3.4: Map of the stations from ECA&D to provide daily temperature gridded products. Source: ECA&D website.

---

<sup>3</sup><https://www.ecad.eu//download/ensembles/download.phpmaps>

---

## Methods

In order to fulfill the objectives of the present work it is necessary to apply different methodologies in each of the results chapters. All of them are explained in detail at the corresponding section of the chapters.

However, in the present chapter the different tools needed for the development of each study are described in a general manner. The three results chapters are based on a **modeling chain** that includes a photovoltaic model that is composed of two steps. First, the transposition to the plane-of-the-array, POA, of the components of the solar radiation, which implies also to assume some models of the sky sphere seen from the generator plane and a model for the electrical performance of the system. Besides, the input of this PV model can be solar radiation measurements, satellite radiation estimations or, as we saw in the previous chapter, the output of atmospheric/climate models.

In chapter 5 the interannual variability and complementarity of solar resource over the Iberian Peninsula is analyzed. A methodology based on **clustering techniques** is applied for that purpose. The regionalization allows us to simplify the spatio-temporal analysis of solar resource. The evaluation of the productivity, defined as the amount of energy produced by a PV system normalized by the power capacity of the system, requires the **modelization of the photovoltaic system**.

Chapter 6 analyses the impact of **aerosols** on photovoltaic productivity over the Euro-Mediterranean area for present climate and past conditions. Some climate simula-

tions forced by the ERA-INTERIM reanalysis are used as the input of the photovoltaic model. The modeling chain allows to make a sensitivity test to quantify the role of aerosols in the area.

Finally, the photovoltaic energy potential is analyzed in the future, using **climate projections** from different climate models. Trends and anomalies with respect to a reference period are evaluated. In this case, a **multi-model analysis** with different RCMs simulations allow us to evaluate the solar resource under climate change scenarios. The representation of aerosols in the climate projections is considered as a fundamental variable for the shortwave downward radiation projections, SSR, and PV productivity.

## 4.1 Clustering algorithm applied to climate data

In a data-driven world, **pattern recognition** is being applied to many disciplines from biology to finance through social science, in order to obtain relevant information from different datasets. When the similarity measurements of the data cannot be defined first, due to unknown previously labeled data, the implemented approach will consist of identifying the similarities afterwards, from a dataset of features, applying clustering algorithms for that purpose.

### 4.1.1 Clustering algorithms

It is not under the scope of this work to analyze in detail all the clustering methods available, due to the vast number of them and its increasing complexity [Jain1999]. However, it is worth giving an overview of its classification and application in order to better understand the choice made in the study of our problem.

There are different types of clustering algorithms based on its application and the criteria applied to construct the clusters. The two main categories are divided in **hierarchical** and **non-hierarchical algorithms**, but there are other taxonomies based on the algorithm construction that can be used to classify different methods [Jain1999].

The **hierarchical clustering algorithms** create a number of nested clusters and they can also be divided themselves in agglomerative or divisive. The first one obtains a smaller number of cluster in each step, whereas the divisive algorithms work towards the other direction.

Most of these hierarchical algorithms are variants of the single-link or complete-link algorithms. They have a different way to measure similarity. In the first case, the distance between two clusters is the minimum of all the pairwise distances measured

between the objects of the two clusters, while, for the complete-link algorithm the distance is considered the maximum of all the pairwise distances.

On the other hand, the non-hierarchical or **partitional clustering algorithms**, create a number of non-overlapping clusters. These methods could be useful when the amount of data involved is large and the construction of a dendrogram, produced by the hierarchical algorithm could be computational expensive.

The partitional methods create the group of clusters using an **optimization function** which defines the similarity. The main inconvenient of these algorithms is the in advanced definition of the number of clusters. Usually, the algorithm is implemented several times for a wide number of partitions and the optimum number of clusters is defined afterwards using validity index criteria.

### 4.1.2 Clustering climate data

As previously commented, the use of pattern recognition and in particular, the clustering analysis, has been widely used across many different disciplines. The use of these techniques to group together atmospheric variables that could help in environmental classifications is a more recent research field [ZMH12]

Historically, the climatic divisions were based mostly on the differences in vegetation types around the globe. The Koppen-Terawatha classification [Kot+06] is the most widely known climate classification and bases its divisions on the vegetation thresholds from precipitation and temperature data. Some authors have already pointed out the limitations of this classification method mostly due to two aspects: the first one is that vegetation thresholds are not well defined and that could be an issue when higher spatial resolution scales want to be defined. On the other hand is the fact that not only precipitation and temperature are influencing the vegetation species but also other atmospheric variables like solar irradiation, as well as other environmental factors that could be related to antropogenic emissions or pollution.

As these classical divisions are not adapted to the necessities of different fields and could be even biased, another way to geo-spatial classification is needed. In this sense it has become frequent to successfully use data-driven classification of different variables [Arg+11; Zag+13; ZIC14; ZPC14; ZMH12].

### 4.1.3 Applied clustering method

In this work a clustering method is applied to classify solar irradiation due to the fact that classical climate divisions are only based on temperature and precipitation. The

spatial pattern that could be extract from the Koppen-Terawatha classification, can not be used for our purpose.

A commonly used partitional clustering method has been selected to classify solar irradiation of the area. The “**k-means**” algorithm is easy to implement and has been largely used over the literature. Moreover, the combination of a **principal component analysis** of the dataset previous to the k-means algorithm application has been proved to be an useful tool to reduce the data-dimensionality and apply the algorithm in a more efficient manner [DH04].

### K-Means algorithm

The k-means algorithm is a partitional clustering method that provides a set of partitions from the application of an optimization function, usually the euclidean distance, 5.1. The algorithm initiates from a pre-defined number of clusters, “k”, and randomly selects a group of centroids equal to the number of clusters. The optimization function is applied to assign each object to one of the clusters, depending on the similarity (distance) to each of the centroids. This process is applied until the algorithm converges.

$$J = \sum_{i=1}^k \sum_{j=1}^n \|x_i - c_j\|^2 \quad (4.1)$$

In equation 5.1: J is the objective function,  $k$  is the number of clusters,  $c_i$  is the centroid of the cluster  $i$  and  $x_i$  is each element inside the cluster.

One of the limitations of this method is its dependency on the first selection of the centroids, that could lead to a local optimum instead of a global optimum. To solve this difficulty, the algorithm can be run many times to test the sensitivity of the algorithm to different initial conditions. Another option is to use an initialization technique to select the centroids.

As the number of clusters “k” is not normally known in advance, the algorithm is applied from 2 to “n” times, with “n” high enough to get the whole variability of the dataset and the optimum number of clusters is defined afterwards. This optimum “k” will define the number of clusters that explains most of the variability and will assure that the increase in the number of clusters does not improve the variance representation.

### Principal Component Analysis

The Principal Component Analysis, PCA [Jol02], consists of a decomposition of the dataset into a number of vectors whose linear combination represents the original

data. The transformation of the original data into a lower dimensional space is a reduction of the dimensionality retaining the maximum of the data variance.

The new orthogonal system has in its first coordinate axis, the projected values of the original data that preserve most of the variance in the dataset, and this is called the principal component. The rest of principal components decrease consecutively the amount of variance explained.

The PCA has been applied in advance to K-means clustering algorithm among the literature [DH04]. Due to the fact that the clustering membership indicators are the eigenvectors given by the PCA, the reduction in dimensionality is linked to K-means. For this reason, it has been applied before the K-means algorithm in order to speed it up.

### **Validity Index**

Clustering validation through the validation or validity index measures the goodness of the clustering results. As well as for the clustering techniques, there is a classification for the methods used to validate the clustering results.

External validation techniques use information from outside of the dataset involved, whereas the internal validation techniques only need the information that is present in the data. The external methods know the number of optimal clusters in advance, so they are applied to select the best clustering algorithm. On the other hand, the internal validation methods will give us the optimum number of clusters after the application of the selected algorithm and only use the information that relies on the data.

Two different indices are used in this study, the **Calinski-Harabasz** index (Eq.:4.2), the **Davies-Bouldin** index (Eq.:4.3). The L-method proposed by Salvador and Chan, 2005 [CH74; DB79; SC04], is also used in an intermediate stage.

In the equation 4.2: The “BCSM” is the Between-Cluster-Scatter-Matrix, and its trace is the sum of squares distances between each cluster center  $c_i$  and the global centroid vector of all the objects of the dataset. The term “WCSM” is the Within-Cluster-Scatter-Matrix and the trace of this matrix is the sum of squares of the distances between the objects inside each cluster and the centroid. “k” is the number of clusters. In the equation 4.3,  $d_i$  is the averaged distance between the data classified into class i and the cluster center  $c_i$  and  $d(c_i, c_j)$  is the distance between the different cluster centers. “k” is the number of clusters.

Similar results are obtained with the CH and DB indexes. In order to analyze the optimum partition, it is important to consider the nature of the variables that we are

analyzing. Most of the atmospheric variables, are continuous variables that could be closely related to other variables such as latitude. For that reason, the regionalization procedure cannot be applied in the same way as for other discrete or non-continuous data. That characteristics should be considered when the results have to be evaluated.

$$CH = \frac{trace_{BCSM}}{trace_{WCSM}} \times \frac{n-k}{k-1} \quad (4.2)$$

$$DB = \frac{1}{k} \sum_{i=1}^k \max_{i=1, \dots, i \neq j} \frac{d_i + d_j}{d(c_i, c_j)} \quad (4.3)$$

## 4.2 Simulating a photovoltaic system

Photovoltaic energy is based on the conversion of incident solar energy into electricity. This process is made by the photovoltaic systems whose basic unit that transforms solar radiation into electricity is the **solar cell**.

The process of simulating a photovoltaic system has two main steps:

1. First, it is necessary to estimate energy that reaches solar cells inside the panels. This energy will be defined as **global effective irradiation**:  $G_{eff}(\alpha, \beta)$ . It is the energy available to be transformed into electricity after being transposed to the tilted plane of the generator and after accounting for the optical losses.
2. Secondly, the amount of energy that the system is able to give depends on the electrical performance of its components. The effect of temperature on cell's efficiency is considered as well as the inverter behavior.

Both stages involve some modeling assumptions and each one will be explained in detail in the following section. In general, due to the fact that it is very unlikely to

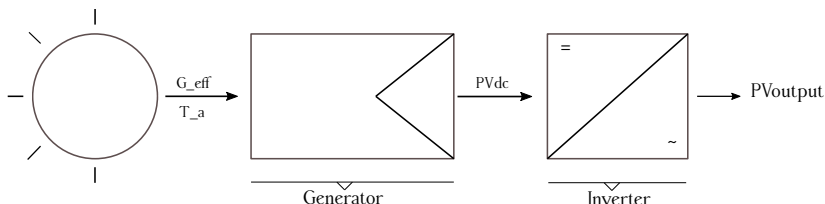


Figure 4.1: Scheme of a photovoltaic system. The effective irradiation is transformed into electricity by the generator and after that, into alternate current by the inverter, to be fed into the grid.

obtain solar radiation measurements in the plane-of-array,  $G(\alpha, \beta)$ ; global horizontal irradiation,  $G(0)$  (the most common variable measured or modeled that can be obtained from different sources), will be the starting point of the simulation. In order to estimate the amount of energy that reaches the generator surface,  $G(\alpha, \beta)$ , it is necessary to do a transposition of the different radiation components from the horizontal plane  $G(0)$  to the plane of the array (POA).

Once the solar irradiation components at the generator surface are calculated, the amount of that energy that can be transformed into electricity is assessed. The relative position between the generator and the sun gives the optical losses according to the difference with the optimum incident angle. After considering the optical losses and dust accumulation, the plane of array irradiation becomes the global effective irradiation  $G_{eff}(\alpha, \beta)$ .

The second step that calculates the energy output, provides the performance of the electrical components from the global effective irradiation and other variables that can influence on cells, like ambient temperature. The whole photovoltaic system includes the generator, the inverter and the transmission elements and wires.

All the processes involved in the stage of simulating a photovoltaic system requires also to compute trackers movements, as well as the relative position between sun and panels throughout the year. All the computations related to the PV system modeling in this thesis have been made using solaR [Per12], an R package that implements all the necessary functions to estimate the energy provided by the system.

#### 4.2.1 Global effective irradiation

Assessing the energy reaching cells of the photovoltaic generator can be summarized in two principle steps:

First, global irradiation on the horizontal plane is decomposed in two components, **direct** and **diffuse** irradiation, Eq.4.4. The third component of global irradiation, the albedo, it is not considered because its contribution is very low. To estimate these quantities we will consider equations proposed by [LJ60] to characterize solar irradiation. The definition of *clearness index*, Eq.4.6, is the ratio between global irradiation and extra-terrestrial irradiation at the horizontal plane. They also proposed to relate that index with the *diffuse fraction*: the ratio of diffuse to global irradiation in Eq.4.5. This relation varies depending on the time scale. For daily values, we estimate the correlation between the clearness index and the diffuse fraction using equations in [ACP92]. After that, the diffuse component is obtained with the definition of the *diffuse fraction*, Eq.4.5.

$$G_d(0) = B_d(0) + D_d(0) \quad (4.4)$$

$$F_{D,d} = \frac{D_d(0)}{G_d(0)} \quad (4.5)$$

$$K_{Td} = \frac{G_d(0)}{B_{0d}(0)} \quad (4.6)$$

The subindex  $d$  means “daily” for these variables. Secondly, daily irradiance profile [ $\frac{W}{m^2}$ ] has to be estimated from irradiation values [ $\frac{Wh}{m^2}$ ]. Considering low variability of solar irradiance during an hour, it is assumed that average irradiance in that interval coincides with solar irradiation in that hour. Regarding equations proposed by [ACP92], the ratio of the diffuse irradiance to diffuse irradiation is assumed to be equivalent to the ratio of extraterrestrial irradiance to extraterrestrial irradiation, Eq.4.7, and the ratio of global irradiance to daily global irradiation follows from the same reference, Eq.4.8.

$$r_D = \frac{D(0)}{D_d(0)} = \frac{B_0(0)}{B_{0d}(0)} \quad (4.7)$$

$$r_G = \frac{G(0)}{G_d(0)} = r_D \cdot (a + b \cdot \cos(\omega)) \quad (4.8)$$

The third step transposes the components to the tilted panel. Only geometrical criteria are considered to compute the direct component.

The difusse component needs to consider the sky sphere seen from the generator at each time step, which depends on the inclination of the panel. The diffuse irradiance is calculated with the anisotropic model proposed in [HM85]. This model, assumes as direct the irradiation coming from the circumsolar region and the rest of the sky sphere is considered as isotropic. An index of anisotropy is considered to calculate the ratio between both regions. When the sky is cloudy, the index presents lower values, which means that diffuse fraction is almost isotropic. Instead, when the sky is clear, the index is higher and the circumsolar region’s contribution increases.

The last step estimates the effective irradiance incident on a generator subtracting dust and angle of incidence losses from the incident irradiance with the model proposed in [MR01].

In figure 4.2 the steps to assess effective irradiation at the plane-of-array is summarized.

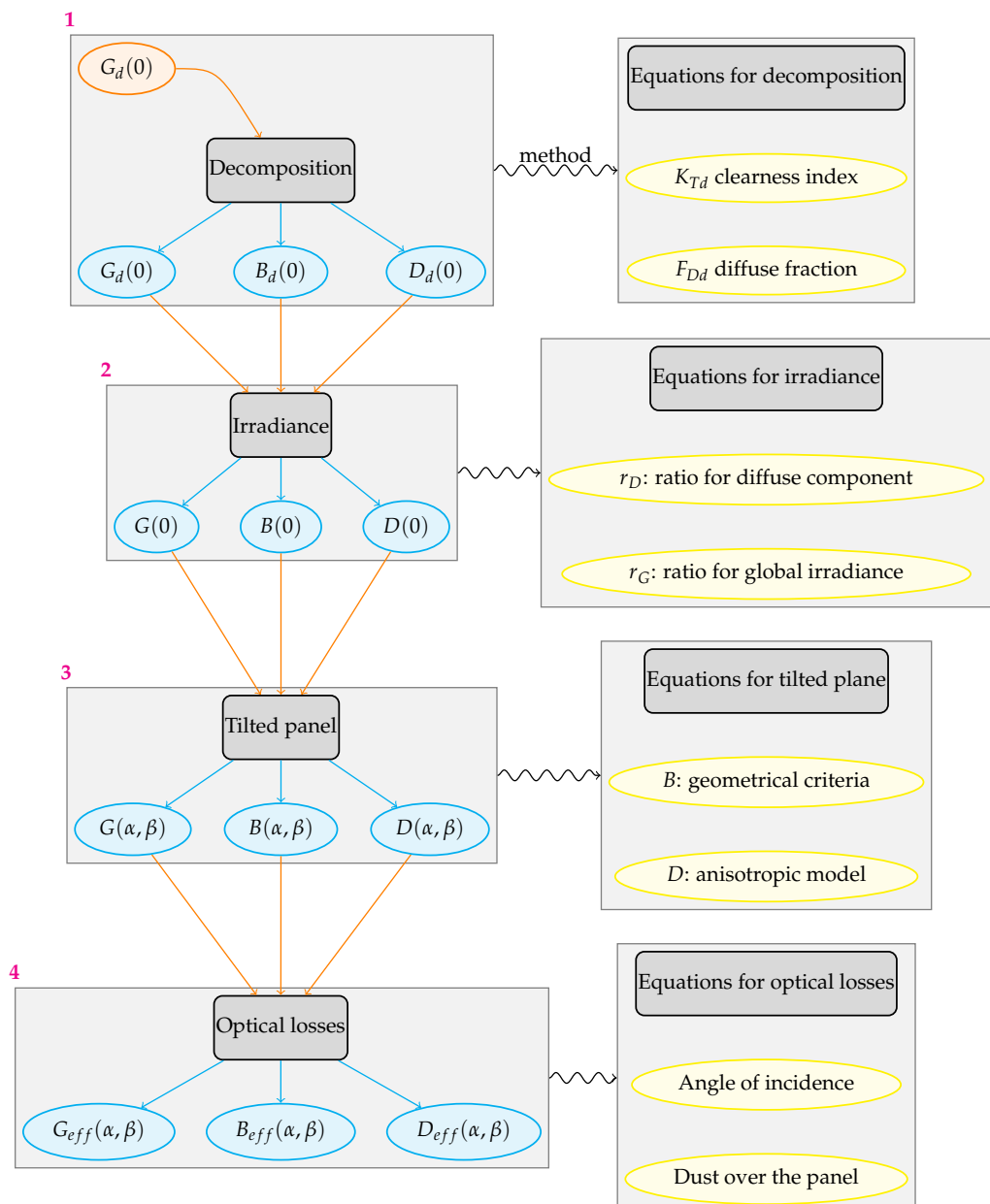


Figure 4.2: Algorithm scheme: steps on the calculation of incident irradiation at the inclined plane. Orange color means input of the calculation and blue color output or results. If a result in a previous step is used in the next one, arrows linking steps are orange. Right side of the scheme represents the method and equations needed.

### 4.2.2 Photovoltaic energy yield

Once the effective irradiation that reaches solar cells is being assessed, the transformation into power output depends on some factors regarding the photovoltaic system. The term “yield”, commonly used, is defined as the ratio between the energy produced and the nominal power of the system [ $\frac{\text{Wh}}{\text{Wp}}$ ]. That energy, comes from the integration in each time step of the power output of the photovoltaic system.

Considering that a photovoltaic generator is composed by modules, the generator nominal power output is calculated by multiplying the power output of a single module by the number of them, assuming the same electric performance of all modules.

The nominal values of the photovoltaic generator are defined by the manufacturer regarding the performance of the modules under certain conditions. However under operating conditions its performance varies and the obtained power depends on how the real conditions affect the cells.

The characterization of the solar cells that composed the modules is made by its I-V curve. The maximum power given by a solar cell can be obtained deriving that curve.

$$\frac{dP}{dV} = 0 \quad (4.9)$$

This point is called the MPP point and the current and voltage corresponding to this point are the  $I_{mpp}$  and  $V_{mpp}$ . The nominal power output of a module comes from the product of  $I_{mpp}$  and  $V_{mpp}$ , Eq. 4.10.

$$P_{out} = I_{m,mpp} \cdot V_{m,mpp} \quad (4.10)$$

The standard conditions applied to characterize the solar cells, thus the modules are:

- $T_c=25^\circ\text{C}$
- $G=800 \left[\frac{\text{W}}{\text{m}^2}\right]$
- $AM=1,5$

The characteristic equation of a solar cell and a module depends on two parameters called: the short-circuit current,  $I_{sc}$  (Eq. 4.11) and the open circuit voltage,  $V_{oc}$  (Eq. 4.12). These two parameters are respectively affected by the incident irradiation and the cell temperature. When the module is exposed to real conditions, the  $I_{mpp}$  and  $V_{mpp}$  are different from those under STC conditions. The  $I_{mpp}$  and  $V_{mpp}$  can be

obtained from the  $I_{sc}$  and the  $V_{oc}$  and the standard  $I_{mpp}$  and  $V_{mpp}$ , from now on:  $I_{mpp}^*$  and  $V_{oc}^*$ :

$$I_{sc} = G_{eff}(\alpha, \beta) \cdot \frac{I_{sc}^*}{G_{STC}} \quad (4.11)$$

$$V_{oc}(T) = V_{oc}^* + (T_c - T_c^*) \frac{dV_{oc}}{T_c} \quad (4.12)$$

The open circuit voltage decreases linearly with cells temperature. Due to that, cells performance depends on cells temperature that is related to ambient temperature as it is shown in Eq. 4.13.

The assumption used for this assessment considers a linear relationship between cell temperature and global effective irradiation, Eq.4.9. NOCT in equation 4.9 is considered constant, being the temperature of a cell when it works under conditions of incident irradiance of 800 [ $\frac{W}{m^2}$ ] and ambient temperature of 20°C.

$$T_c = T_a + G_{eff}(\alpha, \beta) \cdot \frac{NOCT - 20}{800} \quad (4.13)$$

Once the power of the generator is calculated, the power output of the whole system is assessed by the consideration of a common inverter for transforming DC current into AC, also arrangement losses of the generator are included. Other systems factors that influence the performance of the photovoltaic system are shadows over the generator due to the positions of the PV modules over the land. This factor is not considered in our calculations assuming that we look for an estimation of the potential yield of an area, not the product of a real PV plant.

### 4.3 Using Regional Climate Models

The modeling chain to obtain the photovoltaic production of a system starts with the input of the PV model. We can consider the output of an atmospheric or climate model as the input of the PV system instead of solar radiation measurements. The uncertainty of the PV power output will be higher but considering this option allows to make sensitivity studies and also to analyze future projections.

In our context, with the purpose of analyzing solar radiation and the potential PV production from a climatological point of view, climate models are a good tool that allow us to evaluate the resource in present conditions as well as its future evolution and to understand the role of aerosols in solar resource variability.

Element	Method
PV generator	Identical modules with $dV_{oc}/dT_c = 0,475 \frac{\%}{^{\circ}\text{C}}$ and $NOCT = 47^{\circ}\text{C}$ . The MPP point calculated as in [Alo05].
Inverter	Efficiency equation proposed in [JSS92]: $\eta_{inv} = \frac{p_o}{p_o + k_0^o + k_1^o p_o + k_2^o p_o^2} \quad (4.14)$ <p>where <math>p_o = P_{ac}/P_{inv}</math> is the normalized output power of the inverter. The characteristic coefficients of the inverters are: <math>k_0^o = 0.01</math>, <math>k_1^o = 0.025</math>, <math>k_2^o = 0.05</math>.</p>
Other losses	<ul style="list-style-type: none"> <li>• Average tolerance of the set of modules, 3%.</li> <li>• Module parameter dispersion losses, 2%.</li> <li>• Joule losses due to the wiring, 1.5%.</li> <li>• Average error of the MPP algorithm of the inverter, 1%.</li> <li>• Losses due to the MV transformer, 1%.</li> <li>• Losses due to stops of the system, 0.5%.</li> </ul>

Table 4.1: Calculation procedure for the estimation of energy produced by a PV system from irradiation data. Left column represents the element of the PV system and the right column the equations and methods used in each case for the efficiency of the elements.

## Climate Modeling

The history of climate modeling has been linked to the computational development since its beginning. The mathematical representation of the climate system was a consequence of the advance in numerical weather prediction models that took place for the first time in Princeton in 1952 and that had a fast development [Edw11].

Climate modeling is based on a 3-D representation of the whole climatic system, where the Earth is divided in a 3-D spatial grid whose size or resolution has evolved over time with computational power. Equations of motion, momentum and conservation laws are solved for each grid-box. As some of the atmospheric processes occur on a finer spatial scale than the resolution of the model, parametrizations are needed for some processes such as convection. These models were first named as General Circulation Models, GCM, as their aim was to represent main circulation flows in the atmosphere. The development of more complex models that started to include ocean and land, re-named later these models as **Global Climate Models, GCMs**.

Since its origins, there has been an increase and a diversification in research and more groups have developed their own climate models. Also, many international framework initiatives have unified efforts to understand better the future evolution of climate with the intensification and promotion of research collaboration programs, that include all the available models (WCRP, IPCC, CLIVAR...)

Global climate models provide useful information about the possible evolution of climate on large scales. Due to their low horizontal resolution, the model's cells cover areas with very different regional characteristics, which potentially can lead to missing some information that affects particularly to smaller and vulnerable areas.

It was in the early 90s [Dic+89; Gio90] when it was proposed to use global models as the necessary boundary conditions to force a “limited area model LAM”. Those LAMs had been used for numerical weather prediction forecast, but they were applied to predict the weather just few days in advance. The idea of running these simulations for longer periods will result in the development of **Regional Climate Modeling**, which would provide regional climate information of processes that occurs in a spatial scale not resolved by a global models.

In a similar way than the GCMs, the RCMs community has expanded in the last decades and the number of research groups has increased. Also, some international initiatives try to engage different groups and modelers to develop better models and simulations (PRUDENCE, ENSEMBLES, CORDEX, Euro-CORDEX, Med-CORDEX).

In the present work we make use of RCMs focused on the Mediterranean area with finer resolution than GCMs, considering the models and simulations included in the Euro-CORDEX and Med-CORDEX projects [Jac+14; Rut+16].

These RCMs can provide the necessary atmospheric variables for the analysis of renewable energy resources. Due to its complexity and the need of parametrizations for some atmospheric processes, they can have systematic bias that difficults their use for resource assessment. However, due to the low frequency variability observed in some variables and to the importance of considering the future projections, they are a valuable tool for analyzing renewable energy resources and its evolution. Besides, the use of climate models allows to study specific climatic events and to understand their mechanisms, linking the implications of those situations with renewable generation.

Climate simulations from RCMs can be forced by a Global Model, GCM, or by a reanalysis. Reanalysis are model-based climate products for present and past conditions that assimilate observational data. These climate data are normally used to force simulation runs of regional climate models for recent past periods, in order to evaluate the RCMs performance in present climate conditions and analyze their bias compared to other RCMs. These runs are sometimes called evaluation runs. For future conditions, RCMs are then forced by a GCMs that provide the contour conditions for the future.

For chapter 6, “Impact of aerosols in photovoltaic energy production”, only one RCM and three different simulations are used, in order to quantify the sensitivity of PV energy production to changes in atmospheric aerosols content. The test is made in present and past climatic conditions for the Euro-Mediterranean region. The simulations are nested in the ERA-Interim reanalysis and centered in the Mediterranean area, with the domain described by the MED-CORDEX initiative. The simulations length and characteristics of the aerosols dataset included are explained in detail in the corresponding chapter.

### 4.4 Future projections and scenarios

Behind the study of the climate system there is not only the interest of a deeper understanding of the physical processes, but also a concern about the impact that a changing climatic system could have in the ecosystems and different species of the Earth.

The Intergovernmental Panel on Climate Change, IPCC, was launched in 1992 and it is an international organism that was founded by the World Meteorological Association, WMO, and the United Nations Environmental Program, UNEP. Its purpose was to gather together all the scientific information available about the anthropogenic climate change. This information summarizes our knowledge about climate change, its impacts as well as some mitigation strategies to be adopted.

In order to elaborate the climate scenarios, which represent the possible evolution of the climate system, it is also necessary to generate different plausible scenarios of emissions. The development of these emission scenarios of greenhouse gases or aerosols, will be based on the assumptions about technological changes or demographic criteria as well as the socioeconomic development of each region. Those scenarios, with different options for the future evolution, will be the driving force for the climate simulations in order to elaborate the climate projections.

The first emission scenarios were elaborated in the 90s and they have changed since then. For the 5th AR of the IPCC, that was released 2014, the *RCPs* were defined [Sto+13]. They are different “representative concentrations pathways” that correspond to one of the possible scenarios that lead to a specific radiative forcing, i.e, the RCP8.5 represents a radiative forcing of 8.5 ( $\text{W/m}^2$ ) at the end of the present century.

For chapter 7, “Future projections for PV technology”, several RCMs and its corresponding GCMs are used. The simulations include the historical period and the future scenario RCP8.5 or RCP4.5. The analysis of the results will be done with respect to a reference historical period.

In Table 4.2 there is a summary of the climate models and the simulations that are used in chapter 6 and 7.

#### 4. METHODS

---

Study	Climate Model				
	GCM	RCM	Domain	Resolution RCM	Simulation
Aerosols' impact	CNRM-CM5	CNRM-ALADIN53	Med-CORDEX	0.44°	<u>AER</u> <u>NO-AER</u> TREND
Future projections	CNRM-CM5	ALADIN53	Euro-CORDEX	0.11°	HIST/RCP8.5
		RCA4			HIST/RCP8.5
	EC-EARTH	CCLM4	Euro-CORDEX	0.11°	HIST/RCP8.5
		RACMO			HIST/RCP8.5
	CNRM-CM5	RCA4	Med-CORDEX	0.44°	HIST/RCP8.5
		CCLM4			HIST/RCP8.5
	CNRM-CM5	ALADIN-RCSM4	Med-CORDEX	0.44°	HIST/RCP4.5
		PROTHEUS			HIST/RCP4.5

Table 4.2: Summary of the climate models (global, GCM, or regional, RCM) used in chapters 7 and 8. The name of the global model includes the institute that elaborates the simulation and then the global model's name. The domain of the simulations is Med-CORDEX or Euro-CORDEX, described in the referenced paper.

## **Part III**

# **Results**



CHAPTER

5

---

## **Multi-step scheme and spatial analysis of long-term characteristics of photovoltaic productivity over the Iberian Peninsula**

---

This chapter shows the results of the paper published in Solar Energy journal: *A multi-step scheme for spatial analysis of solar and photovoltaic production variability and complementarity*  
<https://doi.org/10.1016/j.solener.2017.09.037>



---

## **Abstract**

In this chapter, we elaborate a comprehensive methodology to analyze variability and complementarity of PV production that can be applied for long-term energy questions and for climate scales. Thanks to the flexibility of the method, it is not limited to those time-scales or to solar resource. The main steps of the method are the application of an objective clustering algorithm for performing a regionalization of the whole domain selected (Iberian Peninsula), the analysis of the temporal variability of solar radiation and photovoltaic energy yield, and the intercomparison of the obtained clusters for examining their complementarity.

Data of 30 years from a satellite dataset are used in this chapter and long-term aspects of solar radiation variability are analyzed. The spatial distribution and variability of photovoltaic (PV) power yield are calculated for different tracking systems. The variability is analyzed on an interannual time scale, which is relevant for energy supply security and year-to-year price stability. It shows robustness and stability of solar radiation and PV production on average for the Iberian Peninsula, but with significant differences among clusters that could allow for spatial compensation of PV production.

The whole process described in this chapter provides the information of how solar resource and the PV energy yield perform in a limited area and provide the tools to analyze the relationships between sub-areas and their variability. In this sense, this method can be applied for isolated or nearly isolated electric systems located in regions with a variety of climates, or for interconnected systems involving several countries.

## 5.1 Introduction

The natural variability of renewable energy resources like solar radiation and wind presents some challenges for the management of electricity systems, which were designed for conventional technologies like nuclear or thermal power plants. For that reason a thorough knowledge and understanding of space-time features of solar radiation is needed. In the case of solar PV energy, its variability [Wid+15] can be studied from the perspective of the resource or from the perspective of the PV power output, which includes some aspects of the PV generators involved in variability, like inverters or tilted and tracking panels which increase the complexity of the assessment. There are many studies focused on the short-term variability [Zam+14] that analyzed PV production ramps due to changes in solar incident irradiation associated with cloud motion [Cro+14; Rem+15]. Also, the smoothing effect that a well-spread site planning has on the PV production is being investigated [Mar+12; PML13].

Not only short-term scales are important to address renewable resources intermittency but also longer time scales are relevant in order to make the system more efficient and reliable [DT12]. Due to that reason, stakeholders can take advantage of climatological studies of renewable energy resources. Operation and management of the system is done in the short-term and in the long run as well. Consequently, policymakers and operators of the electricity system need an accurate evaluation of resources availability in present and future climate conditions for their mid and long-term planning. The analysis of interannual variability has a particular importance in order to assess stability of the resource and the financial viability of renewable energy plants [PBS06; Bry+18], as well as the likelihood of strong electricity price oscillations like the ones associated for example with the large interannual variations of hydroelectric production.

Regarding that perspective of long-term variability of solar resources, there are studies focused on long series from stations [San+09; SLCW13; PV+12] or reanalysis data that identify low frequency changes in solar radiation, as the “dimming” and “brightening” periods [Wil05], which show relationship between solar irradiation and anthropogenic aerosols [Nab+15]. Some studies examine the influence of large-scale circulation atmospheric modes like the NAO (North Atlantic Oscillation) on solar radiation [PV+04; Jer+13b], while others study the spatial variability instead of the temporal variability [GW11].

Some authors make use of regionalization techniques for atmospheric variables in order to analyze them from a climatological point of view [Arg+11] or for solar energy purposes, mainly for operation and short-term assessment [Zag+13; ZIC14; ZPC14].

In this chapter a multi-step scheme that systematizes the time-space comparison of solar irradiation or photovoltaic productivity among sub-regions of the target area is described, taking into account a large set of factors involved in PV production that could affect the variability of photovoltaic energy yield. Spatial complementarity between clusters is analyzed through correlation coefficients of solar irradiation and PV energy yield time series, showing possibilities for compensating PV production shortages in certain clusters.

This chapter is organized as follows: in first place, a description of the methodology is presented. Each stage of the multi-step scheme is summarized in section 5.3 and explained also in the Methodology chapter 4. After that, the clustering algorithm is applied to the irradiation over the Iberian Peninsula and main results are shown.

## 5.2 Data sources

Surface irradiance data is obtained from CM-SAF (Climate Monitoring Satellite Application Facility). A 30-year period of daily irradiance from 1983 to 2013 is obtained from the SARAH data set [Mül+15]. Its accuracy has been analyzed [Pos+12; Mül+15] against ground measurements from the Baseline Surface Radiation Network (BSRN) [Ohm+98]. For shortwave irradiation daily data, limitations reported by providers are related to high clear sky reflection over bright surfaces like desert areas or due to aerosol data, where only climatology of AOD (aerosols optical depth) is used and no variations in monthly to hourly time scales are considered. However, the mean bias requirement threshold of  $25 \text{ W/m}^2$  of the dataset imposed by providers for accuracy is accomplished [Pos+12; Mül+15].

The temperature data needed for the PV output calculations are obtained from the gridded E-OBS dataset. This product is derived from the EU-FP6 project ENSEMBLES [Hay+08], and it includes daily data of mean temperature with a spatial resolution of 0.25 degrees, derived through interpolation of stations data. We apply a bilinear interpolation in order to obtain the data at the same high-resolution as the solar irradiation grid.

## 5.3 Methods

From data of solar irradiation on the horizontal plane as the starting point of the method, the most common variable obtained from different data sources, the scheme will provide different outputs that can be used to evaluate resource and PV production:

- Regionalization of the area to facilitate the spatial analysis.
- Resource and energy yield aggregated by areas.
- Interannual variability of the resource and the PV production.
- Evaluation of the complementarity of the resource and PV production among areas.

### 5.3.1 Regionalization by clustering

Regionalization procedures provide the ability of extracting general information of the areas that could be treated as a coherent unit, facilitating the analysis and not considering those characteristics that are not under study. As it was explained in the methodological chapter, classical climatological classifications have some grade of subjectivity due to the fact that they rely on arbitrary assumptions [Kot+06] and their criteria are based on temperature and precipitation [TH80]. For our purpose, objective and data-derived criteria are more suitable due to the fact that a different variable is analyzed and its classification does not match classical climate divisions. Objective methods based on clustering techniques have been applied successfully over the

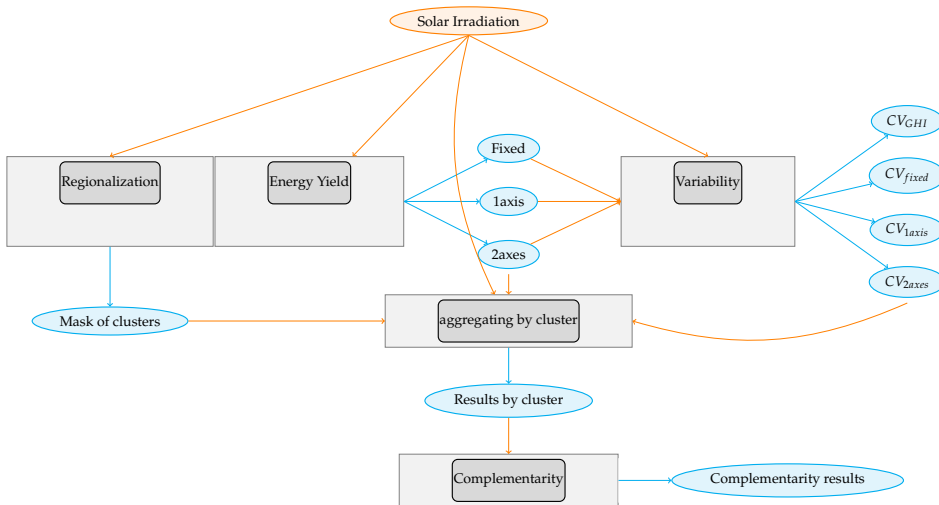


Figure 5.1: Scheme: Each gray block represents each of the operations needed to get the variability and complementarity results. Orange ellipses are the data used and blue ellipses are the results of each stage. If the results of one of the blocks are used as input for another stage, connectors are represented in orange color.

literature for the analysis of renewable energy resources [Pol+15], [Zag+13], [ZIC14], [ZPC14], [Góm+16] and atmospheric variables [Arg+11], [GV+12].

A commonly applied regionalization methodology includes the K-means algorithm after preprocessing the data through Principal Component Analysis [DH04]. This two-step method first reduces redundant information by a Principal Component Analysis that decreases dimensionality of the original dataset. After that, K-means algorithm is applied to the reduced data to find the optimal partition of clusters, which is based on similarity between each element or object inside the cluster and its centroid. This is considered as the most representative element of the cluster, and similarity is measured by an objective function defined in the cluster algorithm.

This method presents some problems regarding the random selection of the cluster centroids in the first step. Different initial centroids can lead to different solution or a local optimum could be found. Also, there could be some computational problems if many iterations are needed to get the final partition.

The procedure used in [Arg+11] and in [ZIC14] is adapted to get the optimal partition in our scheme from a combined clustering grouping and avoiding the above mentioned problems: the **K-means partitional algorithm is initialized with a hierarchical clustering solution of the dimension-reduced data by a Principal Component Analysis**. For the particular case applied in this work, vectors of daily solar irradiation are used for the regionalization. The following steps are needed to get the optimal partition of clusters in the area:

- **To reduce data dimensionality.** Principal components are eigenvectors of an orthogonal matrix after applying a singular value decomposition (SVD) to the original data, daily solar irradiation vectors, whose initial dimension is reduced to the first eigenvectors that retain 95% of the variance. Considering that, a linear combination of these eigenvectors represents the initial data.
- **Hierarchical clustering to initialize k-means.** A hierarchical clustering method classifies data based on a hierarchy. If it is agglomerative, it will start with a cluster for each observation of the data and observations will group together recursively by similarity using the “complete linkage” method. Once the hierarchy is obtained, centroids can be calculated for each emerged partition with a number of clusters between 2 and  $n$ , where  $n$  is a high enough selected number of clusters. Centroids will be the initial seed for the Kmeans algorithm, avoiding the computational problems and favoring reproducibility.
- **K-means algorithm.** The K-means algorithm is a partitional clustering method that minimizes an objective function that defines similarity among the ele-

ments of each cluster. In our case we made use of the Euclidean distance, Eq. 5.1 between the objects or elements in the cluster,  $x_i$ , and its centroid,  $c_j$ , as the objective function. The number of clusters in which the data is divided into has to be known beforehand. In order to overcome the inconvenience, the algorithm is run from 2 to  $n$  clusters and the optimum number is determined by making use of a clustering validity index after that.

$$J = \sum_{i=1}^k \sum_{j=1}^n ||x_i - c_j||^2 \quad (5.1)$$

- **Validity index.** In order to determine the optimal partition, validity clustering techniques are applied. There are two types of validation for the clustering methods. First, external clustering validation methods that make use of external information out of the data; and secondly, there are internal clustering validation methods that rely only on information from the data [Liu+10]. The latter are used to preserve objectivity as much as possible and are based on two criteria: compactness and separation of the clusters emerged. We use one of the most applied validity indices, the Calinski-Harabasz index [CH74], CH, that evaluates the average between and within cluster sums of squares.
- **L-method.** CH index is calculated for every partition from 2 to  $n$  clusters. The resulting CH graph in Figure 5.2 for the Iberian Peninsula regionalization is shown for a number of clusters between 2 and 70 as an example. Theoretically, the partition with the maximum CH is the optimum, but the graph shows a decreasing trend which leads to imprecision in finding the optimum. The large number of data and the continuous variable analyzed are responsible for that. For that reason, the L-method is applied [SC04]. This method selects the intersection of two best-fit lines in the graph CH vs.  $k$ , where  $k$  is the number of clusters of the partition [Zag+13]. All possible pairs of lines that fit linearly to the left and right sequence of data points are created. Each line has at least two points. The total root mean squared error is calculated as in Eq.:5.2:

$$RMSE_T = \frac{c-1}{k-1} RMSE_{left} + \frac{k-c}{k-1} RMSE_{right} \quad (5.2)$$

Where  $c$  is the number of clusters where the graph is split into the two fit-lines,  $k$  is the total number of clusters. The “total root mean square error” is a weighted error with two terms, one for each side of  $c$  in the graph. Each side has a heavier weight depending on the points involved in the fitting. The minimum of  $RMSE_T$  gives us the optimum number of clusters of the data [Zag+13] which are used in the following steps.

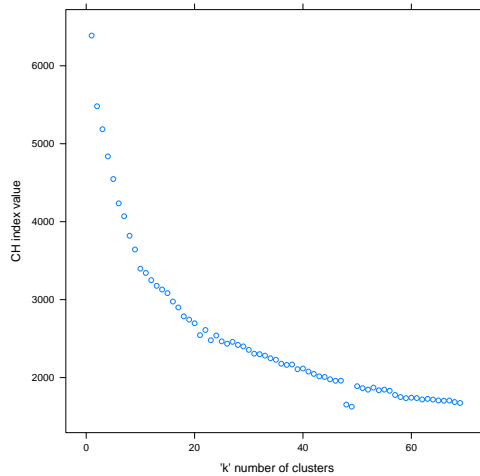


Figure 5.2: Calinski-Harabasz index by “k” number of clusters

### 5.3.2 Photovoltaic energy yield

The simulation of a photovoltaic energy system is carried out in two steps, as described in a previous chapter. The method is summarized here in order not to miss the coherence of the text.

1. In first place, global irradiation at the horizontal plane,  $G(0)$ , is transformed into the plane-of-array irradiation,  $G(\alpha, \beta)$ , where  $\alpha$  is the azimuth angle and  $\beta$  the inclination angle of the generator plane. Due to optical losses (reflection, angle of incidence, and dust), the irradiation available is reduced for the photovoltaic cells inside the panels and the plane-of-array irradiation is then denoted as effective irradiation on the PV generator  $G_{eff}(\alpha, \beta)$ . Three different types of tracking types are considered for the photovoltaic generator, which affect the tilt of the panels:
  - **Fixed:** panels with an optimum angle of inclination that depends on the latitude of the place.
  - **One Axis:** North-South oriented panels that track the sun daily varying the azimuth angle.
  - **Two-axes:** tracking system that allows variation of the azimuth and inclination angles.

2. Once the effective irradiation that reach solar cells has been assessed, the second step is the transformation into power output that depends on the photovoltaic system. The photovoltaic system is composed of a PV generator, consisting of several PV modules, and an inverter to transform the DC current output from the generator into AC current to be integrated into the network.

### 5.3.3 Variability and complementarity

The metric to analyze interannual variability is the coefficient of variation, CV (Eq.5.3), which is defined as:

$$CV = \frac{\sigma}{\bar{X}} \quad (5.3)$$

In this equation,  $\sigma$  is the standard deviation of the variable analyzed and it is divided by the mean of the variable in the period of the study. Sometimes CV is represented in percentage. This measure is dimensionless and can be applied in different time scales, which is helpful for comparisons.

To assess complementarity of the solar resource in the area of study, the Pearson's correlation coefficient between the time series of pairs of clusters is calculated, Eq. 5.4. Different aggregation time steps for the time series (daily, monthly, etc.) can be selected to assess complementarity in different time scales.

$$\rho_{i,j} = \frac{\sigma_{c_i, c_j}}{\sigma_{c_i} \sigma_{c_j}} \quad (5.4)$$

In this equation,  $c_i$  and  $c_j$  are the time series corresponding to the clusters  $i$  and  $j$ .

For a spatial complementarity analysis the range of the area studied has to be taken into account. The area must be large enough to make sense of the comparison between zones, due to the fact that geographically dispersed areas, far from each other, will have very different evolution of atmospheric variables. At the same time, large areas may not be interesting from the electricity generation point of view if, for instance, they are different networks without any market interaction. On the other hand, if the area of study is too small, atmospheric variables and therefore, renewable resources will evolve in a very similar way. For such small areas, local complementarity between different resources can be analyzed, but spatial complementarity of one resource cannot.

The correlation coefficient for an entire long time series may hide changes in complementarity for shorter sub-periods. For that reason a moving correlation window can be applied, in order to provide an indication of how correlation between clusters

varies during the whole period. Width of the window is selected depending on the case under study and the time scale evaluated. For some studies, it can be interesting to assess weekly variations of the correlation coefficient between areas, whereas in other cases, it is more important to consider lower frequency variations in the complementarity.

A 15 years moving window is selected over a 30-years monthly time series in order to look for higher frequency changes in the correlation coefficient patterns inside the entire period. Thus, a collection of correlation coefficients by month for each pair of clusters will be obtained. In order to detect the most important cluster pairs regarding complementarity, the median of the whole set of correlation coefficient series is calculated for each pair of clusters. Then, the sorted coefficients will indicate the cluster pairs that reach lower values of correlation being potentially interesting for the spatial complementarity.

## 5.4 Results

### 5.4.1 Regionalization

The optimal partition after having applied the clustering method is represented in Figure 5.3. The CH validation procedure gives an optimum number of 19 clusters for the area, where each of the clusters has an homogeneous time evolution of solar irradiation. Due to the nature of clustering techniques, there is not a unique/best method to select the optimum partition. Another index (Davies-Boudin, [DB79]) has been applied for comparison, and the obtained optimum number of clusters was of the same order than for CH index.

The ability of the clustering method to select optimum regions and to represent different climates of the area can be highlighted evaluating aggregated values of yearly mean of daily irradiation by cluster. Higher values are found in clusters 14, 15, 17, 18, 19, as can be seen in Table 5.1 which corresponds to the southern half of the Iberian Peninsula. Apart from this latitude-related maximum irradiation, a particularly high value is found in cluster 11, clearly above all surrounding clusters in the northern half of the Iberian Peninsula. This cluster corresponds to the central Ebro basin, which is characterized by a very dry continental climate. It is a deep depression totally surrounded by mountain ranges like the Pyrenees, which frequently cause a Föhn effect which reduces cloudiness and precipitation in comparison with other nearby clusters. Excluding this cluster, irradiation in the northern half of the Iberian Peninsula (1, 2, 3, 4, 5, 6) is lower than in the southern half, and the minimum values are found in clusters in the northern coast and the Pyrenees. The maximum solar irradiation

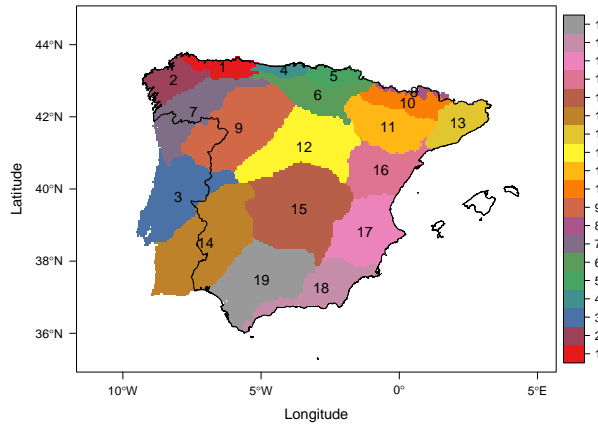


Figure 5.3: Optimal partition of 19 Clusters after applying the algorithm and the validity index. Geographically clusters can be roughly divided: north-west (2,7), north (1,4,5,6), Pyrenees (8), north-east (10,11,13,16), south-east (17,18), centre-north (9,12), west (3), centre-south (14,15,19)

---

is 50 percent higher than the minimum, which reflects the large climatic differences between clusters.

#### 5.4.2 Variability results

After regionalization, an analysis of solar irradiation at the horizontal plane and PV yield by tracking system is performed, including their temporal variability.

Regarding interannual variability, we have calculated the CV of two time-aggregated means of solar irradiation and PV yield:

- On one hand it is applied for the yearly mean of daily irradiation  $G_{d,y}(0)$  and yearly PV yield. This metric gives the variation of the energy from one year to another and if it is low, general stability of the solar resource and PV production is guaranteed.
- On the other hand the interannual variability of the monthly time series  $G_{d,m}(0)$  and monthly energy yield is also investigated in order to quantify differences in the annual cycle.

Zone	$G(0)$	$CV_{G0}$	$Yf_{\text{Fixed}}$	$CV_{\text{Fixed}}$	$Yf_{\text{One}}$	$CV_{\text{One}}$	$Yf_{\text{Two}}$	$CV_{\text{Two}}$
1	3.4	3.6	1047	4.2	1225	4.9	1381	5.1
2	3.8	3.2	1120	3.6	1359	4.3	1520	4.6
3	4.6	2.8	1350	3.4	1720	3.7	1921	4.1
4	3.4	4.1	1024	4.7	1198	5.4	1351	5.7
5	3.4	4.2	1035	4.7	1226	5.5	1374	5.8
6	4.0	3.2	1190	3.7	1465	4.2	1640	4.5
7	4.1	3.4	1224	3.9	1530	4.4	1712	4.8
8	3.6	4.6	1099	6.3	1322	6.4	1473	7.5
9	4.5	2.7	1356	3.0	1725	3.5	1934	3.8
10	4.4	2.7	1367	3.2	1696	3.6	1937	3.9
11	4.7	2.0	1404	2.6	1787	2.7	2024	3.1
12	4.5	2.6	1348	3.1	1701	3.5	1911	3.8
13	4.4	2.7	1340	2.9	1660	3.4	1893	3.7
14	4.9	2.2	1423	2.8	1837	3.0	2047	3.4
15	4.9	2.3	1427	2.9	1837	3.0	2057	3.4
16	4.5	2.6	1374	3.0	1722	3.4	1946	3.7
17	4.9	2.5	1429	2.9	1830	3.3	2052	3.6
18	5.1	2.4	1470	2.9	1906	3.2	2123	3.5
19	5.1	2.1	1456	2.8	1891	2.8	2105	3.7

Table 5.1: Values of yearly mean of daily irradiation  $\left[ \frac{\text{kWh}}{\text{m}^2} \right]$ , yearly yield by tracking system  $\left[ \frac{\text{kWh}}{\text{kWp}} \right]$  and interannual CV of yearly mean in percentage %.

The CV is also aggregated by cluster, in order to facilitate the intercomparison among areas.

### Yearly mean

The results for the CV of the yearly mean of daily irradiation and of the annual mean yield by tracking type, aggregated by cluster, are shown in Table 5.1. Also, yearly mean of daily irradiation is represented, showing differences in resource among areas, as well as yield differences.

The highest values of CV (above 4%) are seen in clusters 8, 4 and 5. These clusters correspond to the Pyrenees and the northern Cantabric coast. This behavior can be explained in part through the influence of variable summer cloudiness, as these areas are not affected by the summer dryness typical of the Mediterranean climate of most of the Iberian Peninsula. Southern and central regions are the least variable. Remarkably, the lowest value of CV is found in cluster 11, corresponding to the central Ebro basin, located at the north of the Iberian Peninsula. Very low values near 2% are also found in the southwestern clusters (4 and 19), a result that coincides with [Gil+15]. Finally, the north-western clusters (2 and 7) show a higher value than the northeastern

cluster 13, despite sharing the same latitude. The north-western clusters are particularly influenced by the Azores high position and interannual variability.

Regarding the electricity production, power from the PV generator depends quasi-linearly on solar irradiation at the plane-of-array ( $G_{eff}(\alpha, \beta)$ ), apart from second order effects (spectrum, wind, etc) [PLC07]. Due to that, the fixed typology is the one with lower yield because the amount of irradiation reaching cells is lower than the amount of energy reaching panels when trackers are allowed to move in one or two axes.

For areas where solar irradiation is higher, yield differences between trackers are higher. This can be seen in Figure 5.4 where yearly mean yield for the 30-years period is aggregated by cluster and tracking system, and clusters are sorted vertically from less to more energy yield. Yield increase from fixed panels to one-axis panels is non-linear. This increase ranges between 17% for the clusters with less solar irradiation, located at the northern coast like clusters 4, 5; and 30% for the southern clusters with more solar irradiation (clusters 18, 19). In contrast, energy yield increase from one-axis to two-axes panels is almost constant, around 12% for all clusters. A consequence of the non-linear PV yield increase from fixed to one-axis panels is that the energy yield differences between clusters are much higher for tracking than for fixed systems. While for fixed panels PV energy yield varies between 1000 and 1450  $\left[\frac{kWh}{kWp}\right]$ , for two-axes systems it varies between 1350 and 2100  $\left[\frac{kWh}{kWp}\right]$ . These average values are coherent with results obtained in [ATCP13].

### **Monthly mean**

Variations in electricity prices from one year to another are significantly dependent on the interannual variation of the monthly renewable electricity production. This time-scale is also mostly influenced by the large scale circulation modes for solar potential in the Iberian Peninsula [JT13] and the winter half of the year, from October to March, is especially variable.

Annual cycles of interannual monthly CV are represented in Figure 5.5. The interannual variability for monthly yield is higher than for the solar irradiation at the horizontal plane. In winter months, these differences in CV are much higher than in summer. This behavior is more pronounced in northern areas (clusters 1, 2, 3, 4, 5, 6, 7). Seasonal patterns can be appreciated in all the areas although some clusters in the north-east area (13, 11) present flatter cycles.

Regarding solar irradiation variability, it is also important to notice the differences in winter months between the eastern and north-western sides of the Iberian Peninsula. Eastern clusters (10, 11, 13, 16, 17, and 18), have smaller values of CV (below 15%) in

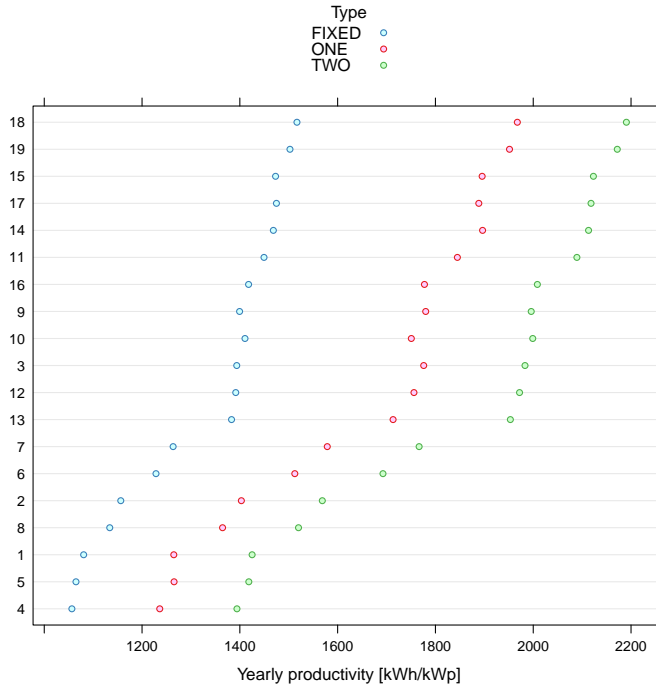


Figure 5.4: Yearly mean of PV yield by cluster and for each tracking system  $\left[ \frac{\text{kWh}}{\text{kWp}} \right]$ . Values are sorted from lower to higher yield values.

winter than northern and north-western clusters (1, 2, 3, 4 and 7), where values above 15% and close to 20% are found. In summer there is a different behavior because the main differences exist between the north and the south of the Iberian Peninsula. Northern clusters (1, 2, 4, 5 and 8) show summer CV values above 7%, while southern clusters (15, 14, 17, 18 and 19) show very low values, around 2%.

Cluster 8, in the Pyrenees region has the highest values in winter, above 25%. Its annual cycle has a wide range between winter and summer, decreasing to 7% in August. On the other hand, north-eastern clusters (13, 11, and 10) show the smallest differences between winter and summer for the CV of solar irradiation.

In order to quantify differences in variability between solar irradiation and solar power output, the ratio between variability of yield by tracking system and solar irradiation is represented in Figure 5.6 for each month and cluster. If CV of energy yield is higher than CV of solar irradiation, values are above one. On the other side, values will be below one if CV of solar irradiation is higher than CV of energy yield.

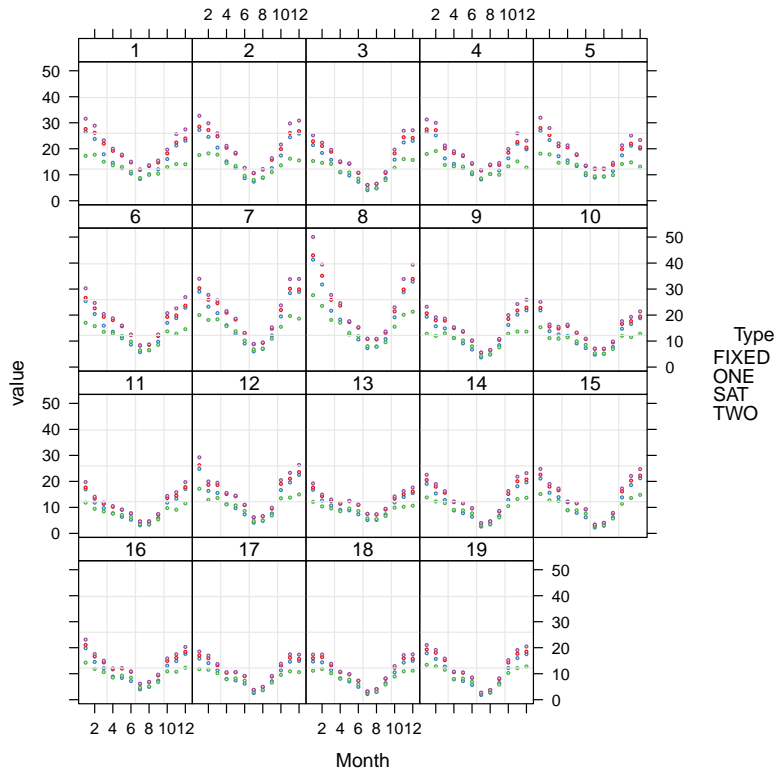


Figure 5.5: Annual cycle of CV (%) by cluster and for each tracking type and global solar irradiation at the horizontal plane.

The highest ratios are obtained between  $CV_{\text{Two}}$  and  $CV_{G0}$ . The ratio of  $CV_{\text{One}}$  is clearly lower in winter months, but in summer it is very similar to the ratio of  $CV_{\text{Two}}$ . Yield with a 'horizontal' axis tracker and 'two-axes' trackers increase the variability between 20% in summer and more than 80% in some areas in winter. The fixed typology ratio,  $CV_{\text{Fixed}}/CV_{G0}$  has a much wider range in the whole year. In winter months, it has values between 1.2 and 1.6, depending on the cluster, and is not far from the other two typologies. In contrast, this ratio decreases rapidly in summer months, reaching values below one between May and August. This means that for that period, variability of the "fixed yield" is smaller than variability of solar irradiation at the horizontal plane.

The results of CV show that variability of PV energy yield at tilted panels is higher than variability of solar resource at the horizontal plane in most cases, which can be

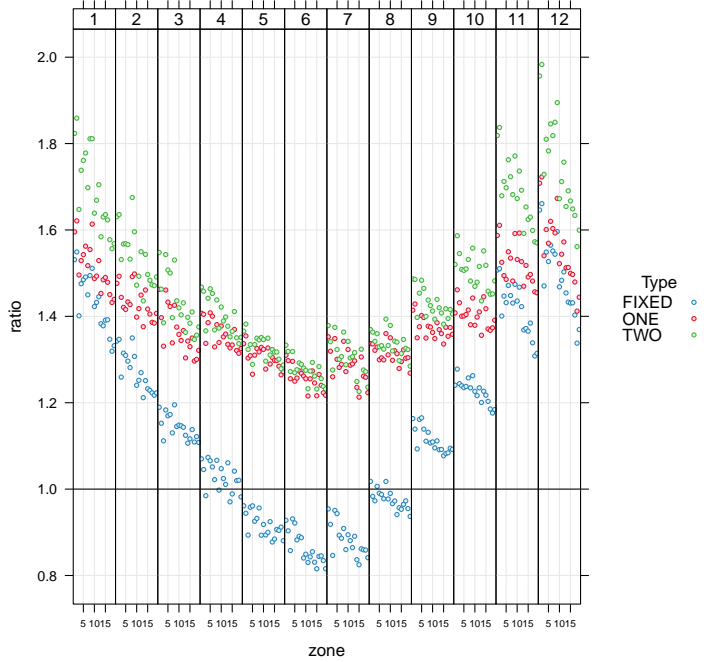


Figure 5.6: CV ratios between each type of tracking system and solar irradiation at the horizontal plane, grouped together by month in the graph. Ratios are calculated for each cluster, represented in the x axis. “Fixed” represents  $\frac{CV_{\text{Fixed}}}{CV_{G0}}$ , “One” is  $\frac{CV_{\text{One}}}{CV_{G0}}$  and “Two” is  $\frac{CV_{\text{Two}}}{CV_{G0}}$

explained by the nature of solar irradiation at tilt panels and its dependency of solar irradiation at the horizontal plane [Per09].

### 5.4.3 Complementarity results

The monthly time series are also selected for the complementarity analysis. Regarding solar power complementarity, opposite-evolving time-series for different areas would strongly increase the reliability of the whole electric system, as shortfalls of solar irradiation in certain areas could be compensated by above-normal irradiation in others. However, this ideal situation is difficult to find in a rather limited area like the IP, at least for monthly time scales over a long time period of 30 years. In this case, the absence of correlation also becomes important, as it avoids simultaneous shortfalls or simultaneous above-normal values and therefore, softens the overall power production. Overall, the 30-year period correlation matrix for each month shows that southern and eastern clusters are uncorrelated at least during part of the year

with northern and northwestern clusters. In some cases, the absence of correlation is found between nearby clusters. A more detailed discussion can be found in the appendix A.

It could be that the obtained clusters present higher complementarity in shorter sub-periods. As explained in section 5.3.3, we have divided the whole 30-year period in sub-periods of consecutive 15 years. The correlation coefficients have been calculated again for the resulting 15-year moving window, for each pair of clusters and for each month. In this way, we obtain how each correlation coefficient evolves during the 30 year period. The analysis has been applied for the four variables in the study: solar irradiation at the horizontal plane and PV energy yield for each tracking system.

The correlation coefficient evolution of the photovoltaic energy yield obtained with fixed panels and for the most important pair of clusters, in terms of complementarity (2-18), is represented in Figure 5.7 to illustrate main results. In addition, the less relevant pair of clusters (15-19), the one with the highest medium value of the correlation coefficient, is also overlapped in the Figure in order to show the differences that exist between the areas that present complementarity in some points of the period and those with high positive values for the whole time series.

Other relevant pairs for complementarity include a northern (1, 2, 4 or 5) and a south-eastern cluster (17 or 18), although they are not shown in the graph. They behave similar to the pair 2-18, with a swinging time series that reaches negative values below -0.6 for the correlation coefficient at some 15-years sub-periods.

Among the first pairs in terms of complementarity, it is important to remark the appearance of 3-4 and 3-5 although they are not shown in the graph. These clusters are closer than the previously commented cases, which highlight the adequacy of the clustering method. All three are Atlantic coast clusters, but while cluster 3 includes part of the western coast, clusters 4 and 5 are northern coastal areas. This fact, together with the position of the main mountain ranges, can explain their partially complementary behavior.

In order to highlight the months with maximum anti-correlation, Figure 5.8 presents, for the same cluster pairs as above, the minimum values of the monthly correlation coefficient (where the minimum for each month is calculated over all 15-year sub-periods). Differences between months are clearly observed in this graph. Only two months (March and June) show consistent positive values of this parameter and therefore, a low complementarity. In the other months, this parameter predominantly has negative values, revealing a certain degree of complementarity for the pair 2-18.

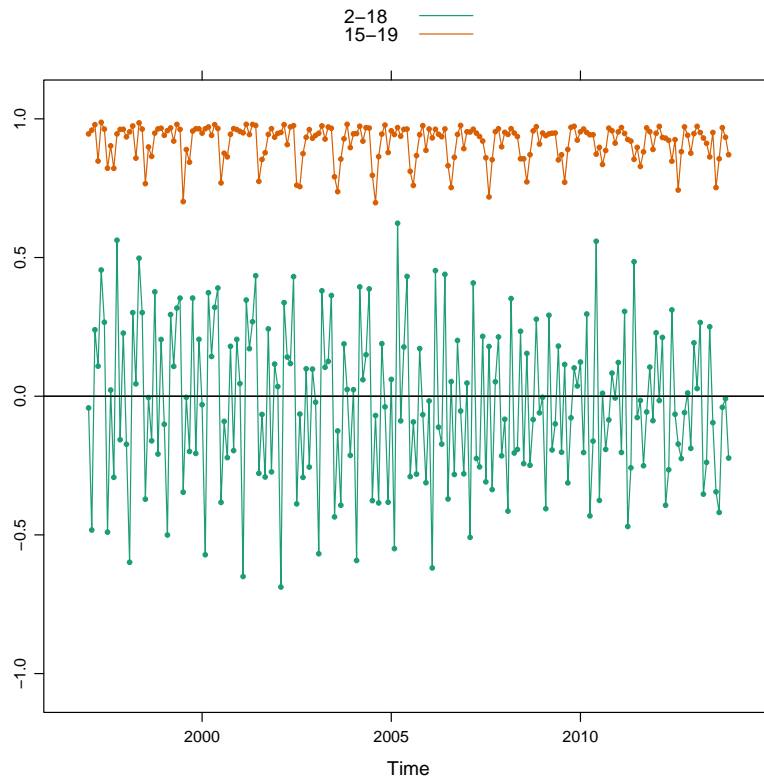


Figure 5.7: Correlation coefficient of photovoltaic energy yield with fixed panels: evolution of a 15-year moving window of monthly values, for the first cluster pair showing the smallest median correlation value (2-18) and the latest with highest median correlation value (15-19).

## 5.5 Conclusion

A detailed understanding of the space-time variability characteristics of renewable energies is fundamental for an adequate planning and management of the electrical system. In this chapter, a multi-step scheme to analyze spatial and temporal variability of renewable resources and production is described, which is implemented here for solar irradiation and photovoltaic energy yield. The method is comprehensive, as it includes 4 different steps covering spatial and temporal variability, spatial complementarity and also a detailed calculation of PV yield that is not usually taken into account in other studies of this subject. The 4 steps are:

1. Regionalization by an objective clustering procedure, that facilitates the inter-comparison between sub-regions and the spatial analysis.

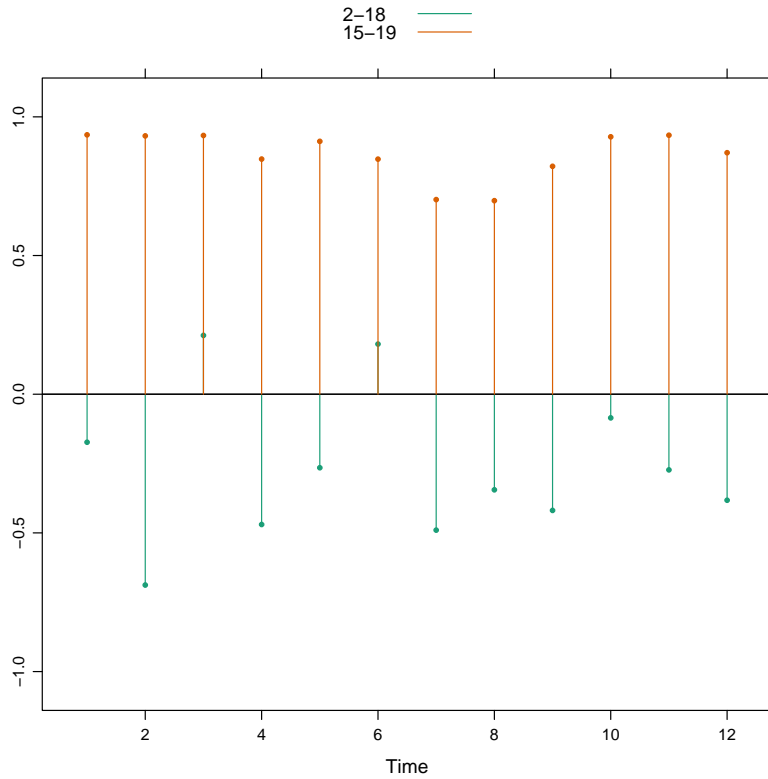


Figure 5.8: Correlation coefficient of photovoltaic energy yield with fixed panels: minimum values of the monthly correlation coefficient, for the same cluster pairs as figure 5.7. The minimum is calculated over all 15-year sub-periods.

---

2. Assessment of energy yield considering different tracking systems, with a model that includes a large number of processes affecting the final power output.
3. Quantification of temporal variability in different time-scales with a robust metric, the coefficient of variation (CV). Due to its dimensionless character, this metric allows for a direct intercomparison of different magnitudes and energy resources.
4. Spatial complementarity assessment using the correlation coefficient, revealing potential options for smoothing out resource and production variability.

The procedure is implemented over the Iberian Peninsula as an example of the scheme applicability. This region has been selected due to its large variety of climates and relevant electricity network characteristics, as it is internally well interconnected but

externally it is poorly integrated with other electrical systems. A 30-year period of satellite data has been applied to analyze variability by subregions. An interannual time scale is selected for the variability analysis, due to its importance for the reliability and the financial viability of renewable energy production. A stable year-to-year production also contributes to reducing year-to-year price oscillations. Relationships between subregions of the IP are investigated in order to assess complementarity and detect possible compensation options. The procedure is applied to solar resource (global horizontal irradiation) and also to the PV yield with different tracking systems. A fundamental contribution of the present study is the consideration of tilted panels and the quantification of differences between tracking systems. It has been proved that this kind of assessment is relevant in the variability analysis. In particular, we show that the increase in PV yield when passing from fixed tilted PV panels to one-axis tracking panels is non-linear, and depends strongly on the value of fixed panel energy yield: subregions with a larger fixed panel productivity show a larger relative increase with the use of a one-axis tracking system. In contrast, the PV yield increase between one-axis and two-axes systems is almost linear.

The clustering method has proved its selective character for detecting sub-regions with relevant differences in solar resource as it is shown in the case of study. This is illustrated, for instance, in the selection of cluster pairs formed by two Atlantic coast subregions as pairs showing a relatively high complementarity. It has been also shown that a moving window is useful to detect sub-periods of higher correlation between regions. The correlation characteristics of cluster pairs change over time if shorter 15-year sub-periods are considered, instead of the whole 30-year period of data. Negative correlation values are detected for most months, with two exceptions: March and June. July, August and September show relatively high anticorrelation between certain clusters, which is important as these months include the summer demand peak.

This work provides a robust and comprehensive methodology that can be extended to other domains and to other timescales. The method can also be adapted to other types of renewable energy generation, like wind or solar thermoelectric, and can also provide combined assessments of different renewable resources, offering for example information about complementarity of solar and wind energy. Future applications of the method will explore such extensions.

## Appendix A

### Yearly mean values and variability

The highest values of CV for solar irradiation (above 4%) are seen in clusters 8, 4 and 5. These clusters correspond to the Pyrenees and the northern Cantabric coast. This behavior can be explained in part through the influence of variable summer cloudiness, as these areas are not affected by the summer dryness typical of the Mediterranean climate of most of the Iberian Peninsula. Southern and Central regions are the least variable. Remarkably, the lowest value of CV is found in cluster 11, corresponding to the central Ebro basin, located at the north of the Iberian Peninsula. Very low values near 2% are also found in the southwestern clusters (4 and 19), a result that coincides with [Gil+15]. Finally, the northwestern clusters (2 and 7) show a higher value than the northeastern cluster (13), despite sharing the same latitude. The northwestern clusters are particularly influenced by the Azores high position and interannual variability.

Irradiation data and their CV are also graphically represented in Figure 5.9, showing their geographical distribution. The functions represented at the margins of the graphs, show respectively the latitudinal and longitudinally aggregated value of the variable. In latitude, both, global irradiation and CV are inversely related. Regarding the longitude axis, a contrast between coastal and interior values is seen for the irradiance, while the CV shows a complex behavior, predominantly with higher values near the western and eastern coast than in the interior parts.

Figure 5.10 shows photovoltaic energy yield by tracking system and their CV values. The increase in the CV with different tracking typologies can be seen. In each case it is possible to appreciate the difference between northern Iberian Peninsula, with higher variability, and the southern Iberian Peninsula, with lower variability. An exception to this latitudinal dependence is again the central Ebro basin, which stands out as the cluster with the lowest variability, particularly for the two-axes tracking. There are also differences between the western and eastern sides of the Iberian Peninsula, showing the last one lower variability on this time scale.

Figure 5.11 shows differences between clusters and tracking typologies combining CV and yield in the same graph. Straight lines are representing mean values for the whole IP. The CV values for yearly yield are around 4% for the two-axes tracking system in the whole area, and close to 3% for the fixed panels. The CV of the annual mean of daily irradiation is about 2.3%. For the x axis, where yield is represented, areas with higher resource have higher PV yield and differences between clusters are larger for those areas. It is easy to notice that by comparing clusters 1 and 19.

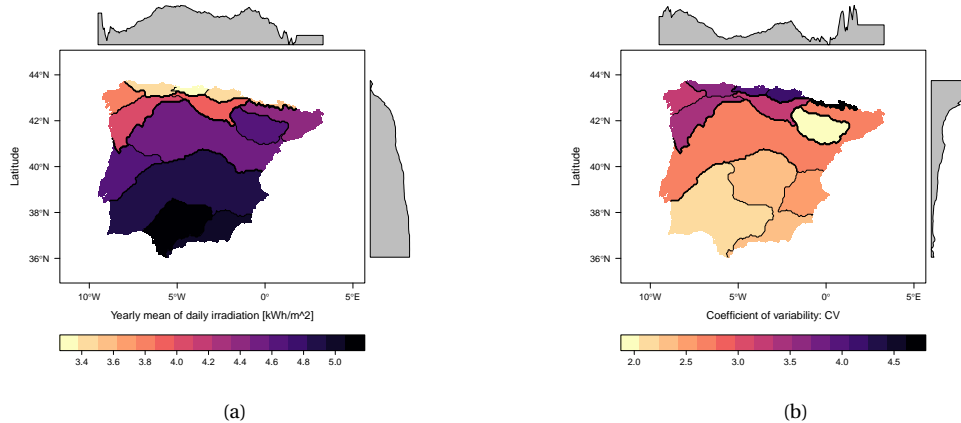


Figure 5.9: Yearly mean of solar irradiation and its CV. Figure [a] shows the yearly mean of daily irradiation period 1983-2013  $\left[ \frac{\text{kWh}}{\text{m}^2} \right]$ . Figure [b] shows the coefficient of variability, CV of the yearly mean of daily irradiation

This figure also facilitates visualization of each cluster's size, due to the fact that each point represents one cell of the domain, and reveals the compactness of most clusters. Only a couple of clusters (8 and 18) show wide dispersion of individual points. Cluster 8 includes the highest mountains of the IP, which could explain this dispersion. For cluster 18, it is seen that although the majority of its points have values of CV below the mean of the IP, there are some of them with high values of CV.

## Complementarity

Figure 5.12 represents the correlation matrix, for each month and for all pairs of clusters, of the solar global irradiation at the horizontal plane, considering the whole period (1983-2013). Correlation coefficient varies in the annual cycle for each pair of clusters. Most of the relationships show a high positive correlation coefficient. This is the case particularly for northern clusters (4, 5, 6), which are highly correlated for every month. For clusters in the southern half of the Iberian Peninsula, from 14 to 19, the correlation coefficient is also positive, although it decreases in July and August for most of the pairs.

However, the high positive correlation is not general. Northern clusters 4 and 5 are slightly correlated, not correlated or slightly positive correlated with southern clusters (14 to 19) for every month. This pattern is amplified in November, where the highest anti-correlation values are found between clusters 5 and 17 and between clusters 5

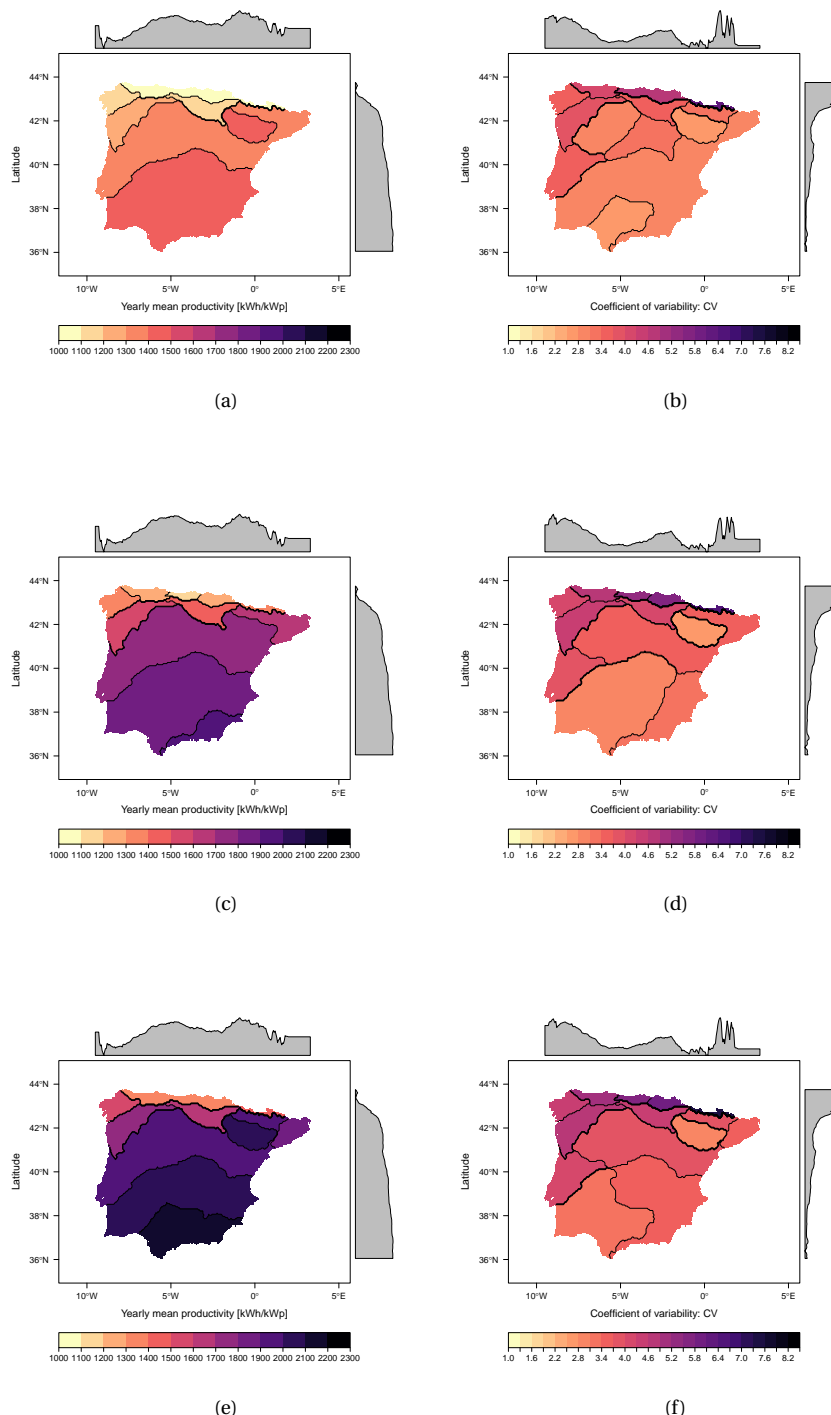


Figure 5.10: First column: maps of yearly mean yield by tracking type  $\left[ \frac{\text{kWh}}{\text{kWp}} \right]$ , mean by cluster (a, fixed; c, 'ona axis'; e, 'two axes'). Second column: maps of interannual coefficient of variability, CV, of the yearly mean yield by tracking type and by cluster (b, 'fixed'; d, 'one axis'; f, 'two axes')

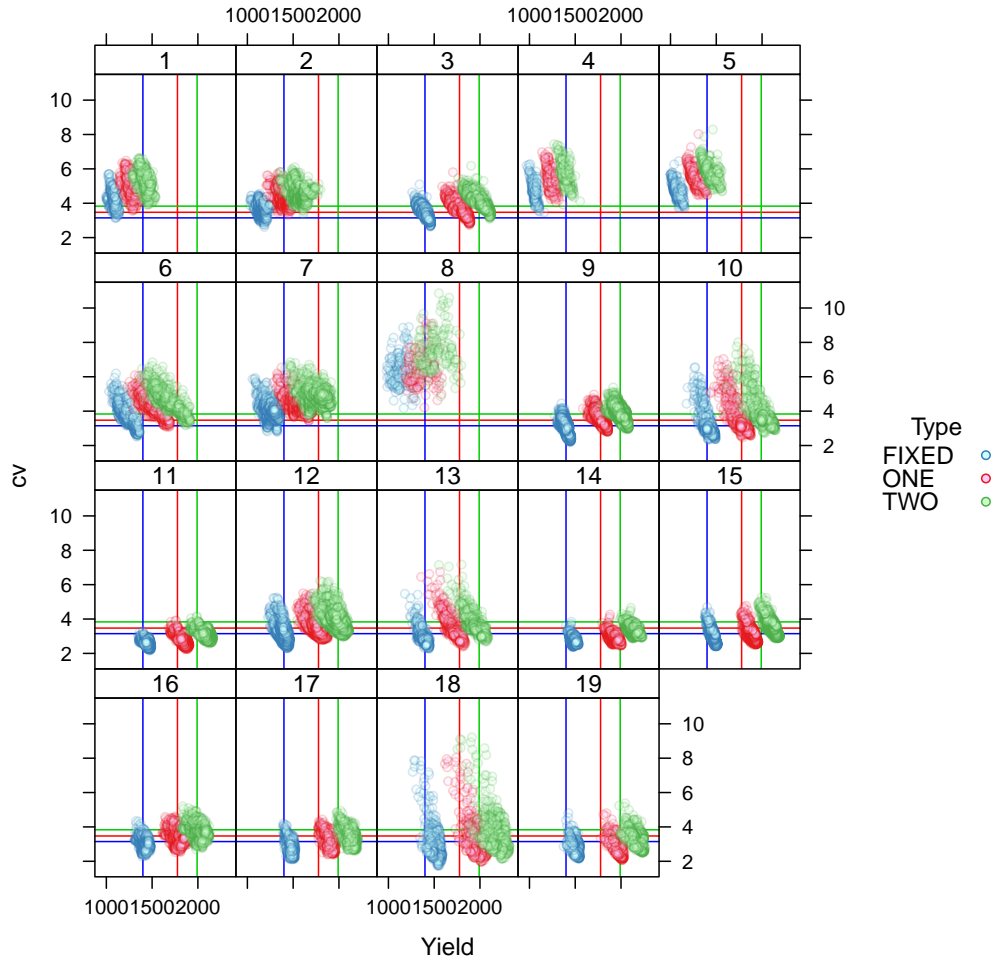


Figure 5.11: Yearly mean of PV yield  $\left[ \frac{\text{kWh}}{\text{kWp}} \right]$  (horizontal axis) and CV (vertical axis in percentage) by cluster and tracking system. The individual points correspond to individual grid points forming part of the clusters. Transparency of dots is applied to show importance of the number of points inside the clusters regarding its value of CV.

and 18. This negative correlation is statistically significant, in contrast to other cases with negative correlation. The absence of positive correlation between southern and northern clusters is more evident between clusters 17 and 18, at the south-east of the IP, and clusters 1 to 5 in the north. Overall, southern and eastern clusters are uncorrelated at least during part of the year with northern and northwestern clusters. In some cases, the absence of correlation is found between nearby clusters: in winter months, the north-eastern cluster 11 (central Ebro valley) is uncorrelated to the closely-lying clusters 4, 5 and 8 (in the northern coast and Pyrenees). This is probably related to persistent atmospheric situations with north to north-westerly winds, that cause cloudiness in the windward clusters and clear skies in the leeward Ebro cluster, due to a Föhn effect.

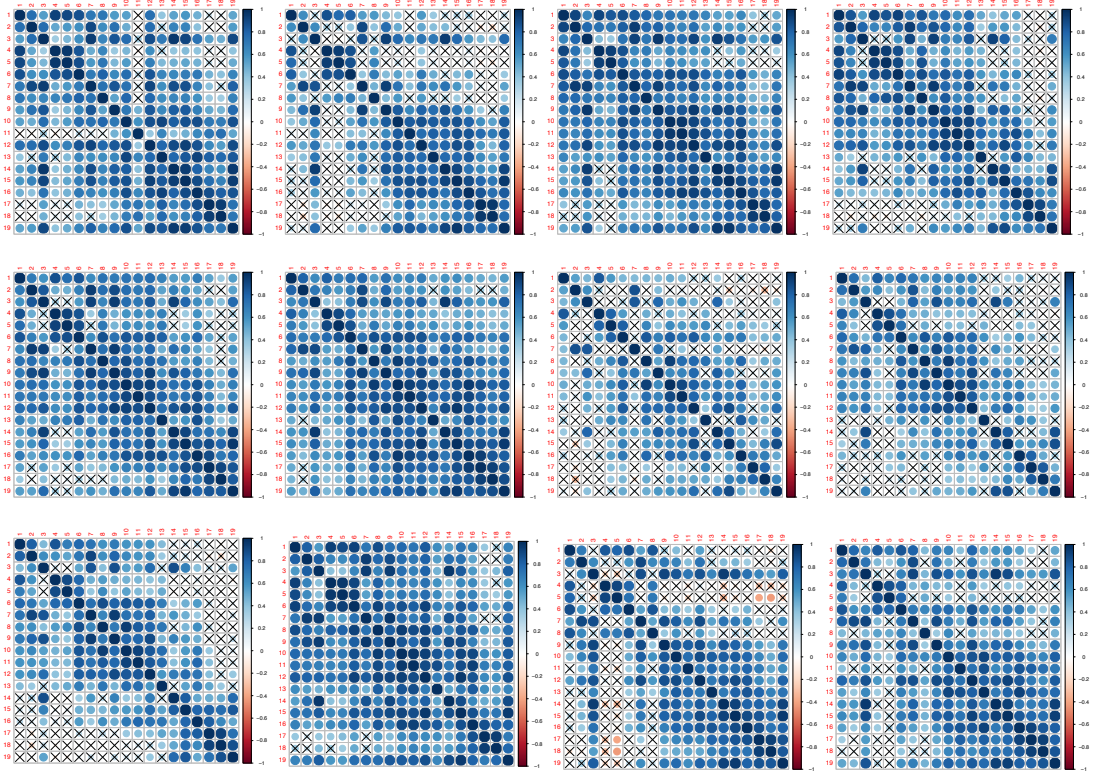


Figure 5.12: Correlation matrix of the monthly time series for the period 1983-2013, between all pairs of clusters. First row: January to April, second row: May to August, third row: September to December. Circle's size means significance of the correlation and the color bar represents the positive correlations in blue and negative correlations in red. Crosses indicate that correlation is not statistically significant. Row and column numbers are cluster numbers.



CHAPTER

# 6

---

## **Impact of aerosols on photovoltaic energy production over the Euro-Mediterranean area**

---

This chapter shows the results of the paper published in Solar Energy journal: *Impact of aerosols on the spatiotemporal variability of photovoltaic energy production in the Euro-Mediterranean area.*  
<https://doi.org/10.1016/j.solener.2018.09.085>



---

## **Abstract**

The aim of this work is to assess the influence of aerosols on photovoltaic energy production from seasonal to multi-decadal time scales. For this purpose we use various coupled aerosol-climate simulations that take into account the complex spatial and temporal patterns of natural and anthropogenic aerosols over the Euro-Mediterranean domain.

The results show that aerosols strongly influence the spatial pattern, seasonal cycle and long-term trend of PV production. The most affected area is Central Europe where sensitivity of PV production to aerosols is higher. The annual production loss due to aerosols ranges from no impact to  $-16\%$  in The Netherlands, with variation depending on the area and on the typology of the tracking system. The summer production loss can even reach  $-20\%$  over regions of Africa and Syria-Iraq.

We conclude that aerosols cannot be neglected in the assessment of PV production at large time scales over the Euro-Mediterranean area. Besides, the potential increase in energy due to reduction in the anthropogenic aerosols is shown in the simulation of the brightening period over Europe, with an increase of  $2000 \frac{\text{kWh}}{\text{kWp}}$  in a PV lifetime for the most affected areas. It illustrates the evolution that PV potential could follow in highly polluted areas through the effective implementation of pollution control measures.

## 6.1 Introduction

Aerosols particles influence the climate system directly, affecting the Earth's radiation budget by scattering or absorption of solar radiation, or indirectly, changing cloud properties. Due to their importance in the amount of solar radiation that reaches the Earth's surface and their effect in the changing climate, the evaluation of their impact on the solar resource for energy purposes is of special interest.

A general lack of well-spread surface stations, previously commented, which provide solar radiation measurements, has made the satellite information the main and most reliable source of data up to now, due to its spatial and time resolution [Pos+12; Ine14]. However, satellite retrievals were not available several decades ago and they do not allow to quantify the effect of specific factors on solar irradiance. Thus for investigating long-term statistics and to disentangle the various factors influencing solar resource, a different approach is needed. Models are the best tool to understand processes that occur in the atmosphere and their link with the resource variability, as individual factors can be included or removed in them, allowing the isolation of their effects.

Due to the increasing concern about the availability of renewable energy resources under climate change scenarios, climate modeling has revealed itself as a valuable tool for evaluating future energy potential [Cro+11; Gae+14; Gae+15; Jer+15b; Jer+15a; Tob+16]. However, representation of the clouds is still one of the main challenges for these models, and the spatio-temporal variability of aerosols is rarely taken into account in some of regional climate models [Bar+17], which could lead to significant errors in PV power forecasting or future energy estimations [Rie+17]. Such climate simulations have to be combined with an accurate PV model capable of reproducing the system performance. Existing studies analyzing the influence of aerosols on solar irradiation lack spatial detail (because of the use of relatively coarse global climate models) and/or do not apply a detailed PV production model [Ber+17].

The Mediterranean region is considered as highly influenced by aerosols coming from different sources [Lel02]. These aerosols have a deep impact on the climate of the region [Nab+14; Nab+15], thus on the shortwave solar radiation reaching the surface [Mal+16]. Regarding possible changes in anthropogenic aerosols in the future [Gae+14; JG+11], the relevance of the near-term climate change scenarios and the expected PV deployment, the study of the Euro-Mediterranean area is important for solar energy.

In this work we use a regional climate model [Nab+14] with a realistic aerosol representation combined with an accurate PV model [Per12]. The influence of these

aerosols in the spatiotemporal variability of PV production over the region is quantified. The analysis is made in present climate conditions for simulations between 2003 and 2009 and different tracking types are considered in the study, due to the different sensitivity of each typology to changes in solar radiation [Gut+17]. On the other hand, the impact that trends in anthropogenic aerosols have in PV energy production is also investigated using longer simulations for the “brightening” [Wil05] period, 1980-2012, reflecting how pollution control policies could benefit the PV energy production in highly polluted areas.

This chapter is organized as follows: in section 6.2 the climate and the photovoltaic model are described. In addition, there is a description of the aerosols and the datasets used for evaluation. Section 6.3 presents the results and shows the impact of aerosols on photovoltaic energy production. It is organized depending on the space-time scale analyzed and there is a subsection for the tracking system sensitivity. Finally, section 6.4 is a discussion section for limitations and future perspectives and section 6.5 shows the main conclusions.

## 6.2 Data and Methods

Different climate simulations are used as an input of a PV power model. These climate simulations provide the daily-mean shortwave solar radiation, SSR, at the surface. The energy production model simulates the performance of a general photovoltaic system as in the previous chapter and includes different tracking types, considering the tilt of photovoltaic panels as a relevant component of the whole assessment. Computation of the photovoltaic energy model is made using the R open-source package named solaR [Per12]. Chapter 4 explains in detail the methodology used for the photovoltaic model.

### 6.2.1 Climate Data

The climate model used in this study (CNRM-RCSM4,[Sev+14]) is a coupled Regional Climate System Model (RCSM) dedicated to the study of the Mediterranean climate. CNRM-RCSM4 is one of the RCSMs contributing to the multi-model Med-CORDEX initiative [Rut+16]. It has the specificity to represent various components (atmosphere, land surface, river, ocean) of the Mediterranean regional climate system at high-resolution as well as their high-frequency coupling. The horizontal resolution is 50 km for the atmosphere, the land surface and the river network, and about 10 km for the Mediterranean Sea. In addition, the atmosphere part of the model, the so-called ALADIN-Climate version 5.2 [Col+10] is one of the few available Regional Climate Models which can take into account a realistic representation of the spatiotem-

poral variability of the aerosols [Nab+14]. The model has been extensively described, evaluated and inter-compared with other Med-CORDEX models in previous studies, [Sev+14; Nab+13; Nab+14; Fla+18; Gae+18; Del+18; Har+18; Cav+18]

The detailed interannual aerosol dataset used in the climate simulations [Nab+13], NAB13, is able to reproduce the spatiotemporal variability of AOD (aerosol optical depth) over the Mediterranean region. It improves the representation of aerosols against older climatologies commonly applied in regional climate studies like Tegen [Teg+97] or Tanré [TGS84].

The NAB13 dataset includes five different aerosol species: Sea Salt, Black Carbon, Sulfate, Organic Carbon and Desert Dust (ss, bc, su, or, sd) with spatial and temporal variability. It is based on a blending of a satellite-derived AOD product and a high-resolution regional climate model using up-to-date interactive aerosols module. This dataset has also been evaluated against ground stations [Nab+13].

During the eighties, some policies against the emissions of certain types of anthropogenic aerosols were implemented in Europe, which has been linked with the observed increase in the shortwave solar radiation in the area [Wil05]. For simulations over this commonly named “brightening period” (1980-2012), a trend for sulfate aerosols is included in NAB13, being able to reproduce the shortwave solar radiation trend observed over Europe since 1980 [Nab+13].

There is a large spatial and seasonal variability of the AOD at 550nm over the Euro-Mediterranean. Spring and summer months are highly influenced by dust aerosols in the south of the domain. In winter, anthropogenic aerosols dominate in central Europe and during autumn, there are few areas with high values in opposition to the rest of the domain.

The domain considered in the simulations covers the Mediterranean area in addition to a large part of Europe (see Figure 6.1).

For the first period, 2003-2009, a pair of runs is analyzed. We refer to them as **AER** and **NO-AER**. The AER simulation includes the NAB13 dataset, whereas no aerosols are included in NO-AER. This pair allows to easily attribute the obtain differences to the aerosols effect, therefore to quantify the impact of aerosols on the Euro-Mediterranean SSR and PV productivity. It is an important point considering the fact that some of the state-of-art RCMs do not include aerosols in their simulations, so it gives an idea of that missing forcing.

Secondly, a longer simulation between 1980 and 2012, **TREND**, covering the “brightening” period observed in Europe is also analyzed. It will show the effect of a decreasing trend in sulfur aerosols on the shortwave solar radiation and on the PV productivity.

A summary of the different simulations is reported in Table 6.1.

### 6.2.2 PV model description

As in the previous chapter, the PV model described in 4 is used with the SSR from the climate model as the input. The procedure is described in [Per09] and the same methodology was applied in [Gut+17]. In this section we make use of the commonly used terms in the PV model description: the shortwave solar radiation, SSR, from the climate model is equivalent to the global irradiation at the horizontal plane  $G(0)$ , which is composed of the beam component,  $B(0)$ , the diffuse irradiation,  $D(0)$ , and the albedo  $R(0)$ .

The two steps followed to obtain the PV output are:

1) Global irradiation at the horizontal plane  $G(0)$ , as an output of the climate model, has to be transformed into the global effective irradiation,  $G_{eff}(\alpha, \beta)$ , which is the amount of energy reaching the tilted surface of the generator (where  $\alpha$  is the azimuth angle and  $\beta$  the inclination angle) after considering reflection losses, angle of incidence and accumulated dust.

Three different tracking types are considered also here for the photovoltaic generator. The equations describing movements and relative position between the system and the sun are described in [Per09]

1. **Fixed panels** with an optimum angle of inclination that depends on the latitude.
2. **One axis trackers**, with a generator rotating on an axis oriented North-South. We will refer to them as “**one**”.
3. **Two-axes** tracking system that allows variation of the azimuth and inclination angles, we will refer to them as “**two**”.

Simulation	Aerosols	Period
AER	NAB13	2003-2009
NO-AER	Not included	2003-2009
TREND	NAB13 + sulfates trend	1980-2012

Table 6.1: Simulations of the CNRM-RCSM4 regional climate model to obtain SSR and temperature as input of the photovoltaic model, period and representation of aerosols in each simulation.

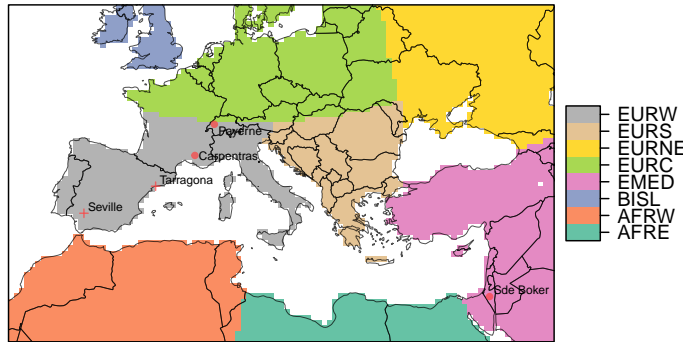


Figure 6.1: Areas defined to evaluate the difference in solar radiation between the satellite and the climate model simulations: Western Europe, EURW; Southern Europe, EURS; North-Eastern Europe, EURNE; Central Europe, EURC; Eastern Mediterranean, EMED; British Island, BISL; Western Africa, AFRW; Eastern Africa, AFRE. The location of the BSRN stations is represented with points “.” and the two PV plants are plotted with “+” in orange.

---

To obtain irradiation components in the tilted surface at daily time scale, it is first necessary to estimate the irradiance profile using empirical relationships [CPR79]. The irradiance profile is then transformed into its components at the tilted surface and integrated in time to obtain the energy reaching the generator surface. Direct irradiance can be transformed to the tilted surface using only geometrical criteria whereas the diffuse fraction is obtained with the model proposed by [HM85]. This model considers an approximation where the sky sphere is seen by the generator as isotropic except for the circumsolar region, which is considered to emit direct irradiance. The albedo component is considered as isotropic, due to the fact that its contribution to global irradiance is low.

Finally, we apply equations from [MR01] to obtain  $G_{eff}(\alpha, \beta)$ . It includes optical losses due to the fact that, except for the two-axis tracking system, the incident irradiation deviates from the normal of the generator. Also, transmittance losses are included for accumulated dust over the surface, considering a “moderate dust degree” in the terms used in the referenced paper [MR01]. In this case, any spatial distinction is considered and the same coefficient values are used to calculate angular and transmittance losses.

2) The second step is the transformation into power output, depending on the electrical characteristics of the components in the photovoltaic system and second order effects like temperature. Detailed information about this step can be found in the Methods chapter and in [Per09].

### 6.2.3 Datasets for evaluation

#### Satellite product: CM-SAF

The SARAH [Mül+15] dataset for daily shortwave solar radiation, SSR, is used with a horizontal resolution of 0.44° to be consistent with the model simulations and for the period 2003 and 2009. For this product, the 85% of absolute differences with shortwave solar radiation measurements is below  $10 \text{ W/m}^2$  for monthly values and  $13 \text{ W/m}^2$  for daily means.

Concerning aerosols representation, the satellite dataset includes information from MACC [Ben+09; Mor+09], provided by the European Centre for Medium-Range Weather Forecasts (ECMWF). Monthly long-term means of a 0.5x0.5 degrees grid are spatially interpolated to assign the values of each pixel.

#### BSRN stations

The three stations of the BSRN network used in this study (Payerne, Carpentras and Sede Boker) covered the period 2003-2009 and provide SSR monthly data [KL+13]. Their location is represented in Figure 6.1 together with the PV plants considered in the study.

#### Temperature data: ECAD

The PV production assessment calculated using the SSR from satellite data needs also the temperature for the performance of cells inside the module. The gridded E-OBS data set from the EU-FP6 project ENSEMBLES [Hay+08] is used in the energy production model at daily resolution. Mean, maximum and minimum temperature from the dataset, in a spatial resolution of 0.25°, are interpolated to the same grid of the climate model.

#### PV production data

Data from two different power plants are used for the evaluation of the simulated PV power and the assessment of the added value of the aerosol inclusion in the climate simulations.

The two power plants are in the Iberian Peninsula and their location represented in Figure 6.1. The first one, located in Tarragona in the North-East area, is a PV system with fixed structure. The second one is a two-axis tracking PV plant located in Seville, in the South of Spain. Details of both PV power plants are in Table 6.2, including the electrical characteristics of their components.

	Seville	Tarragona
Type	two-axes	fixed
Generator	$P_g = 27.31 \text{ kWp}$	$P_g = 100.18 \text{ kWp}$
	$N_{mp} = 12$	$N_{mp} = 27$
	$N_{ms} = 11$	$N_{ms} = 35$
Inverter	$P_{inv} = 25 \text{ kW}$	$P_{inv} = 100 \text{ kWp}$
	$V_{min} = 405 \text{ V}$	$V_{min} = 450 \text{ V}$

Table 6.2: Summary of the electrical components of the two photovoltaic plants, including generator characteristics (generator power  $P_g$ , and modules in parallel and serie,  $N_{mp}$  and  $N_{ms}$ ) and the inverter characteristics (power of the inverter  $P_{inv}$  and the voltage  $V_{min}$ ).

Data of PV production are difficult to obtain due to confidentiality contracts. Moreover, when data are available time series are not always complete. Maintenance, modules substitutions, inverter problems and other stops in the production may lead to common time-gaps in the datasets. These limitations must be taken into account when establishing statistical comparisons between models and real data. In this case, the two PV power plants provide daily data within the period 2003-2009, the details are in Table 6.3. Monthly means of these data are compared against the monthly means of simulated daily PV productivity, energy produced by the power installed  $\frac{\text{kWh}}{\text{kWp}}$ , with the models and the satellite. Only months with more than 15 days of data available are considered for the monthly mean and compared against simulated data.

## 6.3 Results

Although the AOD dataset and the climate simulations used in this study have already been evaluated against observations and satellite datasets in [Nab+13; Nab+14; Nab+15], an additional assessment of the SSR from the climate simulations is also made in this work against the CM-SAF SARAH dataset [Mül+15] for the period 2003-2009 and against some BSRN [KL+13] stations at a local scale.

### 6.3.1 Local scale

Three different stations from BSRN cover the period between 2003-2009 with SSR monthly data. Stations are represented in Figure 6.1 with points. Also, two different power plants in Spain, represented in Figure 6.1 with a cross, are used to evaluate PV power simulations at a local scale. A summary of the data used in this section, the periods and the resolution can be found in Table 6.3.

In Figure 6.2 differences in monthly time series of SSR from simulations and satellite data and the stations measurements are represented.

Data from	Seville	Tarragona	Payerne	Sede Boker	Carpentras
Variable	PV productivity	PV productivity	SSR	SSR	SSR
Time res.	day	day	month	month	month
Period	518 daily values between: 02-07-2007 30-11-2008	300 daily values between: 01-01-2003 19-03-2005	2003-2009	2003-2009	2003-2009
% no data	0	8 %	0	10.71 %	0

Table 6.3: Summary of the local data of PV power plants and SSR from BSRN stations used for the evaluation of the simulations. SSR is evaluated as input of the PV model and the PV output as the result of the whole modeling process.

For the three stations, the satellite has better results than the simulations, although the error magnitude varies depending on the station. There is also a general improvement of the AER simulation against the NO-AER. Carpentras station is the one with lower bias with respect to the observed data 6.2a. In the case of the Sede Boker station 6.2c, there is a seasonal bias in the AER simulation. High negative differences appear from May to August, showing underestimation of the SSR in these months.

Several statistical measurements summarize the general performance of the SSR from the climate model and the PV simulations at each location and are reported in Table 6.4.

For the simulation of PV power output, the daily mean of PV production data averaged for each month is compared with simulated PV energy production at each power plant, using the three possibilities of SSR data as input: AER, NO-AER and SAT. For these simulations, in order to help with the visualization of the results a *violin plot* (6.3) is used to visualize the absolute error and its distribution. For the Seville PV power plant 6.3a, AER performs better than NO-AER and SAT simulations showing lower errors. Besides, only AER has some negative errors, which means underestimation for some months, whereas the satellite and the NO-AER have only positive error values.

The median error for the AER simulation is less than  $0.25 \frac{\text{kWh}}{\text{kWp}}$ . Differences are concentrated around this value, which makes the distribution to peak around it in a narrow shape, although the range is wider due to higher values above  $0.5 \frac{\text{kWh}}{\text{kWp}}$  that spread the distribution.

NO-AER simulation has a wider range of errors than AER and SAT, and a wider distribution. The satellite presents a median error close to  $0.5 \frac{\text{kWh}}{\text{kWp}}$ , as could be expected from the evaluation and report of the CM-SAF dataset.

## 6. IMPACT OF AEROSOLS ON PHOTOVOLTAIC PRODUCTION

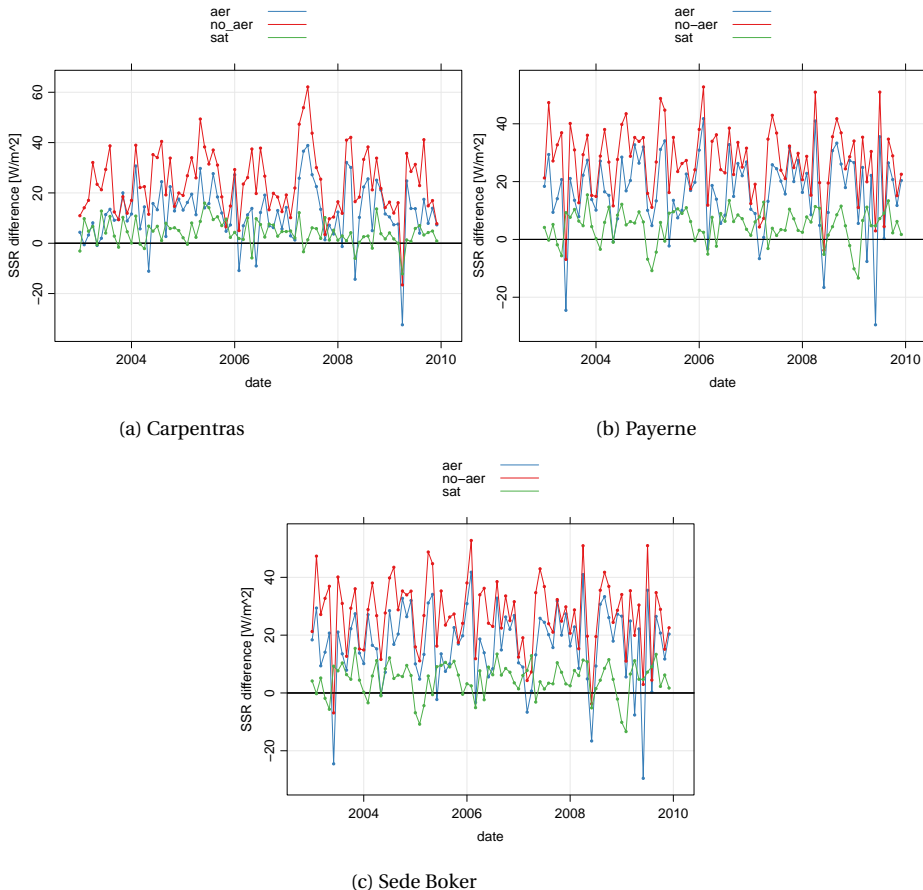


Figure 6.2: Difference in SSR  $\left[ \frac{\text{W}}{\text{m}^2} \right]$  between both simulations and the satellite with respect to the data from BSRN stations (BSRN)

The Tarragona PV power plant presents larger errors. The SAT has slightly better performance than AER and the improvement with respect to NO-AER can be observed in both cases.

AER simulation's median error is 0.60  $\frac{\text{kWh}}{\text{kWp}}$  and NO-AER simulation error has larger values, the median is 0.77  $\frac{\text{kWh}}{\text{kWp}}$ . The SAT error has lower median value: 0.48  $\frac{\text{kWh}}{\text{kWp}}$ .

It can be also appreciated in Figure 6.3b that there are two months in the simulations where errors are specially large. As these values are clear outliers, it might be that some maintenance activities in the plant are the cause of a lower energy output than expected, which would explain the larger errors in those months.

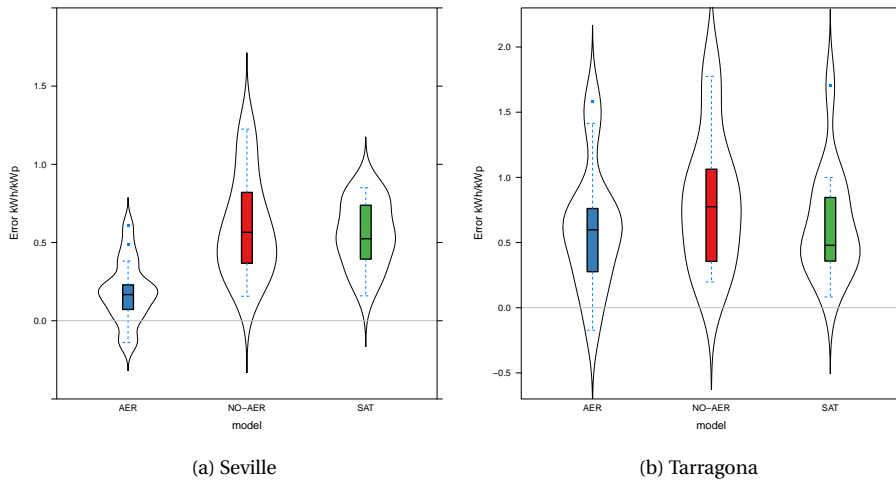


Figure 6.3: Distribution of differences in monthly mean of daily PV productivity [ $\frac{\text{kWh}}{\text{kWP}}$ ] from Seville and Tarragona power plants and the simulated with the model, AER (blue) and NO-AER (red), and the satellite (green) in the same location. The period for Seville is from July 2007 to November 2008 and for Tarragona power plant from January 2003 to December 2005. The violin plot represents at the y-axis the probability density function of the variable, estimated with a kernel density estimation. Along this axis, the plot represents the shape of the variable distribution and it is duplicated by symmetry over an imaginary vertical axis to facilitate visualization. In this way it is easier to see not only statistical parameters represented in the boxplot, that it is also shown inside the violin, but also how the errors are distributed.

The added value of including aerosols in climate simulations for the estimation of PV production is clearly illustrated by our results. The model using climate simulations with a good aerosols representation could be locally as good as the satellite, at least at the location of the PV power plants used (despite of its biases in some areas). The satellite product has revealed itself also as a good dataset, both for SSR (seen in the evaluation with BSRN stations) and for the PV production estimation.

### 6.3.2 Regional scale

The regions defined in Figure 6.1 are the same areas selected in [Nab+14], and the acronyms used in this section are also in the figure. The difference between simulations and satellite data in annual terms is represented in Figure 6.4. The improvement of the simulation including aerosols is noticeable for every region. It can be appreciated also that there are some weak changes in the interannual variability of the bias due to aerosols inclusion, like in the BISL area, AFRE region in 2009 or AFRW.

Western (EURW) and Southern Europe (EURS) have the lowest biases in SSR, as well as eastern Africa (AFRE) and the South of the British Islands (BISL). Negative biases

Location	Simulation	RMSE	MBE	cor	sd
Seville	AER	0.27	0.18	0.98	1.34
	NO-AER	0.67	0.60	0.95	1.29
	SAT	0.59	0.55	0.98	1.45
Tarragona	AER	0.77	0.61	0.87	1.21
	NO-AER	0.96	0.82	0.9	1.29
	SAT	0.76	0.64	0.88	1.13
Payerne	AER	21.21	16.62	0.97	77.4
	NO-AER	29.70	27.07	0.98	81.88
	SAT	7.36	4.6	0.99	83.29
Carpentras	AER	16.59	12.05	0.98	90.05
	NO-AER	27.26	24.10	0.99	90.57
	SAT	6.38	4.26	1.00	88.71
Sede Boker	AER	18.89	8.17	0.98	62.83
	NO-AER	37.42	35.63	0.98	76.06
	SAT	12.00	10.27	0.99	77.62

Table 6.4: Values for the root mean squared error (RMSE), mean bias error (MBE), temporal correlation (cor) and standard deviation (sd) for the simulated PV production in Seville power plant and Tarragona power plant compared with the final productivity data measured  $\left[ \frac{\text{kWh}}{\text{kWp}} \right]$  and the SSR from the climate model simulations and the satellite in comparison with the SSR from BSRN stations  $\left[ \frac{\text{W}}{\text{m}^2} \right]$

only appear for Africa and they could be due to the fact that in some cases the annual amount of aerosols is overestimated, or due to the optical properties of the aerosols in the model. The rest of the areas have positive biases, probably due to an underestimation of the cloud cover in the model [Nab+14]. The eastern side of the domain shows a higher bias (NEEUR), although it is clear that the addition of aerosols improves the representation of SSR.

In order to calculate the impact on photovoltaic production, shortwave solar irradiation, SSR, from the climate model simulations and the satellite dataset is used as an input of the photovoltaic model. For a fixed typology of the panels, the difference between simulations with respect to the satellite dataset as input, in the mean of daily productivity for each month, is represented in Figure 6.5. The productivity is defined as the energy production per unit of power installed kWp.

In general, The NO-AER simulation gives more production than the AER and the satellite, overestimating the PV power potential. Climate model simulations, AER and NO-AER, differ more from satellite PV production output in winter months, whereas in summer months, AER and satellite are close to each other, except for the EURNE

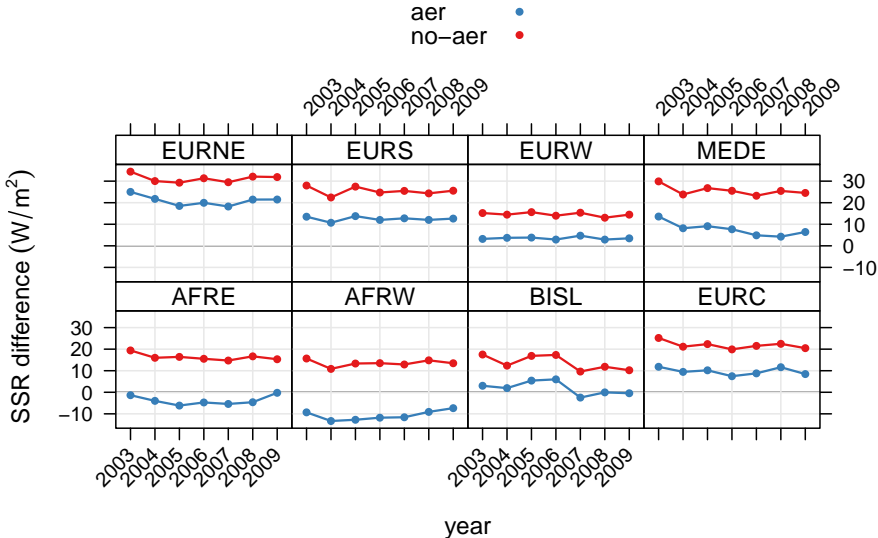


Figure 6.4: Difference in shortwave solar irradiation,  $\text{SSR} \left[ \frac{\text{W}}{\text{m}^2} \right]$ , between simulations and the satellite aggregated by areas defined in figure 6.1 in the period 2003-2009.

region. This area is the most biased area of the model in comparison with the satellite, perhaps due to a bias in the cloud cover.

The regions from North Africa, AFRE and AFRW, are slightly different from the rest with a roughly constant bias curve of the annual cycle, therefore the difference in PV production between summer and winter months is lower due to the mean latitude of the area. Besides, for these areas, the AER simulations give in summer month lower PV production values than the SAT and the NO-AER, which is not the case in the rest of the regions.

The EURS area is the one with largest amplitude between winter and summer months. For April and May, the AER simulations have small differences with the satellite simulation.

### 6.3.3 Impact of aerosols by tracking type

#### Mean behavior. Period 2003-2009

In addition to the absolute difference in PV productivity between AER and NO-AER, the relative difference between simulations is presented in this section, showing the relative impact in each case. It allows us to contextualize the loss with respect of the potential of the place.

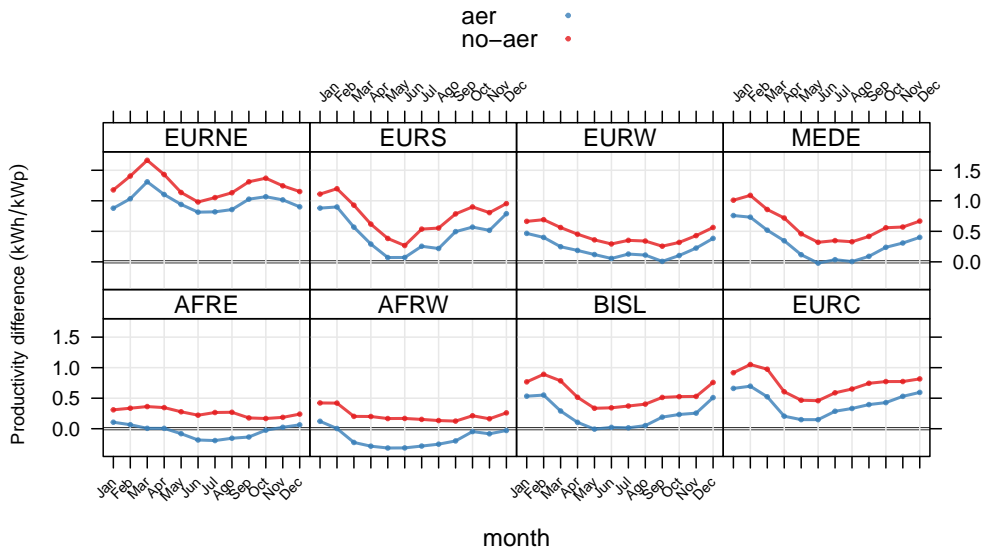


Figure 6.5: Annual cycle of daily energy productivity [ $\frac{\text{kWh}}{\text{kWp}}$ ] differences by area for the AER simulation and NO-AER simulation with respect to the satellite as inputs of the PV model, considering fixed panels.

The difference in yearly PV production between both simulations, for every type of tracking panel, is represented in Figure 6.6a. The spatial pattern shows areas where the aerosols affect more the shortwave solar radiation. Central Europe, Po Valley and the South of the domain, along the African continent coast, are the areas where the differences are more noticeable.

For the fixed panels, the differences are around  $-150 \frac{\text{kWh}}{\text{kWp}}$  for some of these areas in annual terms and reaching  $-200 \frac{\text{kWh}}{\text{kWp}}$  in the Po Valley, Syria, Iraq and between Algeria and Tunisia.

When the two other tracking systems are considered, the difference between both simulations increases, with values of  $-300 \frac{\text{kWh}}{\text{kWp}}$  for the two-axes type over the most affected areas and even higher values like in the south of Turkey. These results are consistent due to the fact that the two-axes and the one-axis tracking systems are more efficient systems to give energy to the generator.

The results of the country averages for the annual productivity are shown in Figure 6.6b. It is shown that the aerosols impact range from  $-4\%$  to the PV production to

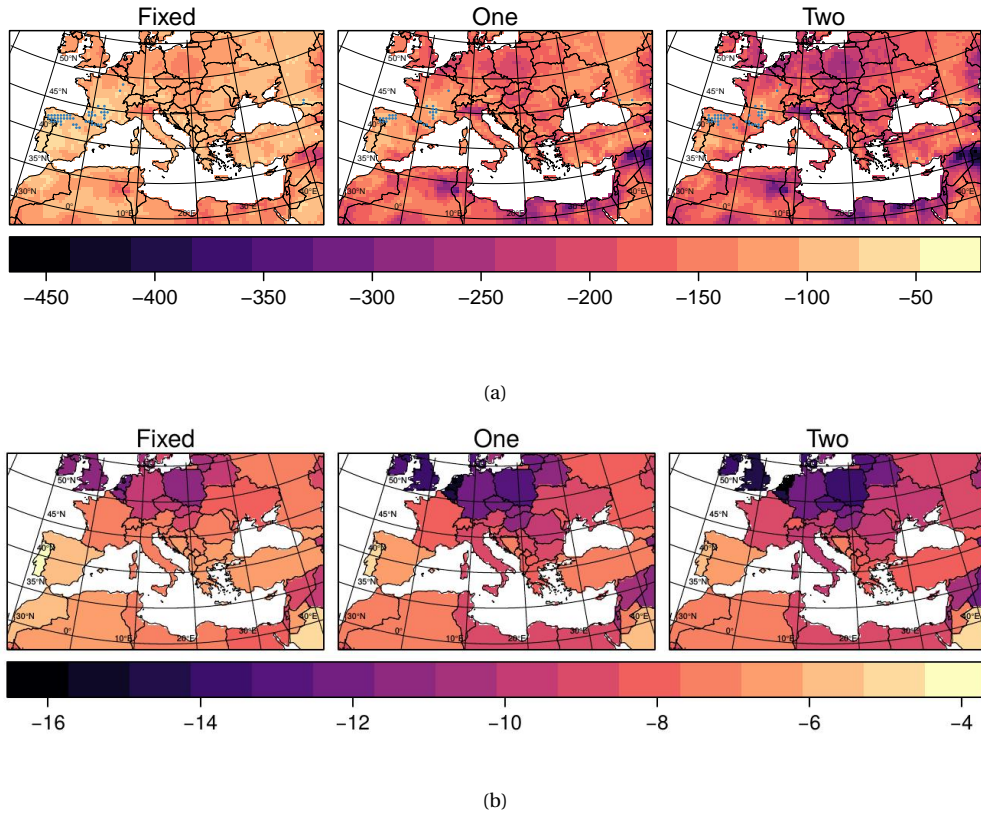


Figure 6.6: Differences in PV yearly productivity: (a) absolute  $\left[ \frac{\text{kWh}}{\text{kWp}} \right]$ , (b) relative averaged by country (%); for the period 2003–2009 between AER and NO-AER and for the three different types of tracking. For the non-significant differences, calculated with a 't-test', a point is over-plotted for (a)

-16%. It can be seen that from the fixed panels to the one-axis, and then to the two-axes tracking type, there is an increase in the productivity losses that is more noticeable in Central Europe, like in Belgium-The Netherlands.

Germany, that has installed a high amount of PV capacity, is affected with values around -10% of loss for fixed system and more than -12% for the one-axis and two-axes panels. Thus, some countries with high PV production have moderate losses due to aerosols in relative terms. For countries in the west and south of the domain like Portugal, Spain, Morocco, Jordanian or the extension of Saudi Arabia included in the domain, the relative amount of energy loss is smaller due to its high potential, with differences between -5% and -6% for fixed panels and reaching -8% in some cases for the other types of tracking systems.

### Seasonal cycle

As can be seen in Figure 6.7, in seasonal terms spring (MAM) and summer months (JJA) show statistically significant values of the PV productivity difference. For winter (DJF) and Autumn (SON), there are few significant areas, mostly located in the south of the domain, in the African continent. An exception can be found for fixed panels in winter, with significant zones in Europe with values above  $-10\%$ , like the Po Valley or the British Islands.

The spatial pattern for the spring season shows higher values in Central-Europe, in specific countries like Poland, Belgium and The Netherlands, or the British Islands, and in northern parts of Syria and Iraq. Maximum values in these areas, range from an impact higher than  $-10\%$  for fixed panels to around  $-15\%$  for the two axes tracking type. Almost the whole African part of the domain shows significant differences, with impact values above  $-5\%$  and local values reaching more than  $-10\%$  between Algeria and Tunisia and in areas of Libya or Egypt.

Summer months have higher loads of aerosols over the Mediterranean. For fixed panels, only a few areas in north Africa, Middle East and north-western Europe show values with a loss higher than  $-10\%$ . One-axis tracking enlarge the extension of areas with a decrease higher than  $10\%$  and some areas with more than  $-15\%$  appear in Belgium and The Netherlands, Algeria and Syria-Iraq border. Also some smaller areas appear with PV production losses above  $-15\%$  within the above mentioned areas. Between the one-axis and the two-axes tracking type, there are no substantial differences in the spatial pattern but maximum values reach in these cases  $-17\%$  to  $-20\%$  in the same areas.

Significance is not clearly linked to the magnitude of the relative difference in productivity. High relative differences in DJF and SON in central and northern Europe are not significant, due to the high climate variability in these areas and seasons, whereas lower relative differences in spring in Africa and in summer in southern and eastern Europe are mostly significant. The fact that JJA changes are significant over most of the domain explains the statistical significance of most yearly differences (Figure 6.6a), due to the high contribution of summer to the yearly production and yearly interannual variability (see e.g. [Gil+15]).

#### 6.3.4 Long-term trends. Period 1980-2012

The impact of long term trends of solar shortwave on PV production can be illustrated with the results of the simulations of the brightening period over Europe. The simulation including the aerosols dataset, NAB13, and the decreasing trend in sulfur aerosols, TREND, is able to reproduce the observed positive trend in SSR [Nab+14].

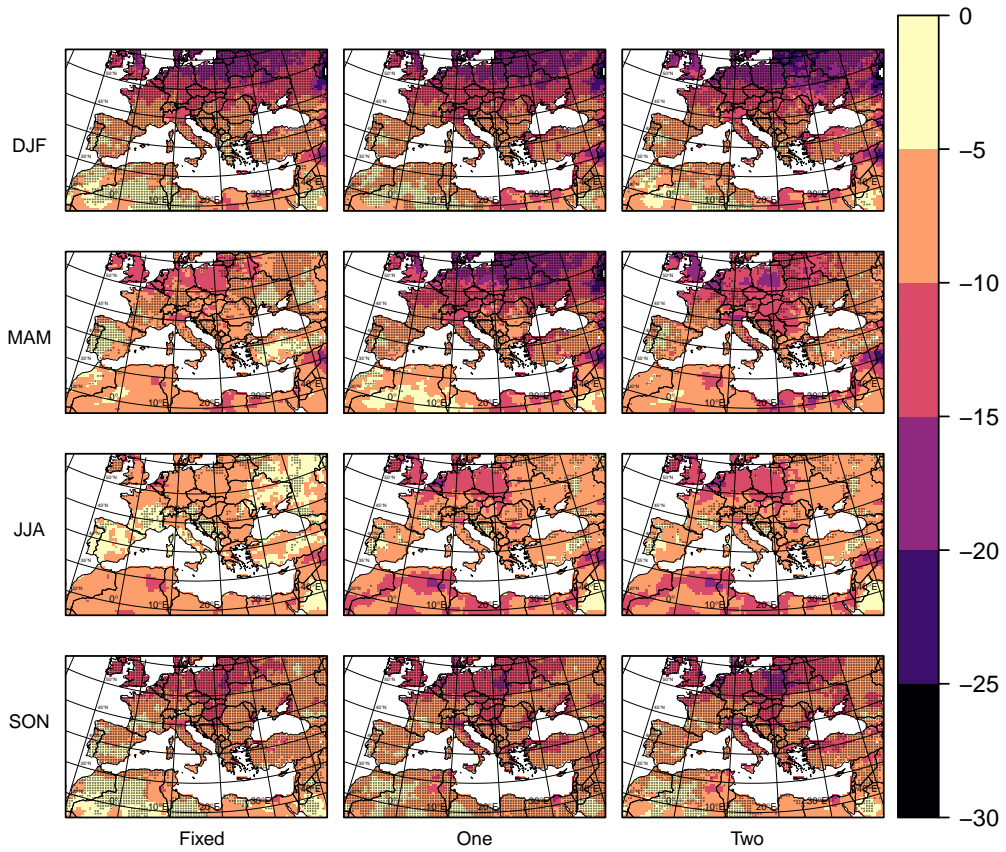


Figure 6.7: Relative difference (%) in seasonal PV productivity between both simulation for all type of panels. For the non-significant absolute differences, calculated with a 't-test', a dot is over-plotted.

As a compromise between the lifetime of a PV plant and the length of the simulation, two 15-year periods (at the beginning and end of the simulated period) are evaluated as a proxy for a PV project and the potential amount of energy that can be obtained during such a project. A fixed system is selected for the panels.

The relative difference between the accumulated energy obtained by a 15-year project between 1997-2012 and energy obtained by a 15-year project between 1980-1995 can be seen in Figure 6.8.

In Central-Europe the differences in the energy obtained are higher, due to the fact that it is the region where anthropogenic aerosols decrease more. Accumulated over 15 years, an increase higher than  $2000 \frac{\text{kWh}}{\text{kWp}}$  is found for this area. It means that about 10-14 % more energy can be produced in the lifetime of a PV plant at the end of the period.

These results highlight the impact that environmental policies could have on the PV energy production, showing that anthropogenic aerosols are able to reduce potential PV power of a project significantly. It also illustrates that future evolution of regional anthropogenic aerosols load is likely to influence expected PV production on a given site on the lifetime of a PV plant.

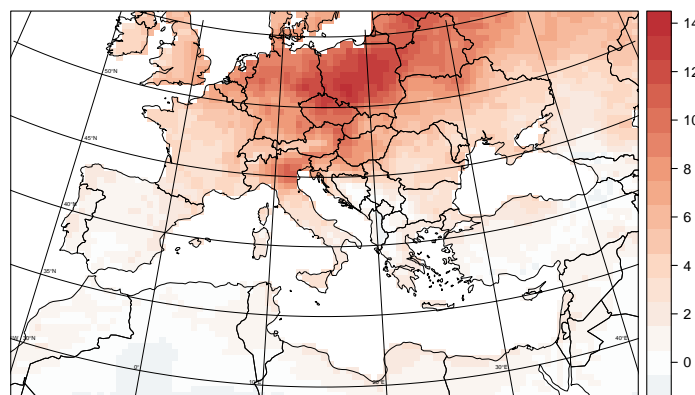


Figure 6.8: Relative difference in PV yearly productivity [%] accumulated for a 15-year period at the end and the beginning of the period: 1980-1994/1998-2012

## 6.4 Discussion

### 6.4.1 Limitations

The coarse resolution of climate models and their bias in some variables, especially in cloud cover, makes difficult their application for solar resource assessment at local scale in most areas. However, the RCMs will evolve to finer resolution and besides, the use of climate models is mandatory to take into account future climate evolution. They are also relevant tools to perform sensitivity tests allowing to disentangle the driving factors of the resource variability such as aerosols.

A multi-model approach would be necessary to obtain a more robust answer applying the same methodology to more models but, up to now, aerosols are poorly considered in many RCMs, which does not allow that type of study considering actual simulations.

For the limitations in the PV model, it is important to notice that in the decomposition of SSR and the transposition to the tilted panels, some empirical relationships are used. If components of solar radiation were an output of the RCM, the additional steps for decomposition could be avoided.

It could also be pointed out that the spectral decomposition of the SSR reaching the panels would give a better input in order to calculate spectral losses of the PV modules, although for periods longer than a day the spectral effects become less significant [MR01].

In the optical losses, deposition of dust over the generator surface is approximated in the assessment but could be underestimated in desert areas because it is not spatially modeled. That could mean a higher drop in transmittance and final energy production.

The time-scale is also important for the AOD representation. Several processes involving aerosols in the atmosphere are in day to weeks time-scales. We have used a realistic interannual dataset of the AOD that improves the state-of the art used in climate modeling but next studies should go further with an improvement in the aerosols representation. This will include a prognostic scheme of aerosols that allows to study finer time-scales and future scenarios, through a fully-coupled and fully-interactive aerosol-climate model.

### 6.4.2 Implications for the climate services dedicated to the energy sector

The results show the necessity of considering aerosols in climate simulations used to deliver energy-related climate services. The inclusion of spatio-temporal variability

of aerosols in RCMs may change the current estimates of future PV production over Europe [Jer+15b]. An accurate ensemble of models is essential for bridging the gap between services providers and potential users considering that some of the discrepancies between model simulations could come from the aerosols inclusion.

#### **6.4.3 PV production data issue**

The scarcity of real power data at PV plant sites is an important issue that has to be overcome in order to improve research in the fields of PV forecasting, climate services or energy modeling. The potential synergies between research institutions and different stakeholders of the energy sector will enhance the PV integration, the management and planning operations as well as the efficiency of the overall system and its development. Not only production data are needed, but also, accurate metadata will be extremely important in order to integrate into the modeling chain important factors such as: days of maintenance activities, cleaning-panel days, installed capacity, electrical characteristics of the PV power plant, among others.

### **6.5 Conclusions**

Two main questions are addressed in this chapter: first, the evaluation of the capacity of an RCM to produce reliable estimations of PV production over the Mediterranean area. Secondly, the role of aerosols in PV production using sensitivity tests performed with the RCM.

It is demonstrated that the use of a RCM as input of a photovoltaic production model is able to reproduce real PV data accurately at monthly time scales for two locations in the domain. Besides, the added value of including aerosols in the simulations is observed over the whole area as the simulation with aerosols shows less bias in SSR than the simulations without aerosols and it is close to the simulated PV using the satellite dataset across the whole area.

The results show that the most impacted areas are (with some exceptions) mostly in central Europe, where the lower resource amount in combination with the influence of aerosols gives a significant reduction in potential electricity production. For the annual averaged by country productivity, the highest relative differences are around -12% for fixed typologies and are seen over Central Europe (Poland and The Netherlands). Differences increase from one axis typology to the two-axes, reaching around -16% between both simulations in Belgium and around -13% and -14% in many countries. In seasonal terms, the loss can reach values of -20% in some areas for summer months.

In the multi-decadal simulation 1980-2012 a noticeable increase in productivity has been obtained in central Europe as a result of the decreasing trend of anthropogenic aerosols observed from the end of the eighties. This trend has been associated with pollution control measures as well as economic crisis in Western Europe. This result has implications beyond the domain of this study: highly polluted countries like India and China could obtain an increase in PV productivity if pollution control policies are effectively implemented.

The non-negligible impact of aerosols on PV production in the area suggests that the inclusion of aerosols in future scenarios is necessary for solar energy assessment.



CHAPTER

7

---

## **Future projections of solar and photovoltaic potential in Europe**



---

## **Abstract**

In the last decades, trends in photovoltaic deployment show an overall increase over the world and it is projected to continue growing for the next years. The comprehensive knowledge of solar resource and its future evolution is demanded by the energy sector. Solar resource and photovoltaic potential have been estimated in several studies using both global and regional climate models, showing a discrepancy between them in the sign of the projected change over Europe. An increase in surface solar radiation and in photovoltaic potential is projected by GCMs, whereas most of the RCMs simulations project a decrease. In this chapter, the role of the aerosol forcing in RCMs as a key explaining factor of this inconsistency is investigated. The results show that RCM simulations including evolving aerosols agree with GCMs in the sign and amplitude of the SSR change over Europe for mid-21st century projections (2021-2050 with respect to 1971-2000, RCP8.5). The opposite signal is projected by the rest of RCMs. The amplitude of the changes depends on the model. In terms of photovoltaic potential, RCMs including evolving aerosols simulate an important yearly increase especially in Central and Eastern Europe with maximum values reaching +10% for some countries in summer (in one of the RCM). On the contrary, the RCMs with no evolving aerosols show a negative anomaly of PV production. This study illustrates the key role of the often-neglected aerosol forcing evolution in RCMs.

## 7.1 Introduction

Due to the link between solar energy production and atmospheric variables, concern has raised about the availability of resources under climate change [Gae+14]. Due to that, climate modeling is a key tool to evaluate future energy potential despite some constraints like its low spatial resolution or known biases in the representation of cloudiness.

Attempts to estimate PV potential in the future under climate change were made in previous works [Cro+11; Pan+14; Gae+14; BBH14]. Some of them were focused locally [Pan+14; BBH14] and others use a single climate model [Cro+11]. Different CMIP5 simulations with different GCMs have also been evaluated to assess the photovoltaic potential under climate change conditions in [Wil+15], projecting an increase over Europe due to the increase in clear-sky and all-sky conditions. Another sensitivity study has shown that projected increase in SSR is also augmented by changes in anthropogenic aerosols emissions for the same area [Gae+14].

However, later studies using regional climate models [Jer+15b; Bar+17] have shown the opposite behavior for some regions in Europe, an overall decrease in surface solar radiation and photovoltaic potential in the same area is projected although no significant change in cloud cover (CLT) was found.

These results constitute one of the few illustrations so far of GCM-RCM inconsistency in the sign of a climate change signal [Bar+17]. In addition, this current inconsistency may lead to diverging messages delivered to the PV production stakeholders depending on the climate information source. So far, this inconsistency has been attributed to an added-value of RCMs with respect to GCMs, due to an improved cloud representation in RCMs and therefore an improved related climate change response in RCMs [Bar+17].

Usually, the added value of regional climate modeling against global simulations lies on the better representation of local climate features due to the increase in resolution of coastal lines or topography that can not be solved with coarser models. However, the increase in resolution has led to a simplification of other processes in order to not compromise the computational time and resources. Many regional climate simulations have been done using a simplified representation of aerosols content, usually aerosol optical depth (AOD) climatologies without variations in time [Nab+13; Nab+14], and without considering their evolution in time for future projections [Bar+17].

In this context, the goals of this study are to further illustrate the GCM-RCM inconsistency by using well-chosen pairs of GCM-RCM within the Euro-CORDEX ensemble,

to attribute this inconsistency to missing evolution of the aerosol forcing in CORDEX RCMs and to deliver trustable future projections of the climate-related PV potential.

In previous studies, the ensemble approach has been considered to evaluate the impact of climate change in renewable resources [Jer+15b; Tob+18; Gil+18; Jer+19]. However, the fact that a large majority of RCMs' simulations do not consider aerosol evolutions in their projections, the impact of aerosols is masked by the ensemble mean approaches.

In this work, we analyze the surface solar radiation (SSR) and the photovoltaic potential over Europe for the mid-21st century and the RCP8.5 scenario using GCM-RCM simulation pairs, from the Euro-CORDEX initiative. We classify different RCM simulations depending on their aerosols representation in the model and their driving GCM. A modelization chain approach is used, where SSR and temperature are the variables used as input of a photovoltaic parametric model used to calculate PV productivity.

Section 7.2 describes the models and simulations used in the study. A description of the aerosols datasets used by them is included here. The methodology is explained in section 7.3 and the main results are explained in 7.4. A discussion and a conclusion section follows.

## 7.2 Climate data

### 7.2.1 CMIP5

The Coupled Model Intercomparison Project Phase Five provides and coordinates global climate simulations from different modeling groups [TSM12] of around the world, using more than 40 models. Different RCP (Representative Concentration Pathway) scenarios are used for radiative forcing of each simulation of CMIP5. In this work, two climate models from CMIP5 are the driving models of different RCMs evaluated in the study for the scenario RCP8.5.

### 7.2.2 Euro-CORDEX

Euro-CORDEX develops climate projections focused on the European continent at different horizontal resolutions ( $0.44^\circ$ ,  $0.11^\circ$ ). These simulations are driven by different CMIP5 GCMs [TSM12].

Among the whole list of simulations included in the Euro-CORDEX database, aerosols are described very differently depending on the RCM. RCMs use different aerosol datasets, different levels of complexity for their representation and different temporal evolutions. In particular, most of the Euro-CORDEX RCMs do not present evolv-

ing aerosols in the future projections. Only two RCMs (namely RACMO22E and ALADIN53) include an aerosol dataset that evolves depending on the year, following the chosen RCP scenarios and the driving GCM.

For our purpose a relevant 6-member ensemble is used, which is a sub-sampling of the whole list of the 0.11° Euro-CORDEX scenario simulations performed under the RCP8.5 hypothesis. Two driving GCMs (EC-EARTH and CNRM-CM5) and four RCMs (RACMO22E, ALADIN53, CCLM4-8-17 and RCA4) are selected. Each GCM drives three RCM simulations, one with evolving aerosols and two with constant aerosols (see Table 7.1 for a detailed description of the GCM-RCM pairs). A group of three RCM simulations driven by the same GCM will be called “family”. Although a small number of the possible Euro-CORDEX GCM-RCM pairs is used, it is largely enough to serve the purpose of the study.

To measure the climate change signal, a 30-year near-future period (2021-2050) is compared to the end of the 20th century (1971-2000). The focus on the near-future allows our results to be nearly independent of the chosen socio-economic scenario (here RCP8.5) and to maximize the aerosol effect with respect to the GHG effect. The choice of 30-year long periods allows to minimize the uncertainty related to the natural climate variability as only one realization of each GCM-RCM pair is usually computed in Euro-CORDEX. In addition, the PV power plants operating during 2021-2050 are the ones that will be planned shortly, so the results are timely for the industry.

### 7.2.3 Aerosols datasets

The information about the aerosols datasets included in the regional climate simulations from Euro-CORDEX, used in this chapter has been included in Table 7.2.

#### Aerosols description in ALADIN53

The aerosols dataset used for ALADIN53 runs is based on AOD fields including 5 different species: black carbon, organic carbon, dust, sea salt, and sulfate. It is described

CMIP5 GCM	Institution	RCM
CNRM-CERFACS-CNRM-CM5	CNRM	ALADIN53
	CLMcom	CCLM4-8-17
	SMHI	RCA4
ICHEC-EC-EARTH	KNMI	RACMO
	CLMcom	CCLM4-8-17
	SMHI	RCA4

Table 7.1: RCMs from Euro-CORDEX grouped by the CMIP5 GCMs drivers generating the 2 families of simulations studied.

Institution	RCM	description	classes	scenarios
CNRM	ALADIN53	Climatology. Szopa 2013	5 classes: sea salt, sulfate, black carbon, desert dust, organic carbon.	evolve with RCP
CLMcom	CCLM4-8-17	Climatology. Tørnås 1984	4 classes: sea, land, desert, urban.	no evolution
SMHI	RCA4	Parametrization in radiation fluxes	Single integrated class.	no evolution
KNMI	RACMO	CAM inventory, Lamarque 2010	6 classes: sulfate, organic matter, desert dust, sea salt, stratospheric aerosols, volcanic	evolve with RCP

Table 7.2: RCMs from Euro-CORDEX and aerosols description.

in [Szo+13] and built from the global LMDz-OR-INCA Climate-Chemistry coupled model. For the historical period it takes into account reference aerosol emissions, including seasonal cycle for each species and trends for the anthropogenic aerosol species. The future simulations include the same temporal variations but following the corresponding RCP8.5 scenario emissions.

### Aerosols description in RACMO22E

A spatial and vertically distributed dataset derived from CAM-inventory [Lam+10] is used in RACMO22E simulations. It also accounts for the same five different species. The historical run also follows the reference emissions [Lam+10] and from 2006 it evolves in time with the RCP.

The resulting changes in AOD for both models in summer months (JJA) between 2021-2050 and a reference period 1971-2000, are represented in Figure 7.1 . An overall decrease for both models is observed with the maximum change in central Europe and with a slightly smaller signal for the RACMO22E simulation.

## 7.3 Methods

### 7.3.1 Spatial analysis

In order to analyze the spatial behavior of solar radiation, SSR, the summer mean change for the period 2021-2050 with respect to the reference period 1971-2000 is calculated. Summer months, June, July and August, JJA, correspond to the season when the AOD (aerosols optical depth) is higher over Europe and the Mediterranean area [Lel02].

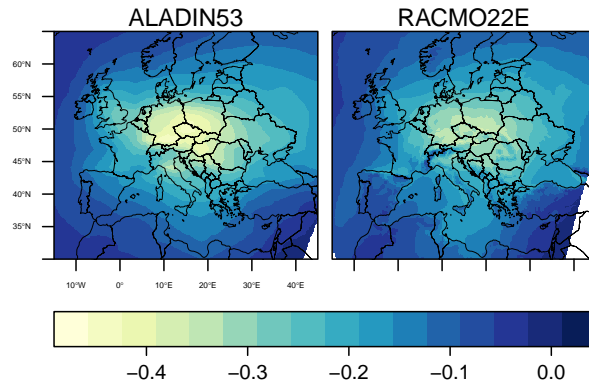


Figure 7.1: Aerosols Optical Depth summer changes between 2021-2050 with respect to the period 1971-2000 for ALADIN53 and RACMO22E models.

---

As an important driver of the variability of SSR the same procedure is applied to the total cloud cover variable, CLT. This allows to know if a correlation exists between both changes and how is modified between models with or without evolving aerosols.

### 7.3.2 PV potential

In order to obtain a projection of the photovoltaic productivity over Europe under climate change scenarios, the modeling chain approach explained in the previous chapters is considered. Solar radiation from the different climate simulations, SSR, is used as an input of the photovoltaic model that gives an estimation of the power output as explained in chapter 4.

The PV modeling process can be summarized in two steps: first, incident solar irradiation that reaches solar cells inside the panels is obtained through the decomposition of global solar irradiation and the transposition to the plane-of-array (POA). After that, the electrical performance of the system is modeled. Surface solar irradiation from climate models is equivalent to global irradiation at the horizontal plane,  $G(0)$ .

Monthly means of surface solar radiation, SSR, from climate models is decomposed first into the diffuse and beam components. The decomposition is made through a regression between the clearness index [LJ60] (which represents the relationship between global irradiation at the horizontal plane and the extra-terrestrial irradiation) and the diffuse fraction (relationships between the diffuse component and  $G(0)$ ) [Pag61].

A monthly average daily profile of the irradiance  $\left[\frac{W}{m^2}\right]$  is obtained for each month [CPR79] which allows to obtain different components in the plane of the array. Direct irradiance in the tilted plane is obtained straightforwardly from geometrical criteria. The diffuse component is obtained using the Hay and McKay model [HM85].

The effective irradiation is then obtained from the consideration of optical losses due to the incident angle and dust accumulation [MR01]. Only a moderate dust accumulation degree is considered.

The second step transforms the ‘effective’ irradiation into power output  $\left[\frac{kWh}{kWp}\right]$  considering the electrical performance of the system. The system includes characteristics of a general PV module and inverter, the arrangement of the generator and some efficiency losses. Characteristics of the general PV system are the same as the ones described in chapter 4.

Yearly PV potential changes for the period 2021-2050 with respect to the reference period 1971-2000 are computed. Yearly values of productivity are considered a good estimation of the performance of a power plant and are considered as a reference for feasibility studies and finance calculations.

Changes in PV potential production for summer months are also calculated, considering that it is the season with higher loads of aerosols and it is when solar energy production peaks.

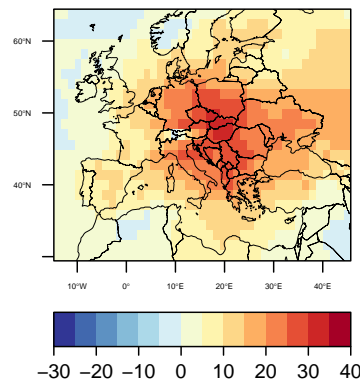
## 7.4 Results

### 7.4.1 Changes in SSR and CLT

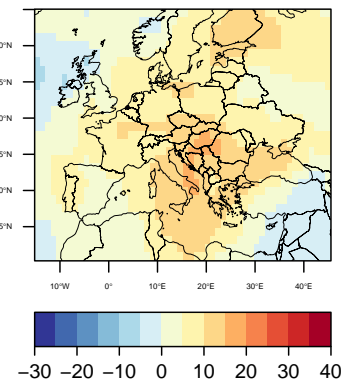
The summer (JJA) mean changes of the period 2021-2050 with respect to the reference period 1971-2000 is represented in Figure 7.2 and Figure 7.3 first for surface solar irradiation, SSR, and then for total cloud cover, CLT.

CMIP5 GCM	RCM	$\Delta SSR$	$\Delta CLT$	$\Delta AOD$	$\rho_{SSR,CLT}$	$\rho_{SSR,AOD}$
CNRM-CERFACS-CNRM-CM5		9.9	0.5		-0.4	
	ALADIN53	12.6	0.3	-0.2	-0.2	-0.9
	CCLM4-8-17	-2.4	-0.8	-	-0.7	-
	RCA4	-2.6	0.2	-	-0.8	-
ICHEC-EC-EARTH		5.6	-0.3		-0.3	
	RACMO	4.8	0.5	-0.1	-0.3	-0.6
	CCLM4-8-17	-2.7	-0.9	-	-0.8	-
	RCA4	-2.1	0.1	-	-0.8	-

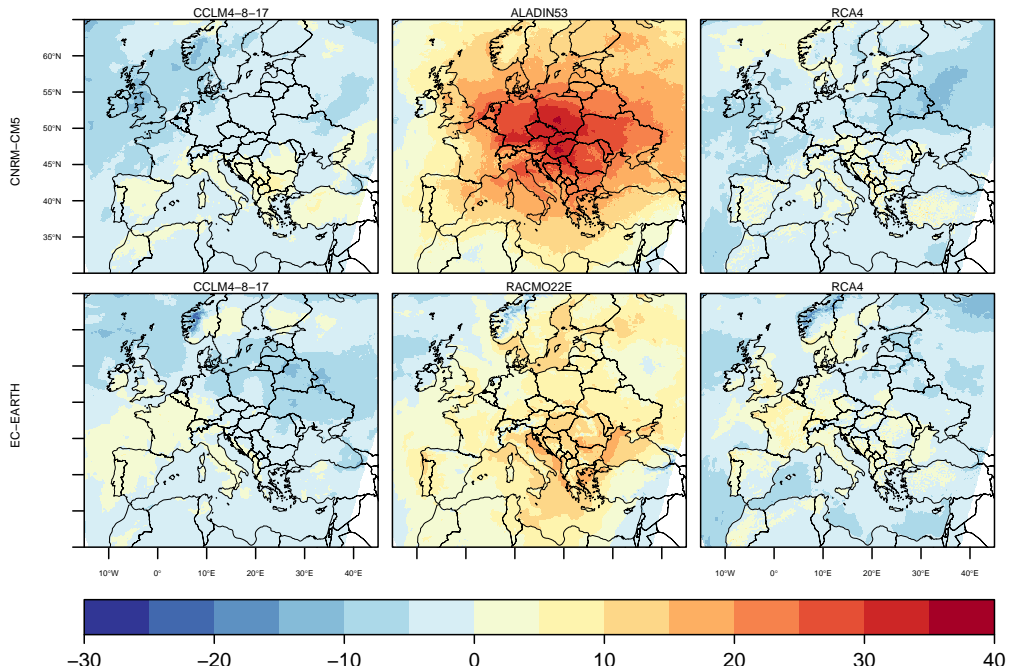
Table 7.3: Spatial changes with respect of the reference period for SSR ( $W/m^2$ ), CLT (%) and AOD; and spatial correlation between SSR,CLT and AOD changes maps.



(a) CNRM-CM5



(b) EC-EARTH



(c) Families of RCMs simulations. First row driven by CNRM-CM5 and second row driven by EC-EARTH.

Figure 7.2: Mean change 2021-2050 with respect to the reference period 1970-2021 of JJA surface solar radiation, SSR.  
 $\left[ \frac{W}{m^2} \right]$

---

Summer mean change shows an increase in Europe, more relevant in Central-Europe, for regional climate models with evolving aerosols in scenarios (ALADIN53 and RACMO22E) although there are differences in the magnitude of the changes. ALADIN53 presents the highest change in the mentioned area, which correlates with the negative change and spatial pattern of AOD of this model, as can be seen in Figure 7.1. For RACMO, the AOD change has a similar spatial pattern but the magnitude is slightly smaller. The projected SSR changes in RACMO are positive for a large area among the domain although they do not reach the higher values of ALADIN53. Mean values for the whole domain are positive for ALADIN ( $12.6 \frac{W}{m^2}$ ) and RACMO ( $4.8 \frac{W}{m^2}$ ) and negative for the others.

The rest of the RCMs from the first and second family present a similar signal in SSR among them, with a slight decrease in SSR with the exception of southern and western Europe that show a small increase.

The changes projected in the two RCMs that account for the evolution of aerosols in the future agree in the sign with the projected changes of the two GCM of the respective families also represented in Figure 7.2. The magnitude and the spatial pattern of the changes in CNRM-CM5 coincide with the ones in ALADIN53. In the same manner, the driving GCM of the second family, EC-EARTH, also presents similar changes to RACMO22E.

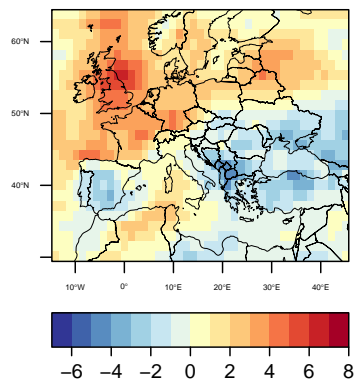
In general, for the whole domain, the mean change in CLT is close to zero for every simulation as can be seen in Table 7.3. The spatial pattern of CLT change in ALADIN53 shows a positive sign in the area where the change in SSR is higher (Central Europe), which is remarkable. For ALADIN53 and RACMO22E the spatial correlation between CLT and SSR is very low, -0.2 and -0.1 respectively, whereas it increases between SSR and AOD, -0.9 for ALADIN53 and -0.6 for RACMO22E.

On the whole, the spatial pattern of CLT explains well the spatial pattern of SSR in RCMs without evolving aerosols whereas both AOD and CLT are required to explain spatial pattern of SSR in GCMs and RCMs with evolving aerosols. The spatial pattern of AOD is even the dominant signal for ALADIN53.

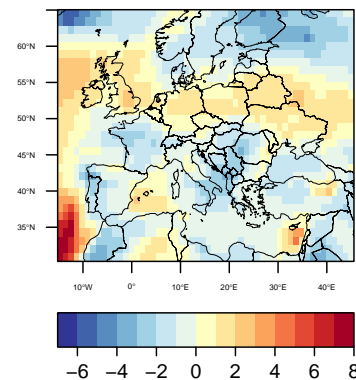
#### 7.4.2 Projected changes in PV production

The photovoltaic yearly productivity, defined as the power output by the power installed, is calculated for each pixel of land in the domain of Euro-CORDEX. Then, the averaged by country difference with respect to the reference period 1971-2000 is represented in Figure 7.4.

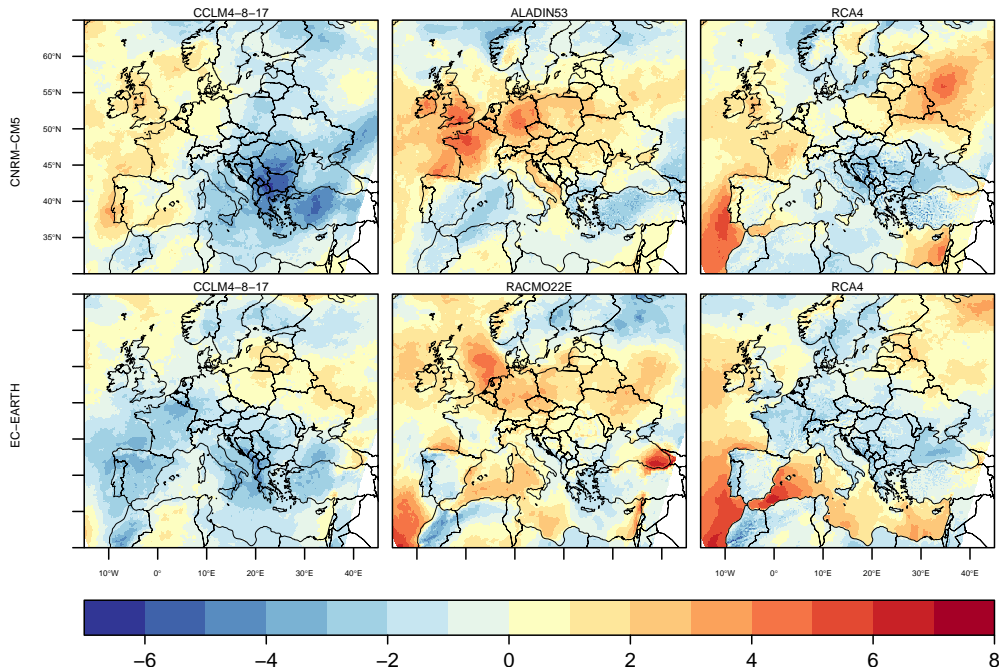
The geographical dependence of the PV potential change is due to the spatial pattern of SSR change, which is closely related to the anomaly of AOD in central Europe pro-



(a) CNRM-CM5



(b) EC-EARTH



(c) Families of RCMs simulations. First row driven by CNRM-CM5 and second row driven by EC-EARTH.

Figure 7.3: Mean change 2021-2050 with respect to the reference period 1970-2021 of JJA total cloud cover, CLT. [%]

---

CMIP5 GCM	RCM	$\Delta PV_{annual}$	$\Delta PV_{JJA}$	Spain	Germany	Italy	Greece	Hungary	Czech Republic
CNRM-CM5	ALADIN53	3.2%	2.7 %	2.4%	10.9%	6.3%	4.6%	11.2%	12.0%
	CCLM4-8-17	-1.4%	-0.8%	-0.6%	-2.2 %	-0.4%	0.3 %	-1.0%	-1.6%
	RCA4	-1.5%	-0.7 %	-0.8 %	-1.5 %	-0.4 %	-0.4 %	-0.5%	-1.1%
EC-EARTH	RACMO	-0.6%	0.6%	0.3%	1.4%	1.6%	2.3%	4.0%	2.5%
	CCLM4-8-17	-2.3%	-1.5%	-0.6%	-1.8%	-0.6%	-1.4%	-1.8%	-1.7%
	RCA4	-2.0%	-0.7%	-0.8%	-0.3%	-0.6%	-0.9%	-0.7%	-0.4%

Table 7.4: Relative change of yearly PV [%] and JJA PV [%] with respect of the reference period for the whole domain and JJA PV relative change averaged by country [%].

jected by ALADIN53 and RACMO22E. The most important result is that the projected change in PV output is positive for both RCMs with evolving aerosols in countries where the other RCMs show the opposite sign. This suggests that for some areas in Europe information from RCMs projections might not be accurate if an ensemble is used for these energy related purposes.

The annual values of PV relative change for the models without aerosol evolution is between -2.3 to -1.4% over the whole domain. ALADIN53 projects a positive annual mean change of 3.2% and RACMO22E of, -0.6%. In absolute terms, values above 100

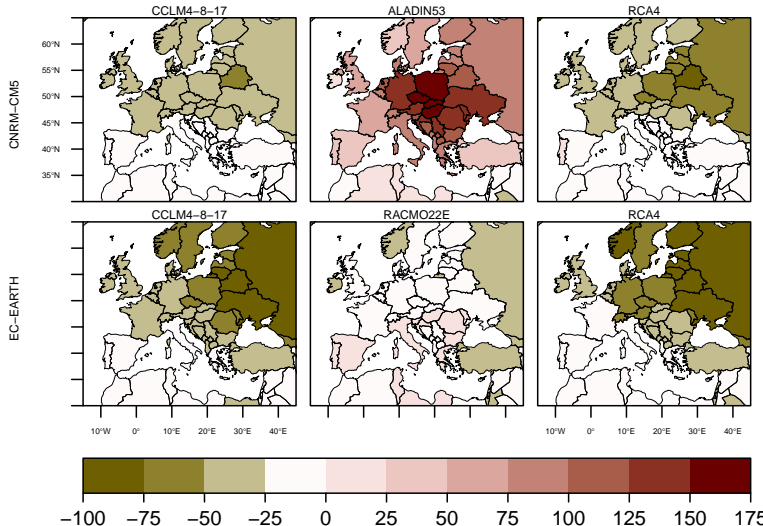


Figure 7.4: Yearly change of PV productivity for 2021-2050 with respect to the reference period 1970-2021  $\left[ \frac{\text{kWh}}{\text{kWp}} \right]$

$\left[ \frac{\text{kWh}}{\text{kWp}} \right]$  are found for countries in Central Europe for ALADIN53 and in north-eastern countries, values are lower than  $-50 \left[ \frac{\text{kWh}}{\text{kWp}} \right]$  for models not including aerosols evolution, as can be seen in Figure 7.4.

For summer months, which is the most important season for solar energy supply, the results are shown in Figure 7.5. In this case, the same pattern as in the annual PV yield is found, with the two models with evolving aerosols showing higher changes. All the simulations not including evolving aerosols have very similar values, close to zero in western and southern Europe a slightly negative for the rest of the countries. On the other hand, ALADIN53 gives a strong change for Central-Europe and countries with a maximum that ranges between 11-13% of increase. RACMO22E has positive values but smaller in magnitude with the maximum values around the eastern-southern European countries.

At the country level, some representative ones have been included in Table 7.4. For ALADIN53 values above 10% are found in Germany, Hungary, and the Czech Republic, whereas lower values are found for Spain (2.4%), Italy (6.3%) or Greece (4.6%), although still positive. In the same countries, RACMO22E shows the highest increase in Hungary, 4%, and smaller values in the rest, from 0.3% in Spain to 2.4% in the Czech Republic.

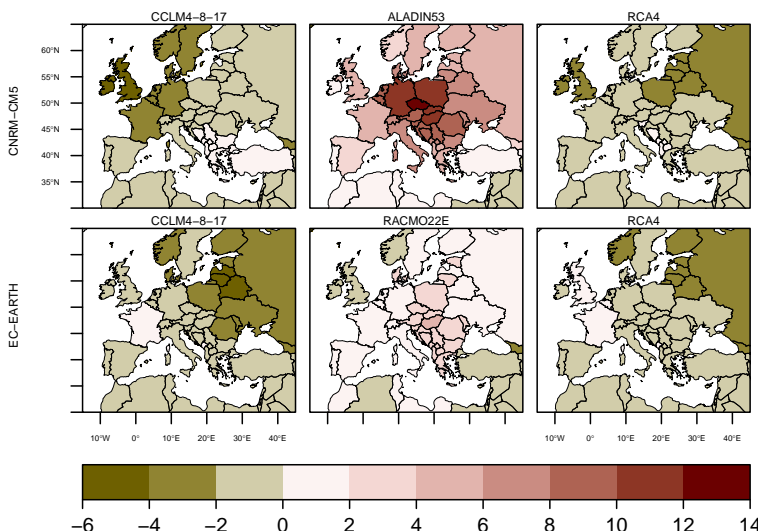


Figure 7.5: PV JJA mean change of 2021-2050 with respect to the reference period 1970-2021 [%]

## 7.5 Discussion

To determine the uncertainty in climate projections is one of the main issues in climate science because the information underlying the simulations is difficult to communicate. In order to isolate the uncertainty sources in a multi-model work it is necessary to design a sensitivity test for each of the models in the study. Up to now, there are not enough simulations from the Euro-CORDEX ensemble including evolving aerosols and for those that include them, there is not the same simulation excluding the aerosols forcing, in order to quantify its impact.

For that reason, this preliminary study, although it highlights very important issues, is the first step in order to understand the role of aerosols in the RCM projections. Uncertainties due to the different AOD datasets used in the two RCMs and in the radiative transfer code of the model difficult the robust answer about the change magnitude.

In addition, although an overestimation of SSR from climate models has been reported extensively, the seek for a robust answer in trends or in the sign in PV potential projected changes justifies the use of climate projections independently from these constraints. They should be undoubtedly addressed later in order to improve the message for potential users and stakeholders of the energy industry.

## 7.6 Conclusion

The study shows that regional climate models with evolving aerosols in the scenarios behave differently to those that have an aerosols climatology constant in time. In model using evolving aerosols, the sign of the SSR change is reversed, agreeing with the positive signal projected by their driving GCMs. This result is a relevant contribution to the explanation of the disagreement found in previous studies between GCMs and RCMs in the sign of future SSR change.

It has been shown also that the change of SSR is not directly linked with change in CLT in the case of the RCMs simulations that include evolving aerosols. The spatial correlation between SSR and CLT in these models is very low and AOD changes are needed to explain the SSR changes.

These results have been derived from the mid of the XXI century. Different changes could be found at the end of the century when the climate change signal is higher.

The results show a general small decrease of SSR for RCMs with no-evolving aerosols, more important in higher latitudes that barely affects the future of PV production, as was pointed out in previous studies [Jer+15b; Jer+19]. However, for ALADIN53 and RACMO2E simulations, a general positive signal in PV projections is found in Central-Europe in the first case and in Southern-Eastern Europe for the second one.

The study shows that regional climate models with time evolving aerosols in the scenario runs behaves different than those that have a fixed climatology. The sign of the anomaly is reversed (for summer mean anomalies), agreeing with the positive signal in PV potential projected by GCMs. The magnitude od the anomalies depends on the country, being the most impacted those in Central-Europe and southern Europe. There is also a small decresase for RCMs with no-evolving aerosols, more important in higher latitudes.

We can conclude that the impact of evolving aerosols on the SSR projections, could affect PV potential projections significantly. Insofar the uncertainty in aerosols datasets and schemes used in RCMs can be narrowed, more accurate projections could be achieved for the energy sector. The fact of the reversed signal in mid century for the PV anomalies in the case of simulations including evolving aerosols, highlights the risk of using an ensemble mean for renewable energy projections and the lack of a robust answer for now.

## Appendix B

### Significance of PV changes in Euro-CORDEX

The statistical significance of the changes of PV potential has been calculated for each simulation. Results of the significance after a t-test and with a threshold of the p-value of 0.05 are represented in Figure 7.6

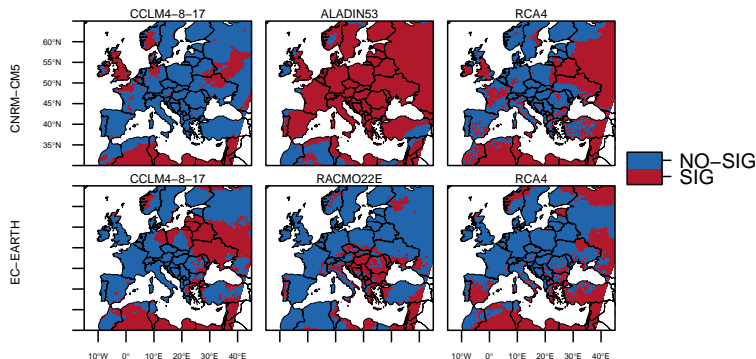


Figure 7.6: Significance of the PV differences between 2021-2050 with respect to the reference period 1970-2021 using a t-test. Red color is for significant results and blue color for no significant.

Significant values are found in ALADIN53 for the whole domain with the exception of certain areas in North-Africa. For the other models in the same family, CCLM and RCA4, the extension of significant areas is smaller. In the last one, significant differences are found in eastern Europe, the North-African continent and some dispersed areas like the British Islands and France. For the CCLM4-8-17 the differences are significant in the north of the African continent, the British Islands and some areas in the continental Eastern-Europe and the south of the Scandinavian Peninsula.

In the second family, driven by the EC-EARTH model, significant differences for the RACMO22E model are less extended than for the other simulations. The significant values are around the south-east of Europe, which correspond to the area of higher PV change. The spatial pattern of significant differences of CCLM and RCA4 is very similar, with significant values in the south of the domain, Eastern Europe and the North of the Scandinavian countries. For RCA4 significant values are also found over the IP.

### **Med-CORDEX analysis**

As part of the CORDEX initiative, scientific groups involved in Med-CORDEX [Rut+16] project provide simulations around the Mediterranean area over a domain that is slightly different to the one used in Euro-CORDEX (see Figure 3.3). An important characteristic in Med-CORDEX ensemble with respect to the Euro-CORDEX is that they provide atmosphere-ocean coupled simulations. A coupled simulation is able to reproduce interactive fluxes between the sea surface and the atmosphere, which will improve the representation of certain climate characteristics, specially in an area like the Mediterranean Sea.

A first look into the Med-CORDEX simulations through an analysis similar to the one developed in the previous chapter is shown in the next section. However, the Med-CORDEX ensemble is limited and only few simulations allow us to apply the pairwise or family comparison principle used before.

### **Climate models**

The only model available with aerosols evolution for scenarios in the Med-CORDEX ensemble is ALADIN-RCSM4 [Sev+14]. In order to isolate the uncertainties coming from the GCMs forcing, RCMs forced with CNRM-CM5 are selected to be compared with ALADIN RCSM4. Only one model apart from ALADIN uses CNRM-CM5 as boundary conditions, the PROTHEUS RCM [Art+10]

The scenario RCP4.5 is the only available for the 2 models. The reference period is 1971-2000 and the future period is 2021-2050 as above.

### Scenario RCP4.5 of relevant variables

The change of SSR and CLT for summer months with respect to the reference period is represented for the two model simulations.

The spatial pattern of SSR change is different in the two simulations. The ALADIN-RCSM4 shows a generalized increase over the domain with values around  $10 \frac{W}{m^2}$  and reaching  $15 \frac{W}{m^2}$  in certain areas. For PROTHeUS, the spatial pattern shows negative changes in the North of the domain. Positive values are around  $5 \frac{W}{m^2}$  in the Southern part of Europe with some areas of  $10 \frac{W}{m^2}$ . The south-western area of the domain, which roughly corresponds to the IP, shows the highest values of change, close to  $15 \frac{W}{m^2}$ .

In Figure 7.8 the change in CLT for the two models can be seen with respect to the reference period. In this case in opposition to the change in SSR, the spatial pattern of both models is similar, projecting a decrease of CLT for the Mediterranean area and a slight increase in Central to Northern Europe. Nevertheless, the decrease of CLT in ALADIN-RCSM4 is smaller.

Differences in spatial pattern suggest that there are other factors affecting the resource change in RCP4.5 projections. Spatial correlation between these variables is presented in Table 7.5.

Mean change for the whole domain is larger for ALADIN-RCSM4 than for PROTHeUS, but the CLT mean change is similar for both. The spatial correlation between CLT and SSR is highly negative for PROTHeUS and less negative for ALADIN-RCSM4.

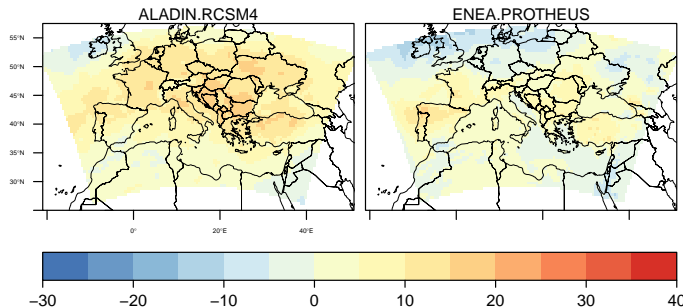


Figure 7.7: SSR change [ $\frac{W}{m^2}$ ] for the period 2021-2050 with respect to the reference period 1971-2000

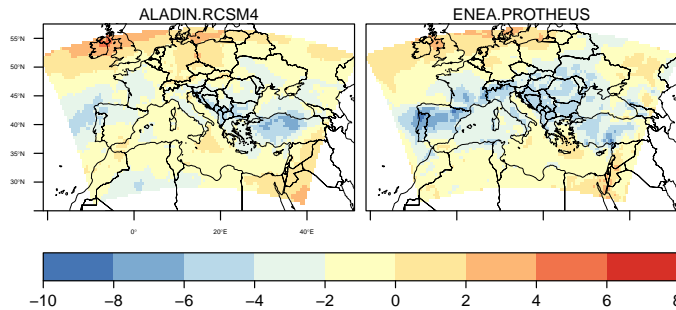


Figure 7.8: CLT change [%] for the period 2021-2050 with respect to the reference period 1971-2000

	$\rho_{SSR,CLT}$	$\rho_{SSR,AOD}$	$\Delta SSR$	$\Delta CLT$
ALADIN-RCSM4	-0.61	-0.66	6.83	-1.17
PROTHEUS	-0.90	-	0.67	-1.76

Table 7.5: Changes in SSR ( $\text{W/m}^2$ ), CLT (%) and spatial correlation between them.

### Final comments

Differences between changes in both climate models indicate that changes in SSR are not only influenced by cloudiness. In addition to the analyses developed in chapter 7, these preliminary results show that a deeper research on how aerosols influence future projections of solar resource should be done, air-sea coupling may also affect changes in SSR indirectly. The results from CORDEX initiative FPS-AEROSOLS, will help to reduce the uncertainty in surface solar radiation future projections, helping in the application of solar energy modeling for the future.

A deeper study on coming simulations from the Med-CORDEX ensemble can be an important contribution to complete the work presented in this chapter, showing differences with the non-coupled models and it is expected to be done in future research.



## **Part IV**

### **Discussion & Conclusion**



---

## Discussion and Conclusion

The main results of this work have shown that solar resource and PV production variability features are found across different time and spatial scales, deserving attention. Some perspectives that arise from the results are also considered in a latter section.

In the three results chapters included in this work, specific questions related to the basic scientific issue have been investigated. Long-term variability problems, that have not been widely considered among the literature, are studied here. The impact of aerosols at climatic time scales is also addressed.

### **Clustering analysis over the IP**

In chapter 5 a multi-step scheme for analysing spatial and temporal variability of PV productivity is applied to the Iberian Peninsula. This is considered as a coherent area in the European electrical grid and energy system, because of its almost isolated character, from a physical and electrical point of view. In addition, the IP is considered as a significant case of study because of its wide variety of climates in a relatively small area, as was remarked in the corresponding chapter. The method includes the application of a detailed photovoltaic production model, allowing to analyse the influence of PV panel tracking on the results. The scientific questions addressed through the clustering methodology can be summarized in three:

- In the first place it is analyzed if there is an optimum spatial distribution of clusters able to explain variability of solar resource within the Iberian Peninsula.
- Secondly, which are the main characteristics grouped together in that spatial distribution and if there are relevant changes in the variability of PV productivity if we consider panel tracking instead of fixed panels.
- Finally, if there is spatial complementarity between sub-areas and if it can be studied with this method.

The scheme presented in 5 allows to characterize an area according to its solar resource variability and systematize the inter-comparison of different areas. The scheme can be applied to different time scales, different resources or different areas.

When the regionalization is applied to the Iberian Peninsula, main climatic features are captured by the method allowing the analysis of the interannual variability and the spatial comparison. In general, the CV of yearly productivity for different clusters among the IP goes from very low variability, 2%, to around 5% which means that PV productivity is roughly stable for interannual time scales, although differences between areas are clear and the interannual variability of monthly series is clearly higher. The CV increases with the complexity of the tracking system, with the two axis tracking type being more sensitive to changes in solar radiation. Due to that, differences between clusters are higher in that case .The annual cycle of the CV of PV productivity shows a clear minimum in summer, specially for fixed panels, which makes PV production in the Iberian Peninsula particularly reliable in summer, precisely when the power demand increases due to cooling needs.

This chapter shows that there is a spatial configuration of clusters that can define different variability characteristics over the Iberian Peninsula, which can be useful for further analysis. Also, this spatial analysis allows to investigate different temporal scales where spatial complementarity can arise.

### **Impact of aerosols over the Mediterranean area**

The results of chapter 6 lead to the conclusion that not only variations in cloudiness are important for long-term solar radiation variability, also aerosols content affects it in different ways. Within this chapter, the following questions are addressed:

- In the first place, it is investigated if aerosols have a significant impact on photovoltaic production over the Euro-Mediterranean area.

- 
- Secondly, how these aerosols influence the spatio-temporal variability of photovoltaic production, from seasonal to multidecadal scales, in present climate conditions is studied.
  - Third, if climate models are adequate for renewable energy studies and renewable energy assessment is investigated.

Past observed trends of SSR over Europe have been simulated using a regional climate model. Only when an accurate aerosols dataset is included in the simulation, one which takes into account sulfates trends over the area, the model is able to reproduce the increase in SSR since the 80's.

The multi-decadal simulation of SSR is used to quantify the impact of that trend in a simulated PV power plant. The results show that the brightening period over Europe would lead to an increase in yearly production of more than 10% in some areas of Central Europe. This means a big impact in a potential PV project over the area.

In the interannual and seasonal scale, no significant impact of aerosols has been observed on the former but indeed, high spatial and seasonal variability is observed.

The added value of simulations including aerosols has been demonstrated with the sensitivity test applied in this chapter. Despite the limitations of RCMs, this illustrates that they are an useful tool in order to advance in the understanding of solar radiation and aerosols interactions.

It is important to remark that due to the difficulties to obtain real PV data, it is difficult to validate the complete modeling chain approach. Nevertheless, the comparison of the modelled PV productivity with some available PV productivity data points also towards a positive impact of the inclusion of detailed aerosol information in RCMs.

### **Future projections of PV potential under climate change scenarios**

The increasing concern about availability of renewable resources under future climate conditions has motivated recent research applying climate models to evaluate possible changes in different resources.

Surface solar radiation under climate change scenarios has been investigated in different works as well as future projections of PV potential. However, the number of research papers dedicated to future renewable energy under climate change is still rather limited.

The discrepancy between global climate models and regional climate models regarding the future change of SSR over Europe is an issue that deserves attention. In chapter 7, the relationship between different climate projections of RCMs and its aerosols representation is investigated in order to answer the next questions:

- Due to the importance that possible changes in solar resource have for planning renewable energy activities, which are the estimations of future PV potential over the Euro-Mediterranean area under climate change scenarios?
- Is the role of aerosols and its evolution in future projections important to understand discrepancies between the GCMs and RCMs SSR projections and photovoltaic potential over that area?

Regional climate simulations from the EURO-CORDEX ensemble are used in the analysis of PV potential. The results show that the use of evolving aerosols in future projections is key to the evaluation of future PV production anomalies. RCMs simulations using time evolving aerosols reproduce an increase in photovoltaic productivity over Europe, coinciding with GCMs and reversing the trend with respect to the rest of RCMs simulations. This shows that including aerosols evolution in the future projections is important in order to assess uncertainties among simulations of different models.

This result is different from previous studies because it focused on the selection of simulations according to their aerosols representation and makes it advisable to discard a simple ensemble approach with equal weights for all members.

For projections including aerosols, the PV potential change for the mid XXI century depends on the area, although higher changes are found in central and southern Europe. This pattern is related to different aerosols' scenarios that project a decrease in anthropogenic aerosols around those areas.

The range of changes varies from one model to another, a result that is important not only because of the need to be careful in the messages given to the solar industry, but also because it points out the way to follow in future works that should quantify the aerosols forcing impact for every model. The projected FPS inside the EURO-CORDEX framework is an ongoing exercise that systematizes the RCM's simulations applying a sensitivity test with and without aerosols and it can help to better understand how aerosol evolution affects not only surface solar radiation but climate as well.

The present dissertation is composed by several studies that addressed different long-term variability problems related to solar resource and photovoltaic generation in climatic framework. The approaches considered in each of the chapters show a methodology that can be applied to different problems, and means the first stage for future research studies. They will be either in the research of aerosols' impact at different scales or in the application of clustering methodologies for the analysis of the resources and production of renewables.

---

## Perspectives

Some perspectives derive from the present work and can lead future research in the field.

In the first place, the methodology applied in chapter 5 can be easily applied to different technologies, areas or time-scales. It would be interesting to apply the methodology to a combination of resources, in order to obtain the spatial distribution that better complements power from different technologies like PV and wind or hydropower. A step forward would be to take into account real power plants locations, although obtaining this kind of information is challenging. Once the spatial distribution of power plants is considered, real applications to improve efficiency of planning and operation activities can be done for the targeted areas.

On the other hand, it would be interesting to investigate if the optimum spatial partition changes in time and under climate change conditions, due to changes in the variability of solar resource. In that case, it would be necessary again to use climate models. The same methodology could be applied for different RCPs scenarios.

By using climate models for the research of solar resource and PV potential, there is a wider spectrum of opportunities for further analysis.

- First, different sensitivity tests can be designed in order to understand different processes affecting solar irradiation.

- Future improvement of RCMs with prognostic aerosols schemes will allow us to design better experiments to understand the role of aerosols in variability for other time scales. Extreme events could be modeled and further investigated. For instance, the reported extreme dust outbreak that has been reported in Germany for the 4th of April in 2014, is an interesting case of study to test in the first place if models are able to reproduce the observed event and afterwards, to estimate the impact of dust on PV production (from local to regional scales) in that kind of episodes.
- The non homogeneous way of representing aerosols in different climate models is an open research field. The *Flagship Pilot Study*, FPS, launched within EURO-CORDEX community, is expected to contribute to the understanding of aerosols and climate interactions over the Euro-Mediterranean area. From the energy perspective, those contributions could lead to a better advice and energy projections for the energy industry and climate services.
- It is also important to notice that different regions around the world can also evolve in similar ways to Europe regarding aerosols. For instance, the observed decrease in anthropogenic aerosols emission in Europe will probably occur in other regions in the future if similar pollution control measures are applied. The quantification of the impact of such likely brightening trends can also contribute to a better development of the PV energy in other regions.



---

## Conclusiones

Los resultados principales del trabajo muestran la amplitud en diferentes escalas temporales y espaciales de la variabilidad del recurso solar y de la productividad fotovoltaica. Los estudios de variabilidad en el largo plazo para la producción eléctrica, y cuya relevancia en la literatura es menor que la de los estudios de caracterización y predicción en el corto plazo, han mostrado tener la capacidad de abordar temas de interés para el desarrollo del sector enegético con alta penetración de energías renovables.

En los tres capítulos de resultados incluidos en este trabajo se investiga la respuesta de cada pregunta específica que emerge del problema científico principal. Estas tres cuestiones pueden resumirse así: la caracterización de la variabilidad interanual, la influencia de los aerosoles como factor determinante en la variabilidad espacio-temporal y la evolución de la producción fotovoltaica en condiciones de cambio climático.

A pesar del evidente marco común para las tres cuestiones, cada una de ellas es discutida de manera individual, por lo que las principales conclusiones derivadas de los tres estudios se resumen a continuación de manera independiente.

### Análisis de variabilidad sobre la PI

En el capítulo 5 se aplica un esquema de varias etapas basado en algoritmos de clustering para estudiar la variabilidad interanual de la producción fotovoltaica en la Península Ibérica. La Península Ibérica es considerada como una unidad eléctrica coherente dentro del sistema europeo, dado su carácter casi aislado desde el punto de vista físico, con la barrera natural de los Pirineos, y desde el punto de vista eléctrico, por las limitaciones en las interconexiones. Además, la gran variedad de climas en su relativamente pequeña extensión, hace que pueda ser considerada como un caso de estudio interesante. Las cuestiones científicas investigadas a través del esquema se resumen en tres:

- En primer lugar, se analiza la existencia de una distribución espacial óptima de clusters o regiones, capaz de explicar la variabilidad de la radiación solar en la PI.
- En segundo lugar se estudian las principales características agrupadas por la distribución espacial, y analizan los cambios al considerar los distintos sistemas de seguimiento en los paneles PV.
- Por último, se analiza si la complementariedad espacial entre las diferentes regiones puede ser estudiada a partir de este método.

El esquema que se presenta en el capítulo 5 permite caracterizar un área de acuerdo a la variabilidad del recurso solar y sistematiza la comparación entre diferentes sub-areas. Su flexibilidad permite aplicarlo a diferentes escalas temporales, diferentes recursos y diferentes áreas.

La regionalización mediante clustering aplicada a la Península Ibérica permite distinguir las principales características climáticas de la zona y la variabilidad interanual del recurso y la producción pueden ser analizadas y comparadas espacialmente. En general, el CV de la productividad anual de los diferentes clusters a lo largo de la Península varía entre muy poca variabilidad, 2% hasta alrededor de un 5%, lo que significa un recurso bastante estable en esas escalas temporales, aunque las diferencias entre áreas son claras. La variabilidad interanual de las series mensuales es más alta, por encima de un 20% para algunas zonas en los meses de invierno. El CV crece con el cambio en el sistema de seguimiento fotovoltaico, siendo el seguidor a doble eje más sensible a cambios en la radiación solar y por tanto las diferencias entre clusters mayores.

Este capítulo muestra como existe una configuración de regiones que se define por las diferentes características de la variabilidad sobre la IP, lo que puede ser

---

útil para un posterior análisis más profundo. Además, este análisis espacial permite investigar diferentes escalas temporales donde la complementariedad entre zonas pueda surgir.

### **Impacto de los aerosoles en la producción fotovoltaica en el área Euro-Mediterránea**

Los resultados del capítulo 6 buscan cuantificar el impacto de los aerosoles en la variabilidad espacio-temporal de la radiación solar y la producción fotovoltaica en escalas climáticas. De manera concreta, en este capítulo encontramos la respuesta a las siguientes tres preguntas:

- En primer lugar se busca conocer si los aerosoles tienen un impacto significativo en la producción fotovoltaica en el área Euro-Mediterránea.
- En segundo lugar se busca cuantificar este impacto en la producción fotovoltaica en escalas que abarcan desde estacionales hasta decadales, en condiciones de clima presente.
- Por último, de manera transversal podemos evaluar si el uso de modelos climáticos para estudios de evaluación de recurso es adecuado.

Las tendencias pasadas observadas en la radiación solar sobre Europa, han sido simuladas con un modelo regional climático. Sólo cuando la tendencia decreciente de los sulfatos es considerada en las simulaciones, el modelo es capaz de reproducir el incremento de la radiación observado en Europa desde los años 80.

La simulación multi-decadal que representa la tendencia en la radiación observada es utilizada para cuantificar el impacto de la misma en una planta de generación fotovoltaica. Los resultados muestran que el periodo de 'brillantez' en Europa, hubiera supuesto un incremento anual en la producción de más de un 10% en algunas áreas de Europa Central, lo que significa un gran impacto para una hipotética planta de generación en esta zona.

A partir de un estudio de sensibilidad se cuantifica el impacto de los aerosoles para la escala interanual y estacional. Aunque la variabilidad no es importante en escala interanual, sí se observa una alta variabilidad espacio-temporal en la escala estacional.

El valor añadido de las simulaciones que incluyen los aerosoles se demuestra mediante el test de sensibilidad aplicado en este capítulo. A pesar de las limitaciones de los RCMs, se ilustra su capacidad como herramienta para investigar

las interacciones entre radiación solar y aerosoles y sus consecuencias no solo en el clima, sino en la radiación como recurso de energía solar.

Es importante remarcar la dificultad de obtener datos reales de plantas de generación eléctrica, en concreto de plantas de generación fotovoltaica, para la validación completa de la cadena de modelado utilizada en este capítulo. Sin embargo, la comparación de la producción obtenida con la de algunas plantas de producción disponibles en escala local, apuntan el impacto positivo de la consideración de información detallada sobre aerosoles en las simulaciones con RCMs.

### **Proyecciones futuras de potencial fotovoltaico en escenarios de cambio climático**

La creciente preocupación acerca de la disponibilidad de los recursos renovables bajo condiciones de cambio climático, ha motivado los recientes estudios de modelos climáticos para evaluar los posibles cambios en los diferentes recursos.

La radiación solar en superficie bajo condiciones de cambio climático, ha sido investigada en diferentes trabajos, así como las proyecciones futuras de potencial fotovoltaico. Sin embargo, la cantidad de estudios dedicados al futuro de los recursos renovables es aún limitado.

La discrepancia entre los modelos climáticos globales y regionales en las proyecciones de SSR sobre Europa es un tema que merece ser considerado para su estudio. En el capítulo 7, la relación entre diferentes proyecciones climáticas y la representación que cada uno de los modelos hace de los aerosoles es investigada para responder a las siguientes preguntas:

- Debido a la importancia que los posibles cambios en el recurso solar tienen para las actividades de planificación en el sector de la energía solar, ¿cómo son las proyecciones de potencial futuro de PV sobre la zona Euro-Mediterránea para los escenarios de cambio climático?
- ¿Es importante el papel de los aerosoles y su evolución para entender las discrepancias entre los modelos globales, GCMs y los modelos regionales RCMs en esa zona?

Las simulaciones regionales de clima del ensemble de EURO-CORDEX se usan para el cálculo del potencial PV. Los resultados muestran que incluir la evolución temporal de los aerosoles en las proyecciones es clave para poder entender los cambios proyectados en la producción PV. Las simulaciones de RCMs

---

que incluyen esta evolución temporal, reproducen el incremento en la productividad fotovoltaica sobre Europa que ha sido proyectada con los modelos globales, mostrando un signo positivo en la anomalía de radiación, al contrario que el resto de RCMs.

Este resultado difiere de los anteriores estudios usando RCMs porque se enfoca a la selección de las simulaciones en función de su representación de aerosoles, descartando el estudio desde el punto de vista del ensemble.

Los resultados muestran que para las proyecciones que incluyen aerosoles, el cambio en el potencial PV para la mitad del siglo XXI presenta valores altos para la zona de Europa Central y el Sur de Europa. Este patrón está relacionado con los escenarios de aerosoles que proyectan un descenso de los aerosoles de origen antropogénico en estas zonas.

La magnitud del cambio varía de un modelo a otro, un resultado que es importante no solo por la cautela con la que deben tomarse estos resultados para dar mensajes a la industria solar, sino también porque señala la manera de proceder en trabajos futuros que deben cuantificar el impacto del forzamiento de aerosoles para cada modelo. En este aspecto, el FPS (flagship pilot study) que trabaja dentro del marco de EURO-CORDEX es un ejercicio que sistematiza las simulaciones de RCMs aplicando distintos estudios de sensibilidad a cada modelo en función los aerosoles empleados. Este trabajo ayudará a comprender mejor como la evolución de los aerosoles va a afectar no solo a la radiación, sino al sistema climático.

Esta disertación comprende un conjunto de estudios que tratan problemas relacionados con la variabilidad en el largo plazo para la radiación solar y para la producción fotovoltaica que se enmarcan dentro del contexto climático. El acercamiento a estos problemas en cada uno de los capítulos, crea una metodología aplicable a distintos problemas y sienta las bases para la elaboración de estudios futuros, tanto en la evaluación del impacto de los aerosoles en otras escalas temporales, como en la aplicación de las metodologías de clustering para el análisis espacio-temporal de los recursos y la producción renovables.





---

## Bibliography

- [ACP92] R. Aguiar and M. Collares-Pereira. “Statistical properties of hourly global radiation”. In: *Solar Energy* 48.3 (1992), pp. 157–167. ISSN: 0038092X. DOI: [10.1016/0038-092X\(92\)90134-V](https://doi.org/10.1016/0038-092X(92)90134-V). URL: <https://linkinghub.elsevier.com/retrieve/pii/0038092X9290134V>.
- [Age17] The International Renewable Energy Agency. *Renewable Energy Statistics*. International Renewable Energy Agency, 2017.
- [Age18] International Energy Agency. *World Energy Outlook 2018*. World Energy Outlook. OECD, 2018, p. 661. ISBN: 9789264064522. DOI: [10.1787/weo-2018-en](https://doi.org/10.1787/weo-2018-en). URL: <https://www.oecd-ilibrary.org/content/publication/weo-2018-en>.
- [APN15] M. P. Almeida, O. Perpiñán, and L. Narvarte. “PV power forecast using a nonparametric PV model”. In: *Solar Energy* 115 (2015), pp. 354–368. ISSN: 0038092X. DOI: [10.1016/j.solener.2015.03.006](https://doi.org/10.1016/j.solener.2015.03.006). URL: <https://www.sciencedirect.com/science/article/pii/S0038092X15001218?via%23Dihub>.
- [Arg+11] D. Argüeso, J. M. Hidalgo-Muñoz, S. R. Gámiz-Fortis, et al. “Evaluation of WRF Parameterizations for Climate Studies over Southern Spain Using a Multistep Regionalization”. In: *Journal of Climate* 24.21 (2011), pp. 5633–5651. ISSN: 0894-8755. DOI: [10.1175/JCLI-D-10-0542.1](https://doi.org/10.1175/JCLI-D-10-0542.1)

- JCLI-D-11-00073.1. URL: <http://journals.ametsoc.org/doi/abs/10.1175/JCLI-D-11-00073.1>.
- [Art+10] V. Artale, S. Calmanti, A. Carillo, et al. “An atmosphere-ocean regional climate model for the Mediterranean area: Assessment of a present climate simulation”. In: *Climate Dynamics* (2010). ISSN: 09307575. DOI: [10.1007/s00382-009-0691-8](https://doi.org/10.1007/s00382-009-0691-8).
- [ATCP13] F. Antonanzas-Torres, F. Cañizares, and O. Perpiñán. “Comparative assessment of global irradiation from a satellite estimate model (CM SAF) and on-ground measurements (SIAR): A Spanish case study”. In: *Renewable and Sustainable Energy Reviews* 21 (2013), pp. 248–261. ISSN: 13640321. DOI: [10.1016/j.rser.2012.12.033](https://doi.org/10.1016/j.rser.2012.12.033). URL: <http://linkinghub.elsevier.com/retrieve/pii/S1364032112007368>.
- [Bar+17] B. Bartók, M. Wild, D. Folini, et al. “Projected changes in surface solar radiation in CMIP5 global climate models and in EURO-CORDEX regional climate models for Europe”. In: *Climate Dynamics* 49.7-8 (2017), pp. 2665–2683. ISSN: 0930-7575. DOI: [10.1007/s00382-016-3471-2](https://doi.org/10.1007/s00382-016-3471-2). URL: <http://link.springer.com/10.1007/s00382-016-3471-2>.
- [Bar10] B. Bartók. “Changes in solar energy availability for south-eastern Europe with respect to global warming”. In: *Physics and Chemistry of the Earth, Parts A/B/C* 35.1-2 (2010), pp. 63–69. ISSN: 14747065. DOI: [10.1016/j.pce.2010.03.008](https://doi.org/10.1016/j.pce.2010.03.008). URL: <https://www.sciencedirect.com/science/article/pii/S1474706510000239>.
- [BBH14] D. Burnett, E. Barbour, and G. P. Harrison. “The UK solar energy resource and the impact of climate change”. In: *Renewable Energy* (2014). ISSN: 09601481. DOI: [10.1016/j.renene.2014.05.034](https://doi.org/10.1016/j.renene.2014.05.034).
- [BC15] M. D. Bartos and M. V. Chester. “Impacts of climate change on electric power supply in the Western United States”. In: *Nature Climate Change* 5.8 (2015), pp. 748–752. ISSN: 1758-678X. DOI: [10.1038/nclimate2648](https://doi.org/10.1038/nclimate2648). URL: <http://www.nature.com/articles/nclimate2648>.
- [Beg+08] M. Begert, E. Zenklusen, C. Häberli, C. Appenzeller, and L. Klok. “An automated procedure to detect discontinuities; performance assessment and application to a large European climate data set”. In: *Meteorologische Zeitschrift* 17.5 (2008), pp. 663–672. ISSN: 0941-2948. DOI: [10.1127/0941-2948/2008/0314](https://doi.org/10.1127/0941-2948/2008/0314). URL: <http://www>.

- [schweizerbart.de/papers/metz/detail/17/56782/An{\\\_}automated{\\\_}procedure{\\\_}to{\\\_}detect{\\\_}discontinuities{\\\_}p?af=crossref](http://schweizerbart.de/papers/metz/detail/17/56782/An{\_}automated{\_}procedure{\_}to{\_}detect{\_}discontinuities{\_}p?af=crossref).
- [Ben+09] A. Benedetti, J.-J. Morcrette, O. Boucher, et al. “Aerosol analysis and forecast in the European Centre for Medium-Range Weather Forecasts Integrated Forecast System: 2. Data assimilation”. In: *Journal of Geophysical Research* 114.D13 (2009), p. D13205. ISSN: 0148-0227. DOI: [10.1029/2008JD011115](https://doi.wiley.com/10.1029/2008JD011115). URL: <http://doi.wiley.com/10.1029/2008JD011115>.
- [Ber+17] M. H. Bergin, C. Ghoroi, D. Dixit, J. J. Schauer, and D. T. Shindell. “Large Reductions in Solar Energy Production Due to Dust and Particulate Air Pollution”. In: *Environmental Science & Technology Letters* 4.8 (2017), pp. 339–344. ISSN: 2328-8930. DOI: [10.1021/acs.estlett.7b00197](https://acs.estlett.acs.org/doi/10.1021/acs.estlett.7b00197). URL: <http://pubs.acs.org/doi/10.1021/acs.estlett.7b00197>.
- [BF18] H. Blanco and A. Faaij. “A review at the role of storage in energy systems with a focus on Power to Gas and long-term storage”. In: *Renewable and Sustainable Energy Reviews* 81 (2018), pp. 1049–1086. ISSN: 13640321. DOI: [10.1016/j.rser.2017.07.062](https://www.sciencedirect.com/science/article/pii/S1364032117311310). URL: <https://www.sciencedirect.com/science/article/pii/S1364032117311310>.
- [Bin+13] N. L. Bindoff, P. A. Stott, K. M. AchutaRao, et al. “Detection and Attribution of Climate Change: from Global to Regional”. In: *Climate Change 2013 - The Physical Science Basis*. Ed. by Intergovernmental Panel on Climate Change. Cambridge: Cambridge University Press, 2013, pp. 867–952. DOI: [10.1017/CBO9781107415324.022](https://doi.org/10.1017/CBO9781107415324.022). URL: <https://doi.org/10.1017/CBO9781107415324.022>.
- [BKK12] A. Beluco, P. Kroeff de Souza, and A. Krenzinger. “A method to evaluate the effect of complementarity in time between hydro and solar energy on the performance of hybrid hydro PV generating plants”. In: *Renewable Energy* 45 (2012), pp. 24–30. ISSN: 09601481. DOI: [10.1016/j.renene.2012.01.096](https://doi.org/10.1016/j.renene.2012.01.096). URL: <https://linkinghub.elsevier.com/retrieve/pii/S0960148112001231>.

- [Blo+16] H. C. Bloomfield, D. J. Brayshaw, L. C. Shaffrey, P. J. Coker, and H. E. Thornton. “Quantifying the increasing sensitivity of power systems to climate variability”. In: *Environmental Research Letters* 11.12 (2016), p. 124025. ISSN: 1748-9326. DOI: [10.1088/1748-9326/11/12/124025](https://doi.org/10.1088/1748-9326/11/12/124025). URL: <http://stacks.iop.org/1748-9326/11/i=12/a=124025?key=crossref.be7b8a57ca6e72c9817ec8df7975>
- [BMN09] P. Bacher, H. Madsen, and H. A. Nielsen. “Online short-term solar power forecasting”. In: *Solar Energy* 83.10 (2009), pp. 1772–1783. ISSN: 0038092X. DOI: [10.1016/j.solener.2009.05.016](https://doi.org/10.1016/j.solener.2009.05.016). URL: <https://linkinghub.elsevier.com/retrieve/pii/S0038092X09001364>.
- [Bof06] S. Bofinger. “Solar electricity forecast—approaches and first results”. In: *21st European Photovoltaic Solar Energy Conference, Dresden* (2006).
- [Bou15] O. Boucher. *Atmospheric Aerosols*. Dordrecht: Springer Netherlands, 2015. ISBN: 978-94-017-9648-4. DOI: [10.1007/978-94-017-9649-1](https://doi.org/10.1007/978-94-017-9649-1). URL: [http://link.springer.com/10.1007/978-94-017-9649-1](https://link.springer.com/10.1007/978-94-017-9649-1).
- [Bry+18] R. Bryce, I. Losada Carreño, A. Kumler, et al. “Consequences of neglecting the interannual variability of the solar resource: A case study of photovoltaic power among the Hawaiian Islands”. In: *Solar Energy* 167 (2018), pp. 61–75. ISSN: 0038092X. DOI: [10.1016/j.solener.2018.03.085](https://doi.org/10.1016/j.solener.2018.03.085). URL: <https://www.sciencedirect.com/science/article/pii/S0038092X18303414>.
- [BT16] P. E. Bett and H. E. Thornton. “The climatological relationships between wind and solar energy supply in Britain”. In: *Renewable Energy* 87 (2016), pp. 96–110. ISSN: 09601481. DOI: [10.1016/j.renene.2015.10.006](https://doi.org/10.1016/j.renene.2015.10.006). URL: <https://www.sciencedirect.com/science/article/pii/S0960148115303591>.
- [CAM19] Copernicus Atmosphere Monitoring Service CAMS. *MACC-II Consortium, 2011: MACC Reanalysis of Global Atmospheric Composition (2003-2012)*. 2019.
- [Can+86] D. Cano, J.M. Monget, M. Albuission, et al. “A method for the determination of the global solar radiation from meteorological satellite data”. In: *Solar Energy* 37.1 (1986), pp. 31–39. ISSN: 0038092X. DOI: [10.1016/0038-092X\(86\)90104-0](https://doi.org/10.1016/0038-092X(86)90104-0). URL: <https://linkinghub.elsevier.com/retrieve/pii/0038092X86901040>.

- [Cav+18] L. Cavicchia, E. Scoccimarro, S. Gualdi, et al. “Mediterranean extreme precipitation: a multi-model assessment”. In: *Climate Dynamics* 51.3 (2018), pp. 901–913. ISSN: 0930-7575. DOI: [10.1007/s00382-016-3245-x](https://doi.org/10.1007/s00382-016-3245-x). URL: <https://doi.org/10.1007/s00382-016-3245-x>.
- [CH74] T. Calinski and J. Harabasz. “A dendrite method for cluster analysis”. In: *Communications in Statistics - Theory and Methods* 3.1 (1974), pp. 1–27. ISSN: 0361-0926. DOI: [10.1080/03610927408827101](https://doi.org/10.1080/03610927408827101). URL: [http://www.tandfonline.com/doi/abs/10.1080/03610927408827101](https://www.tandfonline.com/doi/abs/10.1080/03610927408827101).
- [Col+10] J. Colin, M. Déqué, R. Radu, and S. Somot. “Sensitivity study of heavy precipitation in Limited Area Model climate simulations: influence of the size of the domain and the use of the spectral nudging technique”. In: *Tellus A: Dynamic Meteorology and Oceanography* 62.5 (2010), pp. 591–604. ISSN: 1600-0870. DOI: [10.1111/j.1600-0870.2010.00467.x](https://doi.org/10.1111/j.1600-0870.2010.00467.x). URL: <https://doi.org/10.1111/j.1600-0870.2010.00467.x>.
- [Com91] B. Commoner. “Rapid Population Growth and Environmental Stress”. In: *International Journal of Health Services* 21.2 (1991), pp. 199–227. ISSN: 0020-7314. DOI: [10.2190/B8RU-HA91-JJKW-PKUR](https://doi.org/10.2190/B8RU-HA91-JJKW-PKUR). URL: [http://journals.sagepub.com/doi/10.2190/B8RU-HA91-JJKW-PKUR](https://journals.sagepub.com/doi/10.2190/B8RU-HA91-JJKW-PKUR).
- [CPB15] C. Cornaro, M. Pierro, and F. Bucci. “Master optimization process based on neural networks ensemble for 24-h solar irradiance forecast”. In: *Solar Energy* 111 (2015), pp. 297–312. ISSN: 0038092X. DOI: [10.1016/j.solener.2014.10.036](https://doi.org/10.1016/j.solener.2014.10.036). URL: <https://www.sciencedirect.com/science/article/pii/S0038092X14005234>.
- [CPR79] M. Collares-Pereira and A. Rabl. “The average distribution of solar radiation-correlations between diffuse and hemispherical and between daily and hourly insolation values”. In: *Solar Energy* 22.2 (1979), pp. 155–164. ISSN: 0038092X. DOI: [10.1016/0038-092X\(79\)90100-2](https://doi.org/10.1016/0038-092X(79)90100-2). URL: <https://linkinghub.elsevier.com/retrieve/pii/0038092X79901002>.

- [Cro+11] J. A. Crook, .L. A. Jones, P. M. Forster, and R. Crook. “Climate change impacts on future photovoltaic and concentrated solar power energy output”. In: *Energy & Environmental Science* 4.9 (2011), p. 3101. ISSN: 1754-5692. DOI: [10.1039/c1ee01495a](https://doi.org/10.1039/c1ee01495a). URL: <http://xlink.rsc.org/?DOI=c1ee01495a>.
- [Cro+14] S. Cros, O. Liandrat, N. Sebastien, and N. Schmutz. “Extracting cloud motion vectors from satellite images for solar power forecasting”. In: *International Geoscience and Remote Sensing Symposium (IGARSS)*. Institute of Electrical and Electronics Engineers Inc., 2014, pp. 4123–4126. ISBN: 9781479957750.
- [CSG11] T. Cebecauer, M. Suri, and C. A. Gueymard. “Uncertainty sources in satellite-derived direct normal irradiance: how can prediction accuracy be improved globally”. In: *Proceedings of the SolarPACES Conference, Granada, Spain*. Vol. 2023. 2011.
- [CV12] M. Chiacchio and R. Vitolo. “Effect of cloud cover and atmospheric circulation patterns on the observed surface solar radiation in Europe”. In: *Journal of Geophysical Research: Atmospheres* 117.D18 (2012), n/a–n/a. ISSN: 01480227. DOI: [10.1029/2012JD017620](https://doi.org/10.1029/2012JD017620). URL: <http://doi.wiley.com/10.1029/2012JD017620>.
- [CW10] M. Chiacchio and M. Wild. “Influence of NAO and clouds on long-term seasonal variations of surface solar radiation in Europe”. In: *Journal of Geophysical Research* 115.10 (2010), p. D00D22. ISSN: 0148-0227. DOI: [10.1029/2009JD012182](https://doi.org/10.1029/2009JD012182). URL: <http://doi.wiley.com/10.1029/2009JD012182>.
- [Dam+17] A. Damm, J. Köberl, F. Prettenthaler, N. Rogler, and C. Töglhofer. “Impacts of +2 °C global warming on electricity demand in Europe”. In: *Climate Services* 7 (2017), pp. 12–30. ISSN: 24058807. DOI: [10.1016/j.cliser.2016.07.001](https://doi.org/10.1016/j.cliser.2016.07.001). URL: <https://www.sciencedirect.com/science/article/pii/S2405880716300012>.
- [DB79] D. L. Davies and D. W. Bouldin. “A Cluster Separation Measure”. In: *IEEE Transactions on Pattern Analysis and Machine Intelligence* PAMI-1.2 (1979), pp. 224–227. ISSN: 0162-8828. DOI: [10.1109/TPAMI.1979.4766909](https://doi.org/10.1109/TPAMI.1979.4766909). URL: <http://ieeexplore.ieee.org/document/4766909/>.

- [DDCC09] M. Denault, D. Dupuis, and S. Couture-Cardinal. “Completeness of hydro and wind power: Improving the risk profile of energy inflows”. In: *Energy Policy* 37.12 (2009), pp. 5376–5384. ISSN: 03014215. DOI: [10.1016/j.enpol.2009.07.064](https://doi.org/10.1016/j.enpol.2009.07.064). URL: <https://linkinghub.elsevier.com/retrieve/pii/S0301421509005783>.
- [Del+18] A. Dell'Aquila, A. Mariotti, S. Bastin, et al. “Evaluation of simulated decadal variations over the Euro-Mediterranean region from ENSEMBLES to Med-CORDEX”. In: *Climate Dynamics* 51.3 (2018), pp. 857–876. ISSN: 0930-7575. DOI: [10.1007/s00382-016-3143-2](https://doi.org/10.1007/s00382-016-3143-2). URL: <https://doi.org/10.1007/s00382-016-3143-2>.
- [DH04] C. Ding and Xiaofeng He. “K -means clustering via principal component analysis”. In: *Twenty-first international conference on Machine learning - ICML '04*. New York, New York, USA: ACM Press, 2004, p. 29. ISBN: 1581138285. DOI: [10.1145/1015330.1015408](https://doi.org/10.1145/1015330.1015408). arXiv: [arXiv:0711.0189v1](https://arxiv.org/abs/0711.0189v1). URL: <http://portal.acm.org/citation.cfm?doid=1015330.1015408>.
- [Dia+13] M. Diagne, M. David, P. Lauret, J. Boland, and N. Schmutz. “Review of solar irradiance forecasting methods and a proposition for small-scale insular grids”. In: *Renewable and Sustainable Energy Reviews* 27 (2013), pp. 65–76. ISSN: 13640321. DOI: [10.1016/j.rser.2013.06.042](https://doi.org/10.1016/j.rser.2013.06.042). URL: <https://www.sciencedirect.com/science/article/pii/S1364032113004334>.
- [Dia+87] L. Diabaté, H. Ddemarcq, N. Michaud-Regas, and L. Wald. “Estimating Incident Solar Radiation at the Surface from Images of the Earth Transmitted by Geostationary Satellites: the Heliosat Project”. In: *International Journal of Solar Energy* 5.5-6 (1987), pp. 261–278. ISSN: 0142-5919. DOI: [10.1080/01425918708914425](https://doi.org/10.1080/01425918708914425). URL: <http://www.tandfonline.com/doi/abs/10.1080/01425918708914425>.
- [Dic+89] R. E. Dickinson, R. M. Errico, F. Giorgi, and G. T. Bates. “A regional climate model for the western United States”. In: *Climatic Change* 15.3 (1989), pp. 383–422. ISSN: 0165-0009. DOI: [10.1007/BF00240465](https://doi.org/10.1007/BF00240465). URL: <https://doi.org/10.1007/BF00240465>.
- [DK99] D. Dumortier and Y. Koga. *Status of international daylight measurement programme (IDMP) and its web server (<http://idmp.entpe.fr>)*. 1999.

- [Dor05] M. H. I. Dore. "Climate change and changes in global precipitation patterns: What do we know?" In: *Environment International* 31.8 (2005), pp. 1167–1181. ISSN: 01604120. DOI: [10.1016/j.envint.2005.03.004](https://doi.org/10.1016/j.envint.2005.03.004). URL: <https://www.sciencedirect.com/science/article/pii/S0160412005000553>.
- [Dro+18] P. Drobinski, N. D. Silva, G. Panthou, et al. "Scaling precipitation extremes with temperature in the Mediterranean: past climate assessment and projection in anthropogenic scenarios". In: *Climate Dynamics* 51.3 (2018), pp. 1237–1257. ISSN: 0930-7575. DOI: [10.1007/s00382-016-3083-x](https://doi.org/10.1007/s00382-016-3083-x). URL: <http://link.springer.com/10.1007/s00382-016-3083-x>.
- [DSS13] S. Dubey, J. N. Sarvaiya, and B. Seshadri. "Temperature Dependent Photovoltaic (PV) Efficiency and Its Effect on PV Production in the World – A Review". In: *Energy Procedia* 33 (2013), pp. 311–321. ISSN: 18766102. DOI: [10.1016/j.egypro.2013.05.072](https://doi.org/10.1016/j.egypro.2013.05.072). URL: <https://linkinghub.elsevier.com/retrieve/pii/S1876610213000829>.
- [DT12] R. J. Davy and A. Troccoli. "Interannual variability of solar energy generation in Australia". In: *Solar Energy* 86.12 (2012), pp. 3554–3560. ISSN: 0038092X. DOI: [10.1016/j.solener.2011.12.004](https://doi.org/10.1016/j.solener.2011.12.004). URL: <https://www.sciencedirect.com/science/article/pii/S0038092X11004336>.
- [Dut+06] E. G. Dutton, D. W. Nelson, R. S. Stone, et al. "Decadal variations in surface solar irradiance as observed in a globally remote network". In: *Journal of Geophysical Research Atmospheres* (2006). ISSN: 01480227. DOI: [10.1029/2005JD006901](https://doi.org/10.1029/2005JD006901).
- [Edw11] P. N. Edwards. "History of climate modeling". In: *Wiley Interdisciplinary Reviews: Climate Change* 2.1 (2011), pp. 128–139. ISSN: 17577780. DOI: [10.1002/wcc.95](https://doi.org/10.1002/wcc.95). URL: <https://onlinelibrary.wiley.com/doi/abs/10.1002/wcc.95>.
- [Eng+17] K. Engeland, M. Borga, J. D. Creutin, et al. *Space-time variability of climate variables and intermittent renewable electricity production – A review*. 2017. DOI: [10.1016/j.rser.2017.05.046](https://doi.org/10.1016/j.rser.2017.05.046).
- [Fan86] John C.C. Fan. "Theoretical temperature dependence of solar cell parameters". In: *Solar Cells* 17.2-3 (1986), pp. 309–315. ISSN: 03796787. DOI: [10.1016/0379-6787\(86\)90020-7](https://doi.org/10.1016/0379-6787(86)90020-7). URL: <https://www.sciencedirect.com/science/article/pii/0379678786900207>.

- [Fla+18] E. Flaounas, F. D. Kelemen, H. Wernli, et al. “Assessment of an ensemble of ocean–atmosphere coupled and uncoupled regional climate models to reproduce the climatology of Mediterranean cyclones”. In: *Climate Dynamics* 51.3 (2018), pp. 1023–1040. ISSN: 0930-7575. DOI: [10.1007/s00382-016-3398-7](https://doi.org/10.1007/s00382-016-3398-7). URL: <https://doi.org/10.1007/s00382-016-3398-7>.
- [Fra+16] B. François, M. Borga, J.D. Creutin, et al. “Complementarity between solar and hydro power: Sensitivity study to climate characteristics in Northern-Italy”. In: *Renewable Energy* 86 (2016), pp. 543–553. ISSN: 09601481. DOI: [10.1016/j.renene.2015.08.044](https://doi.org/10.1016/j.renene.2015.08.044). URL: <https://linkinghub.elsevier.com/retrieve/pii/S0960148115302445>.
- [FS10] E. M. Fischer and C. Schär. “Consistent geographical patterns of changes in high-impact European heatwaves”. In: *Nature Geoscience* 3.6 (2010), pp. 398–403. ISSN: 1752-0894. DOI: [10.1038/ngeo866](https://doi.org/10.1038/ngeo866). URL: <http://www.nature.com/articles/ngeo866>.
- [GA+19] J.L. Gómez-Amo, M.D. Freile-Aranda, J. Camarasa, et al. “Empirical estimates of the radiative impact of an unusually extreme dust and wildfire episode on the performance of a photovoltaic plant in Western Mediterranean”. In: *Applied Energy* 235 (2019), pp. 1226–1234. ISSN: 03062619. DOI: [10.1016/j.apenergy.2018.11.052](https://doi.org/10.1016/j.apenergy.2018.11.052). URL: <https://www.sciencedirect.com/science/article/pii/S0306261918317586>.
- [Gae+14] M. Gaetani, T. Huld, E. Vignati, et al. “The near future availability of photovoltaic energy in Europe and Africa in climate-aerosol modeling experiments”. In: *Renewable and Sustainable Energy Reviews* 38 (2014), pp. 706–716. ISSN: 13640321. DOI: [10.1016/j.rser.2014.07.041](https://doi.org/10.1016/j.rser.2014.07.041). URL: <https://www.sciencedirect.com/science/article/pii/S1364032114004936>.
- [Gae+15] M. Gaetani, E. Vignati, T. Huld, and A. Dosio. “Climate modelling and renewable energy resource assessment”. In: (2015).
- [Gae+18] M. Á. Gaertner, J. J. González-Alemán, R. Romera, et al. “Simulation of medicanes over the Mediterranean Sea in a regional climate model ensemble: impact of ocean–atmosphere coupling and increased resolution”. In: *Climate Dynamics* 51.3 (2018), pp. 1041–1057. ISSN: 0930-7575. DOI: [10.1007/s00382-016-3456-1](https://doi.org/10.1007/s00382-016-3456-1). URL: <https://doi.org/10.1007/s00382-016-3456-1>.

- [Gil+15] V. Gil, M. A. Gaertner, E. Sanchez, et al. “Analysis of interannual variability of sunshine hours and precipitation over Peninsular Spain”. In: *Renewable Energy* 83 (2015), pp. 680–689. ISSN: 09601481. DOI: [10.1016/j.renene.2015.05.001](https://doi.org/10.1016/j.renene.2015.05.001). URL: <https://doi.org/10.1016/j.renene.2015.05.001>.
- [Gil+18] V. Gil, M. Á. Gaertner, C. Gutierrez, and T. Losada. “Impact of climate change on solar irradiation and variability over the Iberian Peninsula using regional climate models”. In: *International Journal of Climatology* 0.0 (2018), joc.5916. ISSN: 0899-8418. DOI: [10.1002/joc.5916](https://doi.org/10.1002/joc.5916). URL: <https://rmets.onlinelibrary.wiley.com/doi/abs/10.1002/joc.5916>.
- [Gio+16] F. Giorgi, C. Torma, E. Coppola, et al. “Enhanced summer convective rainfall at Alpine high elevations in response to climate warming”. In: *Nature Geoscience* (2016). ISSN: 17520908. DOI: [10.1038/ngeo2761](https://doi.org/10.1038/ngeo2761).
- [Gio02] F. Giorgi. “Direct radiative forcing and regional climatic effects of anthropogenic aerosols over East Asia: A regional coupled climate-chemistry/aerosol model study”. In: *Journal of Geophysical Research* 107.D20 (2002), p. 4439. ISSN: 0148-0227. DOI: [10.1029/2001JD001066](https://doi.wiley.com/10.1029/2001JD001066). URL: <http://doi.wiley.com/10.1029/2001JD001066>.
- [Gio06] F. Giorgi. “Climate change hot-spots”. In: *Geophysical Research Letters* 33.8 (2006), p. L08707. ISSN: 0094-8276. DOI: [10.1029/2006GL025734](https://doi.wiley.com/10.1029/2006GL025734). URL: <http://doi.wiley.com/10.1029/2006GL025734>.
- [Gio90] F. Giorgi. “Simulation of Regional Climate Using a Limited Area Model Nested in a General Circulation Model”. In: *Journal of Climate* 3.9 (1990), pp. 941–963. ISSN: 0894-8755. DOI: [10.1175/1520-0442\(1990\)003<0941:SORCUA>2.0.CO;2](https://doi.org/10.1175/1520-0442(1990)003<0941:SORCUA>2.0.CO;2).
- [GL08] F. Giorgi and P. Lionello. “Climate change projections for the Mediterranean region”. In: *Global and Planetary Change* 63.2-3 (2008), pp. 90–104. ISSN: 09218181. DOI: [10.1016/j.gloplacha.2007.09.005](https://doi.org/10.1016/j.gloplacha.2007.09.005). URL: <https://www.sciencedirect.com/science/article/pii/S0921818107001750>.
- [GM08] C. A. Gueymard and D. R. Myers. “Solar Radiation Measurement: Progress in Radiometry for Improved Modeling”. In: *Modeling Solar Radiation at the Earth’s Surface*. Ed. by Viorel Badescu. Berlin, Heidelberg: Springer Berlin Heidelberg, 2008, pp. 1–27. ISBN: 978-

- 3-540-77455-6. DOI: [10.1007/978-3-540-77455-6\\_1](https://doi.org/10.1007/978-3-540-77455-6_1). URL: [https://doi.org/10.1007/978-3-540-77455-6\\_1](https://doi.org/10.1007/978-3-540-77455-6_1).
- [GPG06] Xuejie Gao, J. S. Pal, and F. Giorgi. “Projected changes in mean and extreme precipitation over the Mediterranean region from a high resolution double nested RCM simulation”. In: *Geophysical Research Letters* 33.3 (2006), p. L03706. ISSN: 0094-8276. DOI: [10.1029/2005GL024954](https://doi.org/10.1029/2005GL024954). URL: <https://agupubs.onlinelibrary.wiley.com/doi/abs/10.1029/2005GL024954>.
- [Gue12] C. A. Gueymard. “Clear-sky irradiance predictions for solar resource mapping and large-scale applications: Improved validation methodology and detailed performance analysis of 18 broadband radiative models”. In: *Solar Energy* 86.8 (2012), pp. 2145–2169. ISSN: 0038092X. DOI: [10.1016/j.solener.2011.11.011](https://doi.org/10.1016/j.solener.2011.11.011). URL: <http://dx.doi.org/10.1016/j.solener.2011.11.011>.
- [Gue14] C. A. Gueymard. “A review of validation methodologies and statistical performance indicators for modeled solar radiation data: Towards a better bankability of solar projects”. In: *Renewable and Sustainable Energy Reviews* 39 (2014), pp. 1024–1034. ISSN: 13640321. DOI: [10.1016/j.rser.2014.07.117](https://doi.org/10.1016/j.rser.2014.07.117). URL: <https://linkinghub.elsevier.com/retrieve/pii/S1364032114005693>.
- [Gut+17] C. Gutiérrez, M. Á. Gaertner, O. Perpiñán, C. Gallardo, and E. Sánchez. “A multi-step scheme for spatial analysis of solar and photovoltaic production variability and complementarity”. In: *Solar Energy* 158 (2017), pp. 100–116. ISSN: 0038092X. DOI: [10.1016/j.solener.2017.09.037](https://doi.org/10.1016/j.solener.2017.09.037). URL: <https://linkinghub.elsevier.com/retrieve/pii/S0038092X17308241>.
- [Gut+18] C. Gutiérrez, S. Somot, P. Nabat, et al. “Impact of aerosols on the spatiotemporal variability of photovoltaic energy production in the Euro-Mediterranean area”. In: *Solar Energy* 174 (2018), pp. 1142–1152. ISSN: 0038092X. DOI: [10.1016/j.solener.2018.09.085](https://doi.org/10.1016/j.solener.2018.09.085). URL: [http://www.sciencedirect.com/science/article/pii/S0038092X18309794](https://www.sciencedirect.com/science/article/pii/S0038092X18309794).
- [GV+12] J. A. García-Valero, J. P. Montavez, S. Jerez, et al. “A seasonal study of the atmospheric dynamics over the Iberian Peninsula based on circulation types”. In: *Theoretical and Applied Climatology* 110.1–2 (2012), pp. 291–310. ISSN: 0177-798X. DOI: [10.1007/s00704-012-0740-0](https://doi.org/10.1007/s00704-012-0740-0).

- 012-0623-0. URL: <http://link.springer.com/10.1007/s00704-012-0623-0>.
- [GW11] C. A. Gueymard and S. M. Wilcox. “Assessment of spatial and temporal variability in the US solar resource from radiometric measurements and predictions from models using ground-based or satellite data”. In: *Solar Energy* 85.5 (2011), pp. 1068–1084. ISSN: 0038092X. DOI: [10.1016/j.solener.2011.02.030](https://doi.org/10.1016/j.solener.2011.02.030). URL: <https://linkinghub.elsevier.com/retrieve/pii/S0038092X11000855>.
- [GWO98] H. Gilgen, M. Wild, and A. Ohmura. “Means and Trends of Short-wave Irradiance at the Surface Estimated from Global Energy Balance Archive Data”. In: *Journal of Climate* 11.8 (1998), pp. 2042–2061. ISSN: 0894-8755. DOI: [10.1175/1520-0442-11.8.2042](https://doi.org/10.1175/1520-0442-11.8.2042). URL: [http://journals.ametsoc.org/doi/abs/10.1175/1520-0442-11.8.2042](https://journals.ametsoc.org/doi/abs/10.1175/1520-0442-11.8.2042).
- [Góm+16] G. Gómez, W. D. Cabos, G. Liguori, et al. “Characterization of the wind speed variability and future change in the Iberian Peninsula and the Balearic Islands”. In: *Wind Energy* 19.7 (2016), pp. 1223–1237. ISSN: 10954244. DOI: [10.1002/we.1893](https://doi.org/10.1002/we.1893). arXiv: [arXiv:1006.4405v1](https://arxiv.org/abs/1006.4405v1). URL: [http://doi.wiley.com/10.1002/we.1893](https://doi.wiley.com/10.1002/we.1893).
- [Har+18] A. Harzallah, G. Jordà, C. Dubois, et al. “Long term evolution of heat budget in the Mediterranean Sea from Med-CORDEX forced and coupled simulations”. In: *Climate Dynamics* 51.3 (2018), pp. 1145–1165. ISSN: 0930-7575. DOI: [10.1007/s00382-016-3363-5](https://doi.org/10.1007/s00382-016-3363-5). URL: <https://doi.org/10.1007/s00382-016-3363-5>.
- [Hay+08] M .R. Haylock, N. Hofstra, A. M. G. Klein Tank, et al. “A European daily high-resolution gridded data set of surface temperature and precipitation for 1950–2006”. In: *Journal of Geophysical Research* 113.D20 (2008), p. D20119. ISSN: 0148-0227. DOI: [10.1029/2008JD010201](https://doi.org/10.1029/2008JD010201). arXiv: [1201.1509](https://arxiv.org/abs/1201.1509). URL: [http://doi.wiley.com/10.1029/2008JD010201](https://doi.wiley.com/10.1029/2008JD010201).
- [HM85] J. E. Hay and D. C. McKay. “Estimating solar irradiance on inclined surfaces: a review and assessment of methodologies”. In: *International Journal of Solar Energy* 3.4-5 (1985), pp. 203–240.

- [HMB18] L. Hirth, J. Mühlenpfordt, and M. Bulkeley. “The ENTSO-E Transparency Platform – A review of Europe’s most ambitious electricity data platform”. In: *Applied Energy* 225 (2018), pp. 1054–1067. ISSN: 0306-2619. DOI: [10.1016/J.APENERGY.2018.04.048](https://doi.org/10.1016/J.APENERGY.2018.04.048). URL: <https://www.sciencedirect.com/science/article/pii/S0306261918306068>.
- [Hoe+12] M. Hoerling, J. Eischeid, J. Perlwitz, et al. “On the Increased Frequency of Mediterranean Drought”. In: *Journal of Climate* 25.6 (2012), pp. 2146–2161. ISSN: 0894-8755. DOI: [10.1175/JCLI-D-11-00296.1](https://doi.org/10.1175/JCLI-D-11-00296.1). URL: <https://doi.org/10.1175/JCLI-D-11-00296.1>.
- [Hof+09] N. Hofstra, M. Haylock, M. New, and P. D. Jones. “Testing E-OBS European high-resolution gridded data set of daily precipitation and surface temperature”. In: *Journal of Geophysical Research* 114.D21 (2009), p. D21101. ISSN: 0148-0227. DOI: [10.1029/2009JD011799](https://doi.org/10.1029/2009JD011799). URL: <http://doi.wiley.com/10.1029/2009JD011799>.
- [Hol+98] B.N. Holben, T.F. Eck, I. Slutsker, et al. “AERONET—A Federated Instrument Network and Data Archive for Aerosol Characterization”. In: *Remote Sensing of Environment* 66.1 (1998), pp. 1–16. ISSN: 00344257. DOI: [10.1016/S0034-4257\(98\)00031-5](https://doi.org/10.1016/S0034-4257(98)00031-5). URL: <https://www.sciencedirect.com/science/article/abs/pii/S0034425798000315>.
- [HP10] T. E. Hoff and R. Perez. “Quantifying PV power Output Variability”. In: *Solar Energy* 84.10 (2010), pp. 1782–1793. ISSN: 0038092X. DOI: [10.1016/j.solener.2010.07.003](https://doi.org/10.1016/j.solener.2010.07.003). URL: <http://www.asrc.cestm.albany.edu/perez/2010/short.pdf>.
- [HP12] T. E. Hoff and R. Perez. “Modeling PV fleet output variability”. In: *Solar Energy* 86.8 (2012), pp. 2177–2189. ISSN: 0038092X. DOI: [10.1016/j.solener.2011.11.005](https://doi.org/10.1016/j.solener.2011.11.005). URL: <https://www.sciencedirect.com/science/article/pii/S0038092X11004154>.
- [HR11] C. E. Hoicka and I. H. Rowlands. “Solar and wind resource complementarity: Advancing options for renewable electricity integration in Ontario, Canada”. In: *Renewable Energy* 36.1 (2011), pp. 97–107. ISSN: 09601481. DOI: [10.1016/j.renene.2010.06.004](https://doi.org/10.1016/j.renene.2010.06.004). URL: <https://www.sciencedirect.com/science/article/pii/S0960148110002600>.

- [Ine14] P. Ineichen. "Long Term Satellite Global, Beam and Diffuse Irradiance Validation". In: *Energy Procedia* 48 (2014), pp. 1586–1596. ISSN: 18766102. DOI: [10.1016/j,egypro.2014.02.179](https://doi.org/10.1016/j,egypro.2014.02.179). URL: <https://linkinghub.elsevier.com/retrieve/pii/S187661021400441X>.
- [IP99] P. Ineichen and R. Perez. "Derivation of Cloud Index from Geostationary Satellites and Application to the Production of Solar Irradiance and Daylight Illuminance Data". In: *Theoretical and Applied Climatology* 64.1-2 (1999), pp. 119–130. ISSN: 0177-798X. DOI: [10.1007/s007040050116](https://doi.org/10.1007/s007040050116). URL: <http://link.springer.com/10.1007/s007040050116>.
- [IPC13] R. H Inman, H. T.C. Pedro, and C FM. Coimbra. "Solar forecasting methods for renewable energy integration". In: *Progress in Energy and Combustion Science* 39.6 (2013), pp. 535–576. ISSN: 03601285. DOI: [10.1016/j,pecs.2013.06.002](https://doi.org/10.1016/j,pecs.2013.06.002). URL: <http://linkinghub.elsevier.com/retrieve/pii/S0360128513000294>.
- [Iqb83] M. Iqbal. *An Introduction to Solar Radiation*. Elsevier, 1983. ISBN: 9780123737502. DOI: [10.1016/B978-0-12-373750-2.X5001-0](https://doi.org/10.1016/B978-0-12-373750-2.X5001-0). URL: <https://linkinghub.elsevier.com/retrieve/pii/B9780123737502X50010>.
- [Jac+14] D. Jacob, J. Petersen, B. Eggert, et al. "EURO-CORDEX: new high-resolution climate change projections for European impact research". In: *Regional Environmental Change* 14.2 (2014), pp. 563–578. ISSN: 1436-3798. DOI: [10.1007/s10113-013-0499-2](https://doi.org/10.1007/s10113-013-0499-2). URL: <http://link.springer.com/10.1007/s10113-013-0499-2>.
- [Jer+13a] S. Jerez, R.M. Trigo, A. Sarsa, et al. "Spatio-temporal Complementarity between Solar and Wind Power in the Iberian Peninsula". In: *Energy Procedia* 40 (2013), pp. 48–57. ISSN: 18766102. DOI: [10.1016/j,egypro.2013.08.007](https://doi.org/10.1016/j,egypro.2013.08.007). URL: <https://linkinghub.elsevier.com/retrieve/pii/S1876610213016019>.
- [Jer+13b] S. Jerez, R. M. Trigo, S. M. Vicente-Serrano, et al. "The Impact of the North Atlantic Oscillation on Renewable Energy Resources in Southwestern Europe". In: *Journal of Applied Meteorology and Climatology* 52.10 (2013), pp. 2204–2225. ISSN: 1558-8424. DOI: [10.1175/JAMC-D-12-0257.1](https://doi.org/10.1175/JAMC-D-12-0257.1). URL: <http://journals.ametsoc.org/doi/abs/10.1175/JAMC-D-12-0257.1>.

- [Jer+15a] S. Jerez, F. Thais, I. Tobin, et al. “The CLIMIX model: A tool to create and evaluate spatially-resolved scenarios of photovoltaic and wind power development”. In: *Renewable and Sustainable Energy Reviews* 42 (2015), pp. 1–15. ISSN: 13640321. DOI: [10.1016/j.rser.2014.09.041](https://doi.org/10.1016/j.rser.2014.09.041). URL: <https://linkinghub.elsevier.com/retrieve/pii/S1364032114008144>.
- [Jer+15b] S. Jerez, I. Tobin, R. Vautard, et al. “The impact of climate change on photovoltaic power generation in Europe”. en. In: *Nature Communications* 6.1 (2015), p. 10014. ISSN: 2041-1723. DOI: [10.1038/ncomms10014](https://doi.org/10.1038/ncomms10014). URL: <http://www.nature.com/ncomms/2015/151211/ncomms10014/abs/ncomms10014.html>.
- [Jer+19] S. Jerez, I. Tobin, M. Turco, et al. “Future changes, or lack thereof, in the temporal variability of the combined wind-plus-solar power production in Europe”. In: *Renewable Energy* 139 (2019), pp. 251–260. ISSN: 09601481. DOI: [10.1016/j.renene.2019.02.060](https://doi.org/10.1016/j.renene.2019.02.060). URL: <https://www.sciencedirect.com/science/article/pii/S0960148119302149>.
- [JG+11] P. Jimenez-Guerrero, J. Jose Gomez-Navarro, S. Jerez, et al. “Isolating the effects of climate change in the variation of secondary inorganic aerosols (SIA) in Europe for the 21st century (1991–2100)”. In: *Atmospheric Environment* 45.4 (2011), pp. 1059–1063. ISSN: 13522310. DOI: [10.1016/j.atmosenv.2010.11.022](https://doi.org/10.1016/j.atmosenv.2010.11.022). URL: <https://linkinghub.elsevier.com/retrieve/pii/S1352231010009775>.
- [Jol02] I. Jolliffe. “Principal Component Analysis”. In: *International encyclopedia of statistical science*. Springer Series in Statistics. New York: Springer-Verlag, 2002, pp. 1094–1096. ISBN: 0-387-95442-2. DOI: [10.1007/b98835](https://doi.org/10.1007/b98835). URL: <http://link.springer.com/10.1007/b98835>.
- [JSS92] M. Jantsch, H. Schmidt, and J. Schmid. “Results of the concerted action on power conditioning and control”. In: *11th European photovoltaic solar energy conference*. Vol. 1992. 1992, pp. 1589–1592.
- [JT13] S. Jerez and R. M. Trigo. “Time-scale and extent at which large-scale circulation modes determine the wind and solar potential in the Iberian Peninsula”. In: *Environmental Research Letters* 8.4 (2013), p. 044035. ISSN: 1748-9326. DOI: [10.1088/1748-9326/8/4/044035](https://doi.org/10.1088/1748-9326/8/4/044035). URL: <http://stacks.iop.org/1748-9326/8/i=4/a=044035?key=crossref.bd78f653acd03b2f65bd9245c21f41f2>.

- [KC80] F. Kasten and G. Czeplak. "Solar and terrestrial radiation dependent on the amount and type of cloud". In: *Solar Energy* 24.2 (1980), pp. 177–189. ISSN: 0038092X. DOI: 10.1016/0038-092X(80)90391-6. URL: <https://www.sciencedirect.com/science/article/pii/0038092X80903916>.
- [KI16] D. K and I. I. "Solar Power Forecasting: A Review". In: *International Journal of Computer Applications*. Vol. 145. 6. 2016, pp. 28–50. DOI: 10.5120/ijca2016910728. URL: <http://www.ijcaonline.org/archives/volume145/number6/chaturvedi-2016-ijca-910728.pdf>.
- [KL+13] G. König-Langlo, R. Sieger, H. Schmithüsen, et al. *The Baseline Surface Radiation Network and its World Radiation Monitoring Centre at the Alfred Wegener Institute*. 2013. URL: <http://www.wmo.int/pages/prog/gcos/Publications/gcos-174.pdf>.
- [Kle13] J. Kleissl. *Solar Energy Forecasting and Resource Assessment*. Elsevier, 2013. ISBN: 9780123971777. DOI: 10.1016/C2011-0-07022-9. arXiv: arXiv : 1011 . 1669v3. URL: <https://linkinghub.elsevier.com/retrieve/pii/C20110070229>.
- [Klo+08] S. Kloster, F. Dentener, J. Feichter, et al. "Influence of future air pollution mitigation strategies on total aerosol radiative forcing". In: *Atmospheric Chemistry and Physics* 8.21 (2008), pp. 6405–6437. ISSN: 1680-7324. DOI: 10.5194/acp-8-6405-2008. URL: <http://www.atmos-chem-phys.net/8/6405/2008/>.
- [Klo+10] S. Kloster, F. Dentener, J. Feichter, et al. "A GCM study of future climate response to aerosol pollution reductions". In: *Climate Dynamics* 34.7-8 (2010), pp. 1177–1194. ISSN: 0930-7575. DOI: 10.1007/s00382-009-0573-0. URL: <https://doi.org/10.1007/s00382-009-0573-0>.
- [Kot+06] M. Kottek, J. Grieser, C. Beck, B. Rudolf, and F. Rubel. "World Map of the Köppen-Geiger climate classification updated". In: *Meteorologische Zeitschrift* 15.3 (2006), pp. 259–263. ISSN: 0941-2948. DOI: 10.1127/0941-2948/2006/0130. URL: <http://koeppen-geiger.vu-wien.ac.at/present.htm>.

- [Kou+16] I. Kougias, S. Szabó, F. Monforti-Ferrario, T. Huld, and K. Bódis. “A methodology for optimization of the complementarity between small-hydropower plants and solar PV systems”. In: *Renewable Energy* 87.2 (2016), pp. 1023–1030. ISSN: 09601481. DOI: [10.1016/j.renene.2015.09.073](https://doi.org/10.1016/j.renene.2015.09.073). URL: <http://www.ncbi.nlm.nih.gov/pubmed/11292186>.
- [KPO11] V. Kostylev, A. Pavlovski, and Others. “Solar power forecasting performance-towards industry standards”. In: *1st international workshop on the integration of solar power into power systems, Aarhus, Denmark*. 2011.
- [Kro17] B. Krokospi. “Integrating high levels of variable renewable energy into electric power systems”. In: *Journal of Modern Power Systems and Clean Energy* 5.6 (2017), pp. 831–837. ISSN: 2196-5625. DOI: [10.1007/s40565-017-0339-3](https://doi.org/10.1007/s40565-017-0339-3). URL: <https://doi.org/10.1007/s40565-017-0339-3>.
- [KTB02] Y. J. Kaufman, D. Tanré, and O. Boucher. “A satellite view of aerosols in the climate system”. In: *Nature* 419.6903 (2002), pp. 215–223. ISSN: 0028-0836. DOI: [10.1038/nature01091](https://doi.org/10.1038/nature01091). URL: <http://www.nature.com/doifinder/10.1038/nature01091>.
- [Lam+10] J-F. Lamarque, T. C. Bond, V. Eyring, et al. “Historical (1850–2000) gridded anthropogenic and biomass burning emissions of reactive gases and aerosols: methodology and application”. In: *Atmospheric Chemistry and Physics* 10.15 (2010), pp. 7017–7039. ISSN: 1680-7324. DOI: [10.5194/acp-10-7017-2010](https://doi.org/10.5194/acp-10-7017-2010). URL: <http://www.atmos-chem-phys.net/10/7017/2010/>.
- [Lel02] J. Lelieveld. “Global Air Pollution Crossroads over the Mediterranean”. In: *Science* 298.5594 (2002), pp. 794–799. ISSN: 00368075. DOI: [10.1126/science.1075457](https://doi.org/10.1126/science.1075457). URL: <http://www.sciencemag.org/cgi/doi/10.1126/science.1075457>.
- [Liu+10] Yanchi Liu, Zhongmou Li, Hui Xiong, Xuedong Gao, and Junjie Wu. “Understanding of Internal Clustering Validation Measures”. In: *2010 IEEE International Conference on Data Mining*. IEEE, 2010, pp. 911–916. ISBN: 978-1-4244-9131-5. DOI: [10.1109/ICDM.2010.35](https://doi.org/10.1109/ICDM.2010.35). URL: <http://ieeexplore.ieee.org/document/5694060/>.

- [LJ60] B. Y.H. Liu and R. C. Jordan. "The interrelationship and characteristic distribution of direct, diffuse and total solar radiation". In: *Solar Energy* 4.3 (1960), pp. 1–19. ISSN: 0038092X. DOI: [10.1016/0038-092X\(60\)90062-1](https://doi.org/10.1016/0038-092X(60)90062-1). URL: <http://www.sciencedirect.com/science/article/pii/0038092X60900621>.
- [Lor+10] E. Lorenz, J. Hurka, G. Karampela, et al. "Qualified Forecast of Ensemble Power Production by Spatially Dispersed Grid-Connected PV Systems". In: *23rd European Photovoltaic Solar Energy Conference* (2010).
- [Lor+11] E. Lorenz, T. Scheidsteger, J. Hurka, D. Heinemann, and C. Kurz. "Regional PV power prediction for improved grid integration". In: *Progress in Photovoltaics: Research and Applications* 19.7 (2011), pp. 757–771. ISSN: 10627995. DOI: [10.1002/pip.1033](https://doi.org/10.1002/pip.1033). arXiv: [1303.4604](https://arxiv.org/abs/1303.4604). URL: <http://doi.wiley.com/10.1002/pip.1033>.
- [Lun+15] P. D. Lund, J. Lindgren, J. Mikkola, and J. Salpakari. "Review of energy system flexibility measures to enable high levels of variable renewable electricity". In: *Renewable and Sustainable Energy Reviews* 45 (2015), pp. 785–807. ISSN: 13640321. DOI: [10.1016/j.rser.2015.01.057](https://doi.org/10.1016/j.rser.2015.01.057). URL: <https://linkinghub.elsevier.com/retrieve/pii/S1364032115000672>.
- [Mal+16] M. Mallet, F. Dulac, P. Formenti, et al. "Overview of the Chemistry-Aerosol Mediterranean Experiment/Aerosol Direct Radiative Forcing on the Mediterranean Climate (ChArMEx/ADRIMED) summer 2013 campaign". In: *Atmospheric Chemistry and Physics* 16.2 (2016), pp. 455–504. ISSN: 1680-7324. DOI: [10.5194/acp-16-455-2016](https://doi.org/10.5194/acp-16-455-2016). URL: <https://www.atmos-chem-phys.net/16/455/2016/>.
- [Mar+12] J. Marcos, L. Marroyo, E. Lorenzo, and M. García. "Smoothing of PV power fluctuations by geographical dispersion". In: *Progress in Photovoltaics: Research and Applications* 20.2 (2012), pp. 226–237. ISSN: 10627995. DOI: [10.1002/pip.1127](https://doi.org/10.1002/pip.1127). arXiv: [1303.4604](https://arxiv.org/abs/1303.4604). URL: <http://doi.wiley.com/10.1002/pip.1127>.
- [Mat+14] D. Mateos, A. Sanchez-Lorenzo, M. Antón, et al. "Quantifying the respective roles of aerosols and clouds in the strong brightening since the early 2000s over the Iberian Peninsula". In: *Journal of Geophysical Research: Atmospheres* 119.17 (2014), pp. 10,382–10,393. ISSN: 2169897X. DOI: [10.1002/2014JD022076](https://doi.org/10.1002/2014JD022076). URL: <http://doi.wiley.com/10.1002/2014JD022076>.

- [Mee04] G. A. Meehl. "More Intense, More Frequent, and Longer Lasting Heat Waves in the 21st Century". In: *Science* 305.5686 (2004), pp. 994–997. ISSN: 0036-8075. DOI: [10.1126/science.1098704](https://doi.org/10.1126/science.1098704). URL: <http://www.sciencemag.org/cgi/doi/10.1126/science.1098704>.
- [MGV13] A. C. McMahan, C. N. Grover, and F. E. Vignola. "Evaluation of Resource Risk in Solar-Project Financing". In: *Solar Energy Forecasting and Resource Assessment*. Ed. by Jan Kleissl. Boston: Elsevier, 2013, pp. 81–95. ISBN: 978-0-12-397177-7. DOI: [10.1016/B978-0-12-397177-7.00004-8](https://doi.org/10.1016/B978-0-12-397177-7.00004-8). URL: <http://www.sciencedirect.com/science/article/pii/B9780123971777000048>.
- [Mig18] International Organisation for Migration. *Migration Research Analysis: Growth, Reach and Recent Contributions' in IOM* (2017). 2018.
- [MK08] A. Mellit and S. A. Kalogirou. "Artificial intelligence techniques for photovoltaic applications: A review". In: *Progress in Energy and Combustion Science* 34.5 (2008), pp. 574–632. ISSN: 03601285. DOI: [10.1016/j.pecs.2008.01.001](https://doi.org/10.1016/j.pecs.2008.01.001). arXiv: Yahara, Koji, 2014, AReference. URL: <https://linkinghub.elsevier.com/retrieve/pii/S0360128508000026>.
- [Mon+14] F. Monforti, T. Huld, K. Bódis, et al. "Assessing complementarity of wind and solar resources for energy production in Italy. A Monte Carlo approach". In: *Renewable Energy* 63 (2014), pp. 576–586. ISSN: 09601481. DOI: [10.1016/j.renene.2013.10.028](https://doi.org/10.1016/j.renene.2013.10.028). URL: [http://linkinghub.elsevier.com/retrieve/pii/S0960148113005594](https://linkinghub.elsevier.com/retrieve/pii/S0960148113005594).
- [Mor+09] J.-J. Morcrette, O. Boucher, L. Jones, et al. "Aerosol analysis and forecast in the European Centre for Medium-Range Weather Forecasts Integrated Forecast System: Forward modeling". In: *Journal of Geophysical Research* 114.D6 (2009), p. D06206. ISSN: 0148-0227. DOI: [10.1029/2008JD011235](https://doi.org/10.1029/2008JD011235). URL: <http://doi.wiley.com/10.1029/2008JD011235>.
- [MPC13] R. Marquez, H. T.C. Pedro, and C. F.M. Coimbra. "Hybrid solar forecasting method uses satellite imaging and ground telemetry as inputs to ANNs". In: *Solar Energy* 92 (2013), pp. 176–188. ISSN: 0038092X. DOI: [10.1016/j.solener.2013.02.023](https://doi.org/10.1016/j.solener.2013.02.023). URL: <https://www.sciencedirect.com/science/article/pii/S0038092X13000881>.

- [MR01] N. Martin and J.M. Ruiz. “Calculation of the PV modules angular losses under field conditions by means of an analytical model”. In: *Solar Energy Materials and Solar Cells* 70.1 (2001), pp. 25–38. ISSN: 09270248. DOI: [10.1016/S0927-0248\(00\)00408-6](https://doi.org/10.1016/S0927-0248(00)00408-6). URL: <http://linkinghub.elsevier.com/retrieve/pii/S0927024800004086>.
- [MSK12] S. Mekhilef, R. Saidur, and M. Kamalisarvestani. “Effect of dust, humidity and air velocity on efficiency of photovoltaic cells”. In: *Renewable and Sustainable Energy Reviews* 16.5 (2012), pp. 2920–2925. ISSN: 13640321. DOI: [10.1016/j.rser.2012.02.012](https://doi.org/10.1016/j.rser.2012.02.012). arXiv: [12345](https://arxiv.org/abs/12345). URL: [https://linkinghub.elsevier.com/retrieve/pii/S1364032112001050](http://linkinghub.elsevier.com/retrieve/pii/S1364032112001050).
- [Mue+09] R. W. Mueller, C. Matsoukas, A. Gratzki, H. D. Behr, and R. Hollmann. “The CM-SAF operational scheme for the satellite based retrieval of solar surface irradiance — A LUT based eigenvector hybrid approach”. In: *Remote Sensing of Environment* 113.5 (2009), pp. 1012–1024. ISSN: 0034-4257. DOI: [10.1016/j.rse.2009.01.012](https://doi.org/10.1016/j.rse.2009.01.012). URL: <http://www.sciencedirect.com/science/article/pii/S0034425709000224>.
- [Mül+14] B. Müller, M. Wild, A. Driesse, and K. Behrens. “Rethinking solar resource assessments in the context of global dimming and brightening”. In: *Solar Energy* 99 (2014), pp. 272–282. ISSN: 0038092X. DOI: [10.1016/j.solener.2013.11.013](https://doi.org/10.1016/j.solener.2013.11.013). URL: [https://linkinghub.elsevier.com/retrieve/pii/S0038092X13004933](http://linkinghub.elsevier.com/retrieve/pii/S0038092X13004933).
- [Mül+15] R. Müller, U. Pfeifroth, C. Träger-Chatterjee, et al. “Surface Solar Radiation Data Set - Heliosat (SARAH) - Edition 1”. In: *EUMET-SAT Satellite Application Facility on Climate Monitoring (CM SAF)* 1 (2015). DOI: [10.5676/EUM\\_SAF\\_CM/SARAH/V001](https://doi.org/10.5676/EUM_SAF_CM/SARAH/V001). URL: [http://dx.doi.org/10.5676/EUM\\_SAF\\_CM/SARAH/V001](http://dx.doi.org/10.5676/EUM_SAF_CM/SARAH/V001).
- [Nab+13] P. Nabat, S. Somot, M. Mallet, et al. “A 4-D climatology (1979-2009) of the monthly tropospheric aerosol optical depth distribution over the Mediterranean region from a comparative evaluation and blending of remote sensing and model products”. In: *Atmospheric Measurement Techniques* 6.5 (2013), pp. 1287–1314. ISSN: 1867-8548. DOI: [10.5194/amt-6-1287-2013](https://doi.org/10.5194/amt-6-1287-2013). URL: <https://www.atmos-meas-tech.net/6/1287/2013/>.

- [Nab+14] P. Nabat, S. Somot, M. Mallet, A. Sanchez-Lorenzo, and M. Wild. “Contribution of anthropogenic sulfate aerosols to the changing Euro-Mediterranean climate since 1980”. In: *Geophysical Research Letters* 41.15 (2014), pp. 5605–5611. ISSN: 00948276. DOI: [10.1002/2014GL060798](https://doi.wiley.com/10.1002/2014GL060798). URL: <http://doi.wiley.com/10.1002/2014GL060798>.
- [Nab+15] P. Nabat, S. Somot, M. Mallet, et al. “Direct and semi-direct aerosol radiative effect on the Mediterranean climate variability using a coupled regional climate system model”. In: *Climate Dynamics* 44.3-4 (2015), pp. 1127–1155. ISSN: 0930-7575. DOI: [10.1007/s00382-014-2205-6](https://doi.org/10.1007/s00382-014-2205-6). URL: <http://dx.doi.org/10.1007/s00382-014-2205-6>.
- [Neh+17] I. Neher, T. Buchmann, S. Crewell, et al. “Impact of atmospheric aerosols on photovoltaic energy production Scenario for the Sahel zone”. In: *Energy Procedia* 125 (2017), pp. 170–179. ISSN: 18766102. DOI: [10.1016/j.egypro.2017.08.168](https://doi.org/10.1016/j.egypro.2017.08.168). URL: <https://linkinghub.elsevier.com/retrieve/pii/S1876610217336615>.
- [NW07] J. R Norris and M. Wild. “Trends in aerosol radiative effects over Europe inferred from observed cloud cover, solar “dimming,” and solar “brightening””. In: *Journal of Geophysical Research* 112.D8 (2007), p. D08214. ISSN: 0148-0227. DOI: [10.1029/2006JD007794](https://doi.wiley.com/10.1029/2006JD007794). URL: <http://doi.wiley.com/10.1029/2006JD007794>.
- [Ohm+98] A. Ohmura, G. Dutton E, B. Forgan, et al. “Baseline Surface Radiation Network (BSRN/WCRP): New Precision Radiometry for Climate Research”. In: *Bulletin of the American Meteorological Society* 79.10 (1998), pp. 2115–2136. DOI: [10.1175/1520-0477\(1998\)079<2115:BSRNBW>2.0.CO;2](https://doi.org/10.1175/1520-0477(1998)079<2115:BSRNBW>2.0.CO;2); eprint: [https://doi.org/10.1175/1520-0477\(1998\)079<2115:BSRNBW>2.0.CO;2](https://doi.org/10.1175/1520-0477(1998)079<2115:BSRNBW>2.0.CO;2). URL: [https://doi.org/10.1175/1520-0477\(1998\)079<2115:BSRNBW>2.0.CO;2](https://doi.org/10.1175/1520-0477(1998)079<2115:BSRNBW>2.0.CO;2).
- [OMK97] K. Otani, J. Minowa, and K. Kurokawa. “Study on areal solar irradiance for analyzing areally-totalized PV systems”. In: *Solar Energy Materials and Solar Cells* 47.1-4 (1997), pp. 281–288. ISSN: 09270248. DOI: [10.1016/S0927-0248\(97\)00050-0](https://doi.org/10.1016/S0927-0248(97)00050-0). URL: <https://www.sciencedirect.com/science/article/pii/S0927024897000500>.

- [Pag12] J. Page. "The Role of Solar-Radiation Climatology in the Design of Photovoltaic Systems". In: *Practical Handbook of Photovoltaics*. Elsevier, 2012, pp. 573–643. ISBN: 9780123859341. DOI: [10 . 1016 / B978-0-12-385934-1.00017-9](https://doi.org/10.1016/B978-0-12-385934-1.00017-9). URL: <https://www.sciencedirect.com/science/article/pii/B9780123859341000179>.
- [Pag61] J. Page. "The estimation of monthly mean values of daily total short-wave radiation on vertical and inclined surfaces from sunshine records for latitudes 40°N-40°S". In: *UN Conference on New ENergy Sources, paper No. s98*. 1961.
- [Pan+14] I. S. Panagea, I. K. Tsanis, A. G. Koutoulis, and M. G. Grillakis. "Climate Change Impact on Photovoltaic Energy Output: The Case of Greece". In: *Advances in Meteorology* 2014 (2014), pp. 1–11. ISSN: 1687-9309. DOI: [10 . 1155 / 2014 / 264506](https://doi.org/10.1155/2014/264506). URL: [http : // www.hindawi.com/journals/amete/2014/264506/](http://www.hindawi.com/journals/amete/2014/264506/).
- [PBS06] S .C. Pryor, R. J. Barthelmie, and J .T. Schoof. "Inter-annual variability of wind indices across Europe". In: *Wind Energy* 9.1-2 (2006), pp. 27–38. ISSN: 1095-4244. DOI: [10 . 1002 / we . 178](https://doi.org/10.1002/we.178). URL: [http : //doi.wiley.com/10.1002/we.178](http://doi.wiley.com/10.1002/we.178).
- [Per+10] R. Perez, S. Kivalov, J. Schlemmer, et al. "Validation of short and medium term operational solar radiation forecasts in the US". In: *Solar Energy* 84.12 (2010), pp. 2161–2172. ISSN: 0038092X. DOI: [10 . 1016 / j . solener . 2010 . 08 . 014](https://doi.org/10.1016/j.solener.2010.08.014). URL: <https://www.sciencedirect.com/science/article/pii/S0038092X10002823>.
- [Per09] O. Perpiñán. "Statistical analysis of the performance and simulation of a two-axis tracking PV system". In: *Solar Energy* 83.11 (2009), pp. 2074–2085. ISSN: 0038092X. DOI: [10 . 1016 / j . solener . 2009 . 08 . 008](https://doi.org/10.1016/j.solener.2009.08.008). URL: <https://linkinghub.elsevier.com/retrieve/pii/S0038092X09001893>.
- [Per12] O. Perpiñán. "solaR: Solar Radiation and Photovoltaic Systems with R". In: *Journal of Statistical Software* 50.9 (2012). ISSN: 1548-7660. DOI: [10 . 18637 / jss . v050 . i09](https://doi.org/10.18637/jss.v050.i09). URL: [http : // www.jstatsoft.org/v50/i09/](http://www.jstatsoft.org/v50/i09/).
- [Pfe+18a] U. Pfeifroth, J. S. Bojanowski, N. Clerbaux, et al. "Satellite-based trends of solar radiation and cloud parameters in Europe". In: *Advances in Science and Research* 15 (2018), pp. 31–37. ISSN: 1992-0636. DOI: [10 . 5194 / asr - 15 - 31 - 2018](https://doi.org/10.5194/asr-15-31-2018). URL: <https://www.adv-sci-res.net/15/31/2018/>.

- [Pfe+18b] U. Pfeifroth, A. Sanchez-Lorenzo, V. Manara, J. Trentmann, and R. Hollmann. “Trends and Variability of Surface Solar Radiation in Europe Based On Surface- and Satellite-Based Data Records”. In: *Journal of Geophysical Research: Atmospheres* 123.3 (2018), pp. 1735–1754. ISSN: 2169897X. DOI: [10.1002/2017JD027418](https://doi.org/10.1002/2017JD027418). URL: <https://agupubs.onlinelibrary.wiley.com/doi/abs/10.1002/2017JD027418>.
- [PFL95] R. T. Pinker, R. Frouin, and Z. Li. “A review of satellite methods to derive surface shortwave irradiance”. In: *Remote Sensing of Environment* 51.1 (1995), pp. 108–124. ISSN: 00344257. DOI: [10.1016/0034-4257\(94\)00069-Y](https://doi.org/10.1016/0034-4257(94)00069-Y). URL: <http://linkinghub.elsevier.com/retrieve/pii/003442579400069Y>.
- [PL11] O. Perpiñán and E. Lorenzo. “Analysis and synthesis of the variability of irradiance and PV power time series with the wavelet transform”. In: *Solar Energy* 85.1 (2011), pp. 188–197. ISSN: 0038092X. DOI: [10.1016/j.solener.2010.08.013](https://doi.org/10.1016/j.solener.2010.08.013). URL: <https://www.sciencedirect.com/science/article/pii/S0038092X10002811>.
- [Pla+12] S. Planton, P. Lionello, V. Artale, et al. “The climate of the mediterranean region in future climate projections”. In: *The Climate of the Mediterranean Region*. 2012. ISBN: 9780124160422. DOI: [10.1016/B978-0-12-416042-2.00008-2](https://doi.org/10.1016/B978-0-12-416042-2.00008-2).
- [PLC07] O. Perpiñán, E. Lorenzo, and M. A. Castro. “On the calculation of energy produced by a PV grid-connected system”. In: *Progress in Photovoltaics: Research and Applications* 15.3 (2007), pp. 265–274. ISSN: 10627995. DOI: [10.1002/pip.728](https://doi.org/10.1002/pip.728). URL: <http://doi.wiley.com/10.1002/pip.728>.
- [PML13] O. Perpiñán, J. Marcos, and E. Lorenzo. “Electrical power fluctuations in a network of DC/AC inverters in a large PV plant: Relationship between correlation, distance and time scale”. In: *Solar Energy* 88 (2013), pp. 227–241. ISSN: 0038092X. DOI: [10.1016/j.solener.2012.12.004](https://doi.org/10.1016/j.solener.2012.12.004). URL: <https://www.sciencedirect.com/science/article/pii/S0038092X12004197>.
- [Pol+14] J. Polo, F. Antonanzas-Torres, J.M. Vindel, and L. Ramirez. “Sensitivity of satellite-based methods for deriving solar radiation to different choice of aerosol input and models”. In: *Renewable Energy* 68 (2014), pp. 785–792. ISSN: 09601481. DOI: [10.1016/j.renene.2014.01.030](https://doi.org/10.1016/j.renene.2014.01.030).

- renene . 2014 . 03 . 022. URL: <https://www.sciencedirect.com/science/article/pii/S0960148114001670>.
- [Pol+15] J. Polo, M. Gastón, J.M. Vindel, and I. Pagola. “Spatial variability and clustering of global solar irradiation in Vietnam from sunshine duration measurements”. In: *Renewable and Sustainable Energy Reviews* 42 (2015), pp. 1326–1334. ISSN: 13640321. DOI: [10.1016/j.rser.2014.11.014](https://doi.org/10.1016/j.rser.2014.11.014). URL: <http://linkinghub.elsevier.com/retrieve/pii/S1364032114009459>.
- [Pos+12] R. Posselt, R.W. Mueller, R. Stöckli, and J. Trentmann. “Remote sensing of solar surface radiation for climate monitoring — the CM-SAF retrieval in international comparison”. In: *Remote Sensing of Environment* 118 (2012), pp. 186–198. ISSN: 00344257. DOI: [10.1016/j.rse.2011.11.016](https://doi.org/10.1016/j.rse.2011.11.016). URL: <https://linkinghub.elsevier.com/retrieve/pii/S0034425711004111>.
- [PV+04] D. Pozo-Vázquez, J. Tovar-Pescador, S. R. Gámiz-Fortis, M. J. Esteban-Parra, and Y. Castro-Díez. “NAO and solar radiation variability in the European North Atlantic region”. In: *Geophysical Research Letters* 31.5 (2004), n/a-n/a. ISSN: 00948276. DOI: [10.1029/2003GL018502](https://doi.org/10.1029/2003GL018502). URL: <http://doi.wiley.com/10.1029/2003GL018502>.
- [PV+11] D. Pozo-Vázquez, F. J. Santos-Alamillos, V. Lara-Fanego, J. A. Ruiz-Arias, and J. Tovar-Pescador. “The Impact of the NAO on the Solar and Wind Energy Resources in the Mediterranean Area”. In: *Hydrological, Socioeconomic and Ecological Impacts of the North Atlantic Oscillation in the Mediterranean Region*. Springer, 2011, pp. 213–231. DOI: [10.1007/978-94-007-1372-7\\_15](https://doi.org/10.1007/978-94-007-1372-7_15). URL: [http://www.springerlink.com/index/10.1007/978-94-007-1372-7\\_15](http://www.springerlink.com/index/10.1007/978-94-007-1372-7_15).
- [PV+12] D. Pozo-Vázquez, S. Wilbert, C. A. Gueymard, et al. “Interannual variability of long time series of dni and ghi at psa, spain”. In: *Report of Solar Consulting Services* (2012).
- [PZR08] J. Polo, L. F. Zarzalejo, and L. Ramírez. “Solar Radiation Derived from Satellite Images”. In: *Modeling Solar Radiation at the Earth's Surface*. Ed. by Viorel Badescu. Berlin, Heidelberg: Springer Berlin Heidelberg, 2008, pp. 449–462. ISBN: 978-3-540-77455-6. DOI: [10.1007/978-3-540-77455-6\\_18](https://doi.org/10.1007/978-3-540-77455-6_18). URL: [https://doi.org/10.1007/978-3-540-77455-6\\_18](https://doi.org/10.1007/978-3-540-77455-6_18).

- [QR+15] S. Quesada-Ruiz, A. Linares-Rodríguez, J.A. Ruiz-Arias, D. Pozo-Vázquez, and J. Tovar-Pescador. “An advanced ANN-based method to estimate hourly solar radiation from multi-spectral MSG imagery”. In: *Solar Energy* 115 (2015), pp. 494–504. ISSN: 0038-092X. DOI: [10.1016/j.solener.2015.03.014](https://doi.org/10.1016/j.solener.2015.03.014). URL: <https://www.sciencedirect.com/science/article/pii/S0038092X15001322>.
- [RCI11] P. del Río, A. Calvo Silvosa, and G. Iglesias Gómez. “Policies and design elements for the repowering of wind farms: A qualitative analysis of different options”. In: *Energy Policy* 39.4 (2011), pp. 1897–1908. ISSN: 03014215. DOI: [10.1016/j.enpol.2010.12.035](https://doi.org/10.1016/j.enpol.2010.12.035). URL: [http://www.sciencedirect.com/science/article/pii/S0301421510009353](https://www.sciencedirect.com/science/article/pii/S0301421510009353).
- [RD12] E. A. Rosa and T. Dietz. “Human drivers of national greenhouse-gas emissions”. In: *Nature Climate Change* 2.8 (2012), pp. 581–586. ISSN: 1758-678X. DOI: [10.1038/nclimate1506](https://doi.org/10.1038/nclimate1506). URL: [http://www.nature.com/articles/nclimate1506](https://www.nature.com/articles/nclimate1506).
- [Rei09] G. Reikard. “Predicting solar radiation at high resolutions: A comparison of time series forecasts”. In: *Solar Energy* 83.3 (2009), pp. 342–349. ISSN: 0038092X. DOI: [10.1016/j.solener.2008.08.007](https://doi.org/10.1016/j.solener.2008.08.007). URL: <https://linkinghub.elsevier.com/retrieve/pii/S0038092X08002107>.
- [Rem+15] J. Remund, C. Calhau, L. Perret, and D. Marcel. *Characterization of the spatio-temporal variations and ramp rates of solar radiation and PV*. 2015, pp. 1–52. ISBN: 978-3-906042-35-0. URL: [http://iea-pvps.org/index.php?id=336&eID=dam\\_frontend\\_push&docID=2733](http://iea-pvps.org/index.php?id=336&eID=dam_frontend_push&docID=2733).
- [REN18] REN21. *Renewables 2018 Global Status Report*. 2018.
- [Rie+17] D. Rieger, A. Steiner, V. Bachmann, et al. “Impact of the 4 April 2014 Saharan dust outbreak on the photovoltaic power generation in Germany”. In: *Atmospheric Chemistry and Physics Discussions* 17 (2017), pp. 1–31. ISSN: 1680-7375. DOI: [10.5194/acp-2017-441](https://doi.org/10.5194/acp-2017-441). URL: <http://www.atmos-chem-phys-discuss.net/acp-2017-441/>.
- [Rif12] J. Rifkin. “The third industrial revolution: How the internet, green electricity, and 3-d printing are ushering in a sustainable era of distributed capitalism”. In: *World Financial Review* 1.March-April (2012).

- [Rut+16] P. M. Ruti, S. Somot, F. Giorgi, et al. “Med-CORDEX Initiative for Mediterranean Climate Studies”. In: *Bulletin of the American Meteorological Society* 97.7 (2016), pp. 1187–1208. ISSN: 0003-0007. DOI: [10.1175/BAMS-D-14-00176.1](https://doi.org/10.1175/BAMS-D-14-00176.1). URL: <https://doi.org/10.1175/BAMS-D-14-00176.1>.
- [SA+12] F. J. Santos-Alamillos, D. Pozo-Vázquez, J. A. Ruiz-Arias, V. Lara-Fanego, and J. Tovar-Pescador. “Analysis of Spatiotemporal Balancing between Wind and Solar Energy Resources in the Southern Iberian Peninsula”. In: *Journal of Applied Meteorology and Climatology* 51.11 (2012), pp. 2005–2024. ISSN: 1558-8424. DOI: [10.1175/JAMC-D-11-0189.1](https://doi.org/10.1175/JAMC-D-11-0189.1). URL: <http://journals.ametsoc.org/doi/abs/10.1175/JAMC-D-11-0189.1>.
- [San+09] A. Sanchez-Lorenzo, J. Calbó, M. Brunetti, and C. Deser. “Dimming/brightening over the Iberian Peninsula: Trends in sunshine duration and cloud cover and their relations with atmospheric circulation”. In: *Journal of Geophysical Research* 114.D10 (2009), p. D00D09. ISSN: 0148-0227. DOI: [10.1029/2008JD011394](https://doi.org/10.1029/2008JD011394). URL: <https://agupubs.onlinelibrary.wiley.com/doi/abs/10.1029/2008JD011394>.
- [SC04] S. Salvador and P. Chan. “Determining the number of clusters/segments in hierarchical clustering/segmentation algorithms”. In: *16th IEEE International Conference on Tools with Artificial Intelligence*. Ictai. IEEE Comput. Soc, 2004, pp. 576–584. ISBN: 0-7695-2236-X. DOI: [10.1109/ICTAI.2004.50](https://doi.org/10.1109/ICTAI.2004.50). URL: <https://ieeexplore.ieee.org/document/1374239>.
- [Sch+09] J. Schulz, P. Albert, H-D. Behr, et al. “Operational climate monitoring from space: the EUMETSAT Satellite Application Facility on Climate Monitoring (CM-SAF)”. In: 9.5 (2009), pp. 1687–1709.
- [Sch89] J. Schmetz. “Towards a surface radiation climatology: Retrieval of downward irradiances from satellites”. In: *Atmospheric Research* 23.3-4 (1989), pp. 287–321. ISSN: 01698095. DOI: [10.1016/0169-8095\(89\)90023-9](https://doi.org/10.1016/0169-8095(89)90023-9). URL: <http://linkinghub.elsevier.com/retrieve/pii/0169809589900239>.
- [Sen+17a] M. Sengupta, A. Habte, C. A. Gueymard, S. Wilbert, and D. Renne. *Best practices handbook for the collection and use of solar resource data for solar energy applications*. Tech. rep. National Renewable Energy Lab.(NREL), Golden, CO (United States), 2017.

- [Sen+17b] M. Sengupta, A. Habte, C. Gueymard, S. Wilbert, and D. Renne. “Best Practices Handbook for the Collection and Use of Solar Resource Data for Solar Energy Applications: Second Edition”. In: (2017). DOI: [10.2172/1411856](https://doi.org/10.2172/1411856). URL: <http://www.osti.gov/servlets/purl/1411856/>.
- [Sev+14] F. Sevault, S. Somot, A. Alias, et al. “A fully coupled Mediterranean regional climate system model: design and evaluation of the ocean component for the 1980–2012 period”. In: *Tellus A: Dynamic Meteorology and Oceanography* 66.1 (2014), p. 23967. ISSN: 1600-0870. DOI: [10.3402/tellusa.v66.23967](https://doi.org/10.3402/tellusa.v66.23967). URL: <https://doi.org/10.3402/tellusa.v66.23967>.
- [Sil+16] Allan Rodrigues Silva, Felipe Mendonça Pimenta, Arcilan Trevenzoli Assireu, and Maria Helena Constantino Spyrides. “Complementarity of Brazils hydro and offshore wind power”. In: *Renewable and Sustainable Energy Reviews* 56 (2016), pp. 413–427. ISSN: 13640321. DOI: [10.1016/j.rser.2015.11.045](https://doi.org/10.1016/j.rser.2015.11.045). URL: <https://linkinghub.elsevier.com/retrieve/pii/S1364032115013106>.
- [SL+17] A. Sanchez-Lorenzo, A. Enriquez-Alonso, M. Wild, et al. “Trends in downward surface solar radiation from satellites and ground observations over Europe during 1983–2010”. In: *Remote Sensing of Environment* 189 (2017), pp. 108–117. ISSN: 00344257. DOI: [10.1016/j.rse.2016.11.018](https://doi.org/10.1016/j.rse.2016.11.018). URL: <https://linkinghub.elsevier.com/retrieve/pii/S0034425716304655>.
- [SLCW13] A. Sanchez-Lorenzo, J. Calbó, and M. Wild. “Global and diffuse solar radiation in Spain: Building a homogeneous dataset and assessing their trends”. In: *Global and Planetary Change* 100 (2013), pp. 343–352. ISSN: 09218181. DOI: [10.1016/j.gloplacha.2012.11.010](https://doi.org/10.1016/j.gloplacha.2012.11.010). URL: <https://linkinghub.elsevier.com/retrieve/pii/S0921818112002238>.
- [SMH04] C. Schaber, P. Mazza, and R. Hammerschlag. “Utility-Scale Storage of Renewable Energy”. In: *The Electricity Journal* 17.6 (2004), pp. 21–29. ISSN: 10406190. DOI: [10.1016/j.tej.2004.05.005](https://doi.org/10.1016/j.tej.2004.05.005). URL: <https://www.sciencedirect.com/science/article/pii/S1040619004000594>.

- [Sto+13] T. F. Stocker, D. Qin, G.-K. Plattner, et al. “Contribution of Working Group I to the Fifth Assessment Report of the Intergovernmental Panel on Climate Change”. In: *Climate Change 2013 - The Physical Science Basis*. Ed. by Intergovernmental Panel on Climate Change. Cambridge: Cambridge University Press, 2013, pp. 31–116. DOI: [10.1017/CBO9781107415324.005](https://doi.org/10.1017/CBO9781107415324.005). URL: [https://www.cambridge.org/core/product/identifier/CBO9781107415324A011/type/book\\_part](https://www.cambridge.org/core/product/identifier/CBO9781107415324A011/type/book_part).
- [SWC06] D. G. Streets, Ye Wu, and Mian Chin. “Two-decadal aerosol trends as a likely explanation of the global dimming/brightening transition”. In: *Geophysical Research Letters* 33.15 (2006), p. L15806. ISSN: 0094-8276. DOI: [10.1029/2006GL026471](https://doi.org/10.1029/2006GL026471). URL: <https://agupubs.onlinelibrary.wiley.com/doi/abs/10.1029/2006GL026471>.
- [Szo+13] S. Szopa, Y. Balkanski, M. Schulz, et al. “Aerosol and ozone changes as forcing for climate evolution between 1850 and 2100”. In: *Climate Dynamics* 40.9–10 (2013), pp. 2223–2250. ISSN: 0930-7575. DOI: [10.1007/s00382-012-1408-y](https://doi.org/10.1007/s00382-012-1408-y). URL: <http://link.springer.com/10.1007/s00382-012-1408-y>.
- [Sør91] B. Sørensen. “A history of renewable energy technology”. In: *Energy Policy* 19.1 (1991), pp. 8–12. ISSN: 03014215. DOI: [10.1016/0301-4215\(91\)90072-V](https://doi.org/10.1016/0301-4215(91)90072-V). URL: <https://linkinghub.elsevier.com/retrieve/pii/030142159190072V>.
- [Teg+97] I. Tegen, P. Hollrig, M. Chin, et al. “Contribution of different aerosol species to the global aerosol extinction optical thickness: Estimates from model results”. In: *Journal of Geophysical Research: Atmospheres* 102.D20 (1997), pp. 23895–23915. ISSN: 01480227. DOI: [10.1029/97JD01864](https://doi.org/10.1029/97JD01864). URL: <http://doi.wiley.com/10.1029/97JD01864>.
- [TGS84] D. Tanré, J. F. Geleyn, and J. Slingo. “First results of the introduction of an advanced aerosol-radiation interaction in the ECMWF low resolution global model”. In: *Aerosols and their climatic effects* (1984), pp. 133–177.
- [TH80] G. T. Trewartha and L. H. Horn. *An Introduction to climate*. NEW YORK TORONTO LONDON: MC GRAW HILL BOOK COMAPNY INC., 1980, pp. 397–403.

- [Tob+15] I. Tobin, R. Vautard, I. Balog, et al. "Assessing climate change impacts on European wind energy from ENSEMBLES high-resolution climate projections". In: *Climatic Change* 128.1-2 (2015), pp. 99–112. ISSN: 0165-0009. DOI: [10.1007/s10584-014-1291-0](https://doi.org/10.1007/s10584-014-1291-0). URL: <http://link.springer.com/10.1007/s10584-014-1291-0>.
- [Tob+16] I. Tobin, S. Jerez, R. Vautard, et al. "Climate change impacts on the power generation potential of a European mid-century wind farms scenario". In: *Environmental Research Letters* 11.3 (2016), p. 034013. ISSN: 1748-9326. DOI: [10.1088/1748-9326/11/3/034013](https://doi.org/10.1088/1748-9326/11/3/034013). URL: <http://stacks.iop.org/1748-9326/11/i=3/a=034013?key=crossref.7da88a5a7c6dea354ce58294e3c7482b>.
- [Tob+18] I. Tobin, W. Greuell, S. Jerez, et al. "Vulnerabilities and resilience of European power generation to 1.5 °C, 2 °C and 3 °C warming". In: *Environmental Research Letters* 13.4 (2018), p. 044024. ISSN: 1748-9326. DOI: [10.1088/1748-9326/aab211](https://doi.org/10.1088/1748-9326/aab211). URL: <http://stacks.iop.org/1748-9326/13/i=4/a=044024>.
- [Tro18] A. Troccoli. *Weather & Climate Services for the Energy Industry*. Ed. by Alberto Troccoli. Cham: Springer International Publishing, 2018. ISBN: 978-3-319-68417-8. DOI: [10.1007/978-3-319-68418-5](https://doi.org/10.1007/978-3-319-68418-5). URL: <http://link.springer.com/10.1007/978-3-319-68418-5>.
- [TSM12] K. E. Taylor, R. J. Stouffer, and G. A. Meehl. "An Overview of CMIP5 and the Experiment Design". In: *Bulletin of the American Meteorological Society* 93.4 (2012), pp. 485–498. ISSN: 0003-0007. DOI: [10.1175/BAMS-D-11-00094.1](https://doi.org/10.1175/BAMS-D-11-00094.1). arXiv: [arXiv:1011.1669v3](https://arxiv.org/abs/1011.1669v3). URL: <http://journals.ametsoc.org/doi/abs/10.1175/BAMS-D-11-00094.1>.
- [Vig+12] F. Vignola, C. Grover, N. Lemon, and A. McMahan. "Building a bankable solar radiation dataset". In: *Solar Energy* 86.8 (2012), pp. 2218–2229. ISSN: 0038092X. DOI: [10.1016/j.solener.2012.05.013](https://doi.org/10.1016/j.solener.2012.05.013). URL: <https://linkinghub.elsevier.com/retrieve/pii/S0038092X1200182X>.
- [VPB14] C. Vernay, S. Pitaval, and P. Blanc. "Review of Satellite-based Surface Solar Irradiation Databases for the Engineering, the Financing and the Operating of Photovoltaic Systems". In: *Energy Procedia* 57 (2014), pp. 1383–1391. ISSN: 18766102. DOI: [10.1016/j.energy.2014.08.001](https://doi.org/10.1016/j.energy.2014.08.001).

- egypro . 2014 . 10 . 129. URL: <https://www.sciencedirect.com/science/article/pii/S1876610214014969>.
- [WHD13] L. J. Wilcox, E. J. Highwood, and N. J. Dunstone. “The influence of anthropogenic aerosol on multi-decadal variations of historical global climate”. In: *Environmental Research Letters* 8.2 (2013), p. 024033. ISSN: 1748-9326. DOI: [10.1088/1748-9326/8/2/024033](https://doi.org/10.1088/1748-9326/8/2/024033). URL: <http://stacks.iop.org/1748-9326/8/i=2/a=024033?key=crossref.a1c3c3b215836ca46672972ba973400c>.
- [Wid+15] J. Widén, N. Carpman, V. Castellucci, et al. “Variability assessment and forecasting of renewables: A review for solar, wind, wave and tidal resources”. In: *Renewable and Sustainable Energy Reviews* 44 (2015), pp. 356–375. ISSN: 13640321. DOI: [10.1016/j.rser.2014.12.019](https://doi.org/10.1016/j.rser.2014.12.019). URL: <http://www.sciencedirect.com/science/article/pii/S1364032114010715>.
- [Wie+01] E. Wiemken, H.G. Beyer, W. Heydenreich, and K. Kiefer. “Power characteristics of PV ensembles: experiences from the combined power production of 100 grid connected PV systems distributed over the area of Germany”. In: *Solar Energy* 70.6 (2001), pp. 513–518. ISSN: 0038092X. DOI: [10.1016/S0038-092X\(00\)00146-8](https://doi.org/10.1016/S0038-092X(00)00146-8). URL: <https://www.sciencedirect.com/science/article/pii/S0038092X00001468>.
- [Wil+15] M. Wild, D. Folini, F. Henschel, N. Fischer, and B. Müller. “Projections of long-term changes in solar radiation based on CMIP5 climate models and their influence on energy yields of photovoltaic systems”. In: *Solar Energy* 116 (2015), pp. 12–24. ISSN: 0038092X. DOI: [10.1016/j.solener.2015.03.039](https://doi.org/10.1016/j.solener.2015.03.039). URL: <http://www.sciencedirect.com/science/article/pii/S0038092X15001668>.
- [Wil05] M. Wild. “From Dimming to Brightening: Decadal Changes in Solar Radiation at Earth’s Surface”. In: *Science* 308.5723 (2005), pp. 847–850. ISSN: 0036-8075. DOI: [10.1126/science.1103215](https://doi.org/10.1126/science.1103215). arXiv: [arXiv:1308.5367](https://arxiv.org/abs/1308.5367). URL: <http://www.sciencemag.org/cgi/doi/10.1126/science.1103215>.
- [Wil09] M. Wild. “Global dimming and brightening: A review”. In: *Journal of Geophysical Research* 114.D10 (2009), p. D00D16. ISSN: 0148-0227. DOI: [10.1029/2008JD011470](https://doi.org/10.1029/2008JD011470). URL: <http://doi.wiley.com/10.1029/2008JD011470>.

- [Wil12] M. Wild. "Enlightening Global Dimming and Brightening". In: *Bulletin of the American Meteorological Society* 93.1 (2012), pp. 27–37. ISSN: 0003-0007. DOI: [10.1175/BAMS-D-11-00074.1](https://doi.org/10.1175/BAMS-D-11-00074.1). URL: <http://journals.ametsoc.org/doi/abs/10.1175/BAMS-D-11-00074.1>.
- [WM03] R. C. Willson and A. V. Mordvinov. "Secular total solar irradiance trend during solar cycles 21-23". In: *Geophysical Research Letters* 30.5 (2003), n/a–n/a. ISSN: 00948276. DOI: [10.1029/2002GL016038](https://doi.org/10.1029/2002GL016038). URL: <http://doi.wiley.com/10.1029/2002GL016038>.
- [Yan+14] Hong-Tzer Yang, Chao-Ming Huang, Yann-Chang Huang, and Yi-Shiang Pai. "A Weather-Based Hybrid Method for 1-Day Ahead Hourly Forecasting of PV Power Output". In: *IEEE Transactions on Sustainable Energy* 5.3 (2014), pp. 917–926. ISSN: 1949-3029. DOI: [10.1109/TSTE.2014.2313600](https://doi.org/10.1109/TSTE.2014.2313600). URL: <http://ieeexplore.ieee.org/document/6802349/>.
- [Yin05] J. H. Yin. "A consistent poleward shift of the storm tracks in simulations of 21st century climate". In: *Geophysical Research Letters* 32.18 (2005), n/a–n/a. ISSN: 00948276. DOI: [10.1029/2005GL023684](https://doi.org/10.1029/2005GL023684). URL: <https://agupubs.onlinelibrary.wiley.com/doi/abs/10.1029/2005GL023684>.
- [Zag+13] A. Zagouras, A. Kazantidis, E. Nikitidou, and A.A. Argiriou. "Determination of measuring sites for solar irradiance, based on cluster analysis of satellite-derived cloud estimations". In: *Solar Energy* 97 (2013), pp. 1–11. ISSN: 0038092X. DOI: [10.1016/j.solener.2013.08.005](https://doi.org/10.1016/j.solener.2013.08.005). URL: <http://dx.doi.org/10.1016/j.solener.2013.08.005>.
- [Zam+14] M. Zamo, O. Mestre, P. Arbogast, and O. Pannekoucke. "A benchmark of statistical regression methods for short-term forecasting of photovoltaic electricity production. Part II: Probabilistic forecast of daily production". In: *Solar Energy* 105 (2014), pp. 804–816. ISSN: 0038092X. DOI: [10.1016/j.solener.2014.03.026](https://doi.org/10.1016/j.solener.2014.03.026). URL: <http://linkinghub.elsevier.com/retrieve/pii/S0038092X13005239>.
- [ZIC14] A. Zagouras, R. H. Inman, and C. FM. Coimbra. "On the determination of coherent solar microclimates for utility planning and operations". In: *Solar Energy* 102 (2014), pp. 173–188. ISSN: 0038092X. DOI: [10.1016/j.solener.2014.01.021](https://doi.org/10.1016/j.solener.2014.01.021). URL: <http://dx.doi.org/10.1016/j.solener.2014.01.021>.

- [ZMH12] J. Zscheischler, M. D. Mahecha, and S. Harmeling. “Climate Classifications: the Value of Unsupervised Clustering”. In: *Procedia Computer Science* 9 (2012), pp. 897–906. ISSN: 18770509. DOI: [10.1016/j.procs.2012.04.096](https://doi.org/10.1016/j.procs.2012.04.096). URL: <http://www.sciencedirect.com/science/article/pii/S1877050912002177>.
- [ZPC14] A. Zagouras, H. T.C. Pedro, and C. F.M. Coimbra. “Clustering the solar resource for grid management in island mode”. In: *Solar Energy* 110.0 (2014), pp. 507–518. ISSN: 0038092X. DOI: [10.1016/j.solener.2014.10.002](https://doi.org/10.1016/j.solener.2014.10.002). URL: <https://linkinghub.elsevier.com/retrieve/pii/S0038092X14004836>.
- [ZRP05] L. F. Zarzalejo, L. Ramirez, and J. Polo. “Artificial intelligence techniques applied to hourly global irradiance estimation from satellite-derived cloud index”. In: *Energy* 30.9 (2005), pp. 1685–1697. ISSN: 03605442. DOI: [10.1016/j.energy.2004.04.047](https://doi.org/10.1016/j.energy.2004.04.047). URL: <https://linkinghub.elsevier.com/retrieve/pii/S036054420400249X>.
- [Alo05] M. C. Alonso García. *Caracterización y modelado de asociaciones de dispositivos fotovoltaicos*. CIEMAT, 2005. ISBN: 84-7834-495-0.

# List of Figures

1.1	Conceptual scheme: climate, energy and societies interactions . . . . .	9
2.1	Irradiance, wind and wave, forecasting methods depending on the time horizon . . . . .	20
3.1	Map of BSRN stations . . . . .	38
3.2	Retrieval of solar irradiation from satellites . . . . .	40
3.3	The EURO and MED-CORDEX projects domains . . . . .	41
3.4	Map of ECAD stations . . . . .	44
4.1	Scheme of a photovoltaic system . . . . .	50
4.2	Steps for obtaining $G_{eff}$ . . . . .	53
5.1	Stages of the multi-step scheme for variability and complementarity analysis . . . . .	68
5.2	Calinski-Harabasz index by number of clusters . . . . .	71
5.3	Optimal partition of clusters over the Iberian Peninsula . . . . .	74
5.4	Yearly mean of PV yield by cluster and tracking type over the Iberian Peninsula . . . . .	77
5.5	Annual cycle of CV by cluster and tracking type over the Iberian Peninsula . . . . .	78
5.6	CV ratios of PV by tracking type and solar irradiation at horizontal plane . . . . .	79

5.7	Correlation coefficients of the yearly energy yield for the two pairs of clusters with the highest and smallest correlation values over the Iberian Peninsula . . . . .	81
5.8	Correlation coefficients of the monthly energy yield for the two pairs of clusters with the highest and smallest correlation values over the Iberian Peninsula . . . . .	82
5.9	Yearly mean of solar irradiation and variability over the Iberian Peninsula . . . . .	85
5.10	Yearly mean yield and variability by tracking type and cluster over the Iberian Peninsula . . . . .	86
5.11	Yearly mean of solar irradiation and variability by tracking type and cluster for each cell over the Iberian Peninsula . . . . .	87
5.12	Correlation matrix between clusters over the Iberian Peninsula . . . . .	89
6.1	Euro-Mediterranean areas defined and local points . . . . .	98
6.2	Time series of differences between SSR from simulations, satellite data and BSRN stations . . . . .	102
6.3	Distribution of differences in monthly mean of daily PV productivity between simulations and real PV data . . . . .	103
6.4	Differences between climate simulations and satellite in SSR in defined areas . . . . .	105
6.5	Differences in annual cycle of daily energy productivity between PV simulations with SSR from climate models and from satellite . . . . .	106
6.6	Differences in yearly PV productivity between simulations with and without aerosols . . . . .	107
6.7	Differences in seasonal PV productivity between simulations with and without aerosols . . . . .	109
6.8	Difference in PV productivity in the brightening period . . . . .	110
7.1	Aerosol optical depth summer change between 2050-2021 with respect to 1971-2000 over Europe . . . . .	122
7.2	Summer mean SSR change over Europe for the period 2021-2050 with respect of 1971-2000 with different climate models . . . . .	124
7.3	Change in summer CLT over Europe for the period 2021-2050 with respect of 1971-2000 with different climate models . . . . .	126
7.4	Yearly change of PV productivity over Europe for the period 2021-2050 with respect of 1971-2000 . . . . .	127
7.5	JJA mean relative change of PV productivity over Europe for the period 2021-2050 with respect of 1971-2000 . . . . .	128

7.6	Statistical significance of PV changes . . . . .	130
7.7	Summer SSR change over Med-CORDEX domain for the period 2021- 2050 with respect of 1971-2000 with different climate models . . . .	132
7.8	Summer CLT change over Med-CORDEX domain for the period 2021- 2050 with respect of 1971-2000 with different climate models . . . .	133

# List of Tables

4.1	Calculation procedure for the estimation of energy produced by a PV system. Equations and methods for the efficiency of the elements	56
4.2	Summary of the climate models (global, GCM, or regional, RCM) used in chapters 7 and 8	60
5.1	Values of yearly mean of daily irradiation, yearly yield by tracking system and interannual CV of yearly mean by cluster over the Iberian Peninsula	75
6.1	Simulations of the CNRM-RCSM4 used as input of the PV model, period and aerosols representation	97
6.2	Electrical components of the PV power plants	100
6.3	Summary of the local PV data from power plants and SSR from BSRN stations	101
6.4	Statistical analysis at local scale of the simulations with climate models	104
7.1	RCMs from Euro-CORDEX grouped by the CMIP5 GCMs drivers generating the 2 families of simulations studied	120
7.2	RCMs from Euro-CORDEX and aerosols description	121
7.3	Changes of SSR, CLT, AOD and spatial correlations	123
7.4	Relative change of yearly PV [%] and JJA PV [%] with respect of the reference period for the whole domain and JJA PV relative change averaged by country [%].	127
7.5	Changes in SSR, CLT and spatial correlation for Med-CORDEX models	133